Technical Sciences

16(4) 2013

The Technical Sciences is indexed and abstracted in BazTech (http://baztech.icm.edu.pl)
and in IC Journal Master List (http://journals.indexcopernicus.com)

The Journal is also available in electronic form on the web sites
http://www.uwm.edu.pl/techsci (subpage Issues)
http://wydawnictwo.uwm.edu.pl (subpage Czytelnia)

The print edition is the primary version of the Journal

PL ISSN 1505-4675

Contents

A MOVABLE STRING SIEVE – ANALYSIS OF SEED SCREENING

Zdzisław Kaliniewicz[1], *Jerzy Domański*[2]

[1] Department of Heavy Duty Machines and Research Methodology,
University of Warmia and Mazury, Poland
[2] Department of Mechanical Engineering and Machine Construction,
University of Warmia and Mazury, Poland

A b s t r a c t

The conditions of seed movement in a string sieve set into reciprocating motion have been formulated for cereal, vetch, pea, lupine and faba bean seeds. In the analyzed string sieve, seed movement was determined by a combination of the following parameters: angular velocity of the crank, crank radius, seed size, seed's coefficient of external friction, string diameter and angle of inclination of the separator screen. A string sieve for cleaning and sorting most farm-produced seeds was analyzed. The width of the separating groove was set at 1 mm at the beginning of the screen and 11 mm at the end of the screen, and the strings had the diameter of 4 mm. Our results indicate that seeds cannot be effectively graded in the modeled string sieve. The angular velocity of the crank exceeds the velocity which is applied to power conventional separator buckets, and it could damage the separator. A reduction in the angular velocity of the crank to the recommended level caused seeds to become jammed directly before the screening site. The above problem can be solved by propelling seeds into motion with the use of special sweeping brushes.

Symbols

a_s – horizontal longitudinal acceleration of the screen, $\mathrm{m \cdot s^{-2}}$,
d – equivalent diameter of seeds, mm,
d_s – string diameter, mm,
g – gravitational acceleration, $\mathrm{m \cdot s^{-2}}$,
G, G_y, G_z – gravity force and gravity force components, N,
F, F_y, F_z – inertia force and inertia force components, N,
m – seed weight, kg,
N_1, N_2 – the string's normal ground reaction forces, N,
r – crank radius, m,
s – width of the groove in a given screen location, mm,
T_1, T_2 – frictional force components, N,
T_s, W_s, L_s – thickness, width and length of a seed, mm,
v_s – horizontal longitudinal velocity of the screen, $\mathrm{m \cdot s^{-1}}$,

* Corespondence: Zdzisław Kaliniewicz, Katedra Maszyn Roboczych i Metodologii Badań, Uniwersytet Warmińsko-Mazurski w Olsztynie, ul. Oczapowskiego 11/B112, 10-719 Olsztyn, phone: 48 89 523 39 34, e-mail: zdzislaw.kaliniewicz@uwm.edu.pl

x, SD – mean value and standard deviation of physical parameters characterizing different seed groups,

x_{min}, x_{max} – minimum and maximum value of a parameter,

α – angle of inclination of a string sieve, °,

μ_s – coefficient of static friction of seed on steel,

φ – included angle between a seed's gravity force component and a string's normal ground reaction force, °,

ω – angular velocity of the crank, s^{-1}.

Introduction

String sieves are applied in the process of cleaning and sorting seeds (GROCHOWICZ 1994, RAWA 1992, RAWA et al. 1990, WIERZBICKI et al. 1991). The separator bucket is the main operating element of a string sieve. Mesh screens are made of wire or metal sheet, and they feature openings of regular shape and size across the entire screen. A single mesh screen can be applied to separate seeds into two fractions only: seeds that are captured by the mesh and seeds that pass through the mesh. Several mesh screens are placed in the separator bucket to separate seeds into the desired number of fractions. A seed mixture is separated by choosing a set of screens with mesh openings that correspond to the dimensions (width and/or thickness) of graded seeds. In practice, different screens are used to separate various seed species or differently sized seeds of the same species (GROCHOWICZ 1994).

Some screening operations, in particular in the mining industry, involve groove or rod separators (DOMAGAŁA 1976, LEŚKIEWICZ et al. 1971, SKIRŁO et al. 1989, WITKOWICZ et al. 1974, 1977) where rods or wires are fixed perpendicularly to the longer sides of the screen frame. The resulting grooves have identical dimensions across the entire screen. When seeds are graded into several fractions, a set of mesh screens grouped in a large separator bucket may be required.

The above problems are not encountered in the string sieve designed by KALINIEWICZ (2011, 2013a). In this solution, strings are stretched between two horizontal bars. This arrangement creates separating grooves between strings whose size changes gradually with distance from the beginning of the screen. Seeds are sorted into various size fractions by changing the position of collecting buckets under the screen. In view of the average size of farm-produced seeds, the width of the separating groove should be set at 1 mm at the beginning of the screen and 11 mm at the end of the screen. In sieves designed for grading cereal seeds, the width of the separating groove can be set at 1 mm and 5 mm, respectively (KALINIEWICZ 2013a). The results of a preliminary study (KALINIEWICZ 2013d) demonstrated that in separators with a fixed screen, the working surface should be set at an angle of 45° to propel seeds into

motion and at 50° to ensure the continuity of the screening process. Such a large setting angle is not recommended, however, because the graded mixture contains plump seeds with a small coefficient of external friction which will travel at high speeds. The above deteriorates the quality of the separation process. The screen should be set at a small inclination angle and it move in reciprocating motion to ensure that seeds move along the screen.

The majority of seeds produced on agricultural farms are ellipsoid in shape. This group of seeds includes cereal seeds (wheat, rye, barley, oats and triticale), lupine and faba bean seeds, as well as spherical flattened seeds such as pea and vetch seeds. Since the average coefficient of sliding friction is higher that the average coefficient of rolling resistance (KALINIEWICZ 2013c), it is much more difficult to set ellipsoid seeds in motion, compared with spherical seeds. Thus, a string sieve whose operating parameters have been adapted to ellipsoid seeds can also be used to separate spherical seeds.

In this study, the movement of ellipsoid seeds on the working surface of a string sieve moving in reciprocating motion was described to support the selection of optimal operating parameters of a string sieve.

Theoretical analysis of the separation process

The analyzed string sieve was developed according to the concept proposed by KALINIEWICZ (2103a). In the original solution, the working surface is made of steel wires, rods or strings with circular cross-section. The conceptual diagram of the discussed device is presented in Figure 1. The separator bucket is supported by two rockers, and it is set into reciprocating motion by a crank system powered by an electric motor. Deflection amplitude and frequency are controlled by changing crank radius and rotational speed. The crank radius is much smaller than rocker length (1:100 ratio), therefore, it can be assumed that the sieve screen moves in linear motion. Due to a significant difference in the dimensions of the crank and the connecting rod (1:50 ratio), it can also be assumed that the motion is harmonic (GROCHOWICZ 1994). In extreme positions of the separator bucket, the differences in absolute acceleration do not exceed 4%.

The working surface of the string sieve was set at angle α relative to the horizontal plane (Fig. 1), which was smaller than the smallest coefficient of static friction of the analyzed seeds, to immobilize the seeds when the screen was not in motion. For the sake of simplicity, the following angles were disregarded: opening angle between strings in bottom rows, angle of inclination of bottom strings in the first row relative to top strings, and angle of inclination of bottom strings in the second row relative to top strings. The
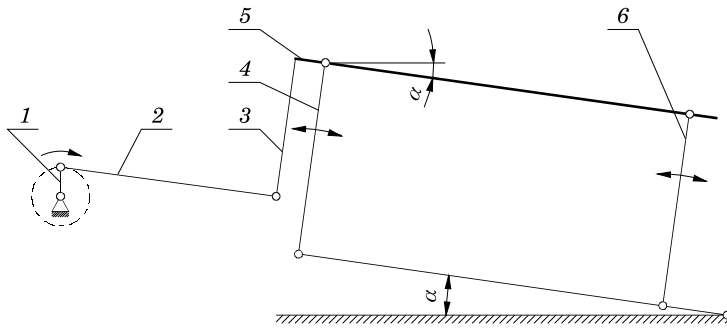
Fig. 1. Conceptual diagram of a string sieve: *1* – electric motor with a crank, *2* – connecting rod, *3* – frame of the screen bucket, *4* – front rocker, *5* – mesh screen, *6* – rear rocker, α – screen's angle of inclination relative to the horizontal plane

above angles did not exceed 1.5° (KALINIEWICZ 2013a). Assuming that the sieve is set into motion beginning from the position indicated in Fig. 1, horizontal longitudinal velocity and acceleration of the screen can be determined with the use of the below formulas:

$$v_s = r \cdot \omega \cdot \cos \omega t \tag{1}$$

$$a_s = -r \cdot \omega^2 \cdot \sin \omega t \tag{2}$$

It was assumed that seeds would be fed in a narrow stream to the initial section of the string sieve. The elastic strain of screen strings, the interactions between seeds and the influence of centripetal acceleration on seed motion were not taken into account for the sake of simplicity. This study analyzed only the sliding motion of seeds across the surface of a string sieve, therefore, the geometric model of the analyzed seeds was adopted in the form of a rotating ellipsoid (GASTON et al. 2002, GROCHOWICZ 1994, HEBDA, MICEK 2005, 2007, ŻABIŃSKI, SADOWSKA 2010). The major axis of the ellipsoid was seed length, and the minor axis was the average of seed thickness and width. The seeds had a circular cross-section whose equivalent diameter was determined based on the following equation:

$$d = \frac{T_s + W_s}{2} \tag{3}$$

In the first stage of the analysis, a seed was placed on the surface of a string sieve with its longitudinal axis parallel to the strings (Fig. 2), i.e. the seed was supported by two adjacent strings. The following forces acted upon the seed:

– gravity *G*,

– normal ground reaction force, as the resultant force exerted by strings N_1 and N_2,

– friction, as the resultant force exerted by T_1 and T_2,

– inertia *F*, in a direction opposite to acceleration, calculated from the following formula:

$$F = m \cdot r \cdot \omega^2 \cdot \sin \omega t \tag{4}$$
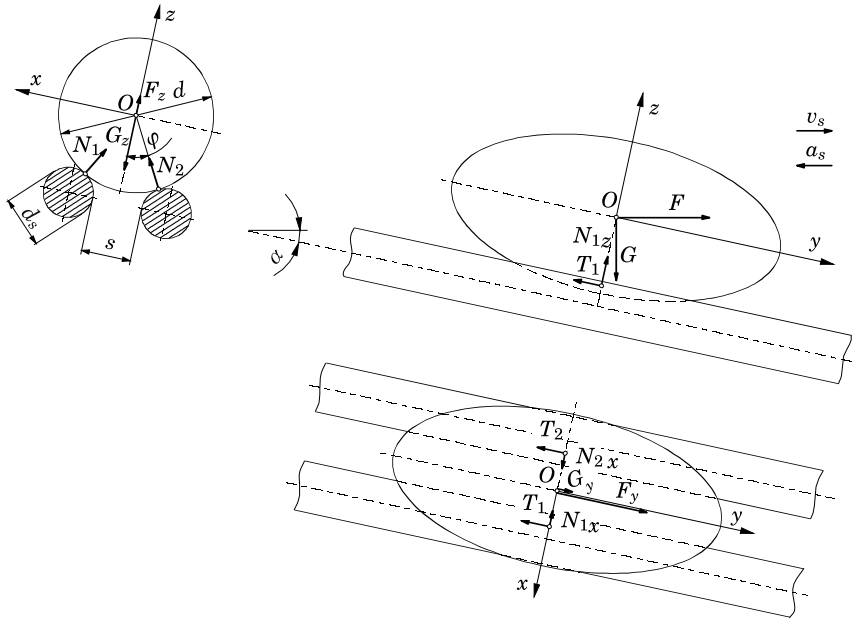
Fig. 2. Distribution of forces acting upon an ellipsoid seed in the first quarter of a string sieve's operating cycle

Gravity force components can be expressed with the use of the below formulas:

$$G_y = m \cdot g \cdot \sin\alpha \tag{5}$$

$$G_z = m \cdot g \cdot \cos\alpha \tag{6}$$

The string's normal ground reaction force was determined based on the below formula:

$$N_1 = N_2 = \frac{G_z - F_z}{2\cos\varphi} = \frac{m \cdot g \cdot \cos\alpha - m \cdot r \cdot \omega^2 \cdot \sin\omega t \cdot \sin\alpha}{2\cos\varphi} \tag{7}$$

Frictional forces counteract the movement of seeds across strings, and in extreme cases, they can reach:

$$T_1 = \mu_s \cdot N_1 = \mu_s \cdot N_2 = T_2 \tag{8}$$

In the critical position of a seed (at the beginning of motion across the screen), frictional forces were projected to the y-axis to produce:

$$-2T_1 + G_y + F_y = 0 \tag{9}$$

Dependencies (8), (7) and (5) were substituted into equation (9), the inertia component was introduced and seed weight was reduced to produce:

$$\frac{\mu_s \cdot g \cdot \cos\alpha - \mu_s \cdot r \cdot \omega^2 \cdot \sin\omega t \cdot \sin\alpha}{\cos\varphi} = g \cdot \sin\alpha + r \cdot \omega^2 \cdot \sin\omega t \cdot \cos\alpha \tag{10}$$

Assuming that seeds should remain in motion at least upon the achievement of extreme delay (at $\omega t = 90°$), equation (10) can be transformed to

$$\mu_s \cdot r \cdot \omega^2 \cdot \sin\alpha + r \cdot \omega^2 \cdot \cos\alpha \cdot \cos\varphi = \mu_s \cdot g \cdot \cos\alpha - g \cdot \sin\alpha \cdot \cos\varphi \tag{11}$$

The above formula can be used to determine the angular velocity or the radius of the crank when the values of the remaining parameters are known. The remaining parameters condition the sliding motion of seeds across the surface of the string sieve, which is a prerequisite for separation. Formula (11) was used to determine the angular velocity of the crank:

$$\omega = \sqrt{\frac{g \cdot (\mu_s \cdot \cos\alpha - \sin\alpha \cdot \cos\varphi)}{r \cdot (\mu_s \cdot \sin\alpha + \cos\alpha \cdot \cos\varphi)}} \tag{12}$$

Angle φ is determined from a geometric function given by KALINIEWICZ (2013d):

$$\varphi = \text{arc} \sin\frac{s + d_s}{d + d_s} \tag{13}$$

Materials and methods

A comprehensive analysis of seed motion across the working surface of a string sieve requires the determination of the physical parameters of selected seed species, including dimensions (length, width, thickness) and the coeffi-

cient of external friction. The studied cereal species were wheat, rye, barley, oats and triticale, which were classified into a homogenous group of cereals. Other seed species (vetch, pea, lupine and faba bean) were analyzed as separate groups. One hundred and twenty seeds of each species were randomly selected for analysis. Oblong seeds which met the set criteria, in particular seeds whose motion was initiated by sliding (KALINIEWICZ 2013b, 2013c), were selected manually. The final sample sizes were as follows: cereals – 600 seeds, vetch – 60 seeds, pea – 46 seeds, lupine – 103 seeds, faba bean – 89 seeds. The length, width and thickness of seeds were determined under the MWM 2325 laboratory microscope, and the coefficient of external friction was determined with the use of a device described by KALINIEWICZ (2013b). The equivalent diameter of seeds was determined.

The results were processed statistically to determine differences between the mean values of geometric parameters and the correlations between equivalent diameters and coefficients of static friction (for a given group of seeds). The results were processed by one-way analysis of variance with a post-hoc test and correlation analysis (LUSZNIEWICZ, SŁABY 2008, RABIEJ 2012).

The analysis was carried out for a sieve with steel strings where the width of the separating groove was set at 1 mm at the beginning of the screen and 11 mm at the end of the screen (KALINIEWICZ 2013a).

Results and Discussion

Seed dimensions and the results of the comparison of the analyzed seed groups are presented in Table 1. In most cases, different results were reported for the examined seed groups (species). Significant differences were not observed only in a comparison of the length of pea seeds and lupine seeds and in a comparison of the coefficients of static friction of pea seeds and cereal seeds. A comparison with other authors' findings (ALTUNTAS, DEMIRTOLA 2007, COBORU 2012, LEMA et al. 2005, RYBIŃSKI et al. 2009, SADOWSKA, ŻABIŃSKI 2011, TASER et al. 2005, YALÇIN, ÖZARSLAN 2004, YALÇIN et al. 2007) indicates that vetch seeds were characterized by low plumpness, faba bean seeds – by medium plumpness, and lupine and pea seeds – by high plumpness. The analyzed seed groups were arranged in the following ascending order based on the average values of the equivalent diameter: cereals, vetch, lupine, pea and faba bean.

KALINIEWICZ (2013b, 2013c) demonstrated that physical dimensions (length, width, thickness), weight, volume, density and shape of seeds do not significantly affect their frictional properties. Similar results were reported during attempts to determine correlations between the seeds' equivalent

Table 1

The results of measurements and statistical calculations of selected physical properties of the analyzed seed groups

Seed group	Physical property	x_{min}	x_{max}	x	SD
Cereals	thickness, mm	1.75	3.41	2.67^e	0.30
	width, mm	1.83	4.40	3.23^e	0.49
	length, mm	5.40	13.70	8.24^b	1.51
	equivalent diameter, mm	1.79	3.81	2.95^e	0.37
	coefficient of static friction	0.23	0.33	0.34^a	0.06
Vetch	thickness, mm	2.60	3.64	3.16^d	0.28
	width, mm	3.42	4.70	4.15^d	0.29
	length, mm	3.63	5.14	4.45^d	0.34
	equivalent diameter, mm	3.13	4.11	3.66^d	0.25
	coefficient of static friction	0.23	0.43	0.30^b	0.04
Pea	thickness, mm	4.73	6.93	6.08^b	0.49
	width, mm	5.71	8.06	7.02^b	0.56
	length, mm	6.56	8.83	7.66^c	0.49
	equivalent diameter, mm	5.35	7.44	6.55^b	0.49
	coefficient of static friction	0.29	0.42	0.34^a	0.03
Lupine	thickness, mm	4.37	6.02	5.15^c	0.35
	width, mm	5.40	7.55	6.33^c	0.43
	length, mm	6.16	8.80	7.58^c	0.51
	equivalent diameter, mm	5.03	6.70	5.74^c	0.34
	coefficient of static friction	0.23	0.36	0.28^c	0.03
Faba bean	thickness, mm	5.55	8.91	7.39^a	0.71
	width, mm	6.55	10.20	8.63^a	0.84
	length, mm	7.38	13.00	10.34^a	1.13
	equivalent diameter, mm	6.05	9.54	8.01^a	0.75
	coefficient of static friction	0.19	0.36	0.22^d	0.03

a, b, c, d, e – values marked with the same letters in the superscript do not differ statistically

diameter and their coefficients of external friction. Significant correlations where the coefficient of correlation exceeded 0.4 were not observed, and the results of the cited studies are not discussed in this analysis. Every seed from a given group can be thus assigned a coefficient of sliding friction from the entire range of values determined for a given cereal species.

In the analyzed string sieve, string diameter was $d_s = 4$ mm (KALINIEWICZ 2013a). Formulas (12) and (13) contain a total of 6 variable parameters. For this reason, only exemplary minimum angular velocities of the crankshaft were presented as a function of one of the parameters, where the value of the remaining parameters was kept constant (Fig. 3). An analysis of changes in the examined parameters indicates that the minimum angular velocity of the crank which is required to set seeds into motion increases rapidly at the place where the width of the working groove becomes equal to the seeds' equivalent diameter, i.e. at the potential screening site. The above results from a rapid
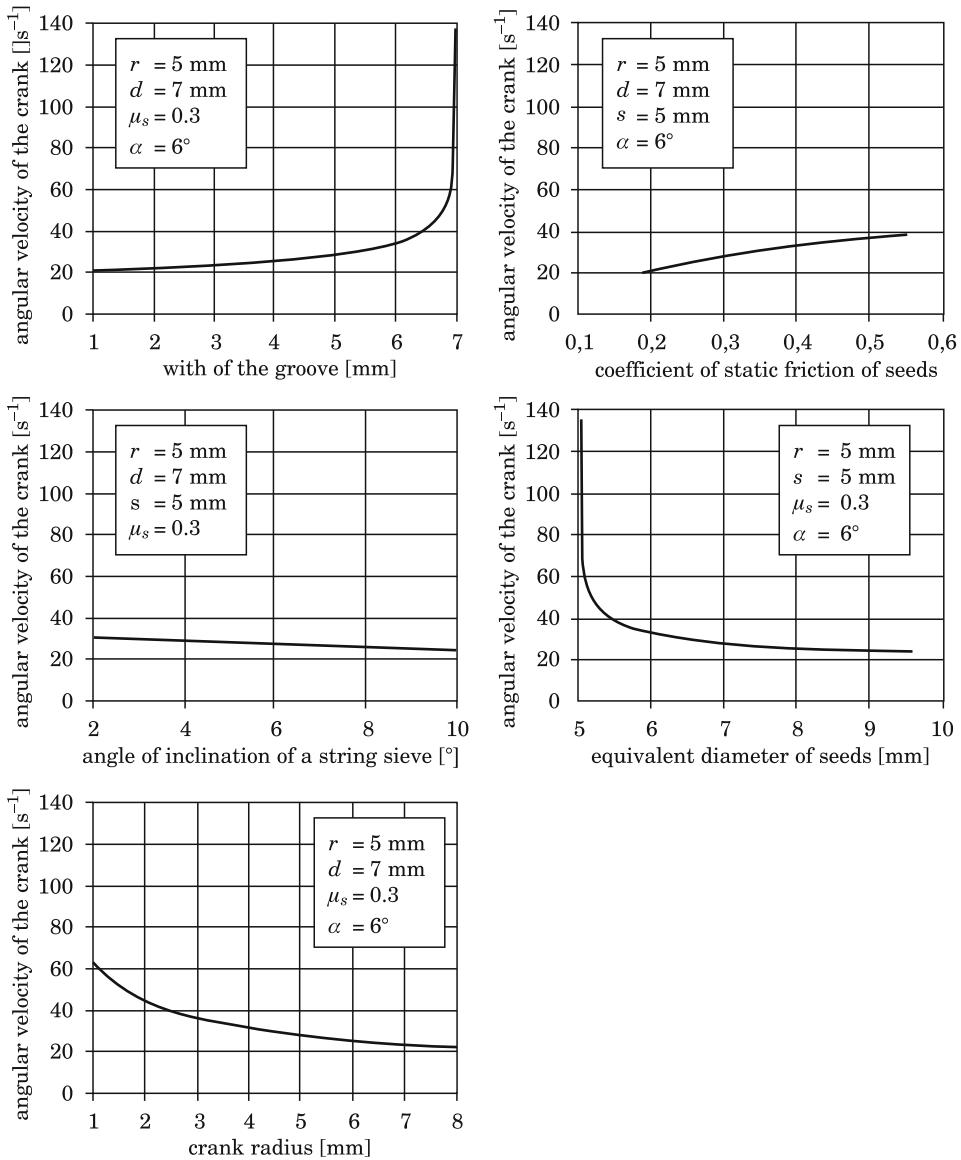
Fig. 3. The correlation between the minimum angular velocity of the crank in a string sieve, structural parameters and seed parameters

increase in normal ground reaction forces, which leads to the formation of powerful frictional forces that counteract seed motion across the screen. The crank radius significantly affects minimum angular velocity which is required to propel seeds into motion. Minimum angular velocity decreases with an

increase in radius, and the higher the crank radius, the slower the decrease in angular velocity. According to published data (GROCHOWICZ 1994), the amplitude of bucket deflections should range from 5 to 12 mm, which implies that the crank should have the radius of 2.5 to 6 mm. To initiate the motion of seeds with a high coefficient of friction, the minimum angular velocity should be nearly twice that required for seeds with a low coefficient of friction. In the analyzed range of constant values, the sieve's angle of inclination does not significantly influence the minimum angular velocity of the crank. Minimum angular velocity decreases with an increase in the angle of inclination, and the noted change is nearly linear.

In the final stage of seed movement, i.e. when seeds reach the location where they pass through the screen, the required crank angular velocity increases rapidly. The equation (12) noted in the potential screening sites are presented in Fig. 4. Within the set range of values of the sieve's inclination angle and crank radius, the angular velocity of the crank can be estimated in the range of 83 to 530 s^{-1}. The above velocities significantly exceed the recommended values. According to GROCHOWICZ (1994), the angular velocity of a crank in a string sieve should range from 30 to 63 s^{-1}. Higher velocities can damage the separator bucket. Even the highest angular velocity values given in literature will not guarantee continuous seed motion, therefore the structure
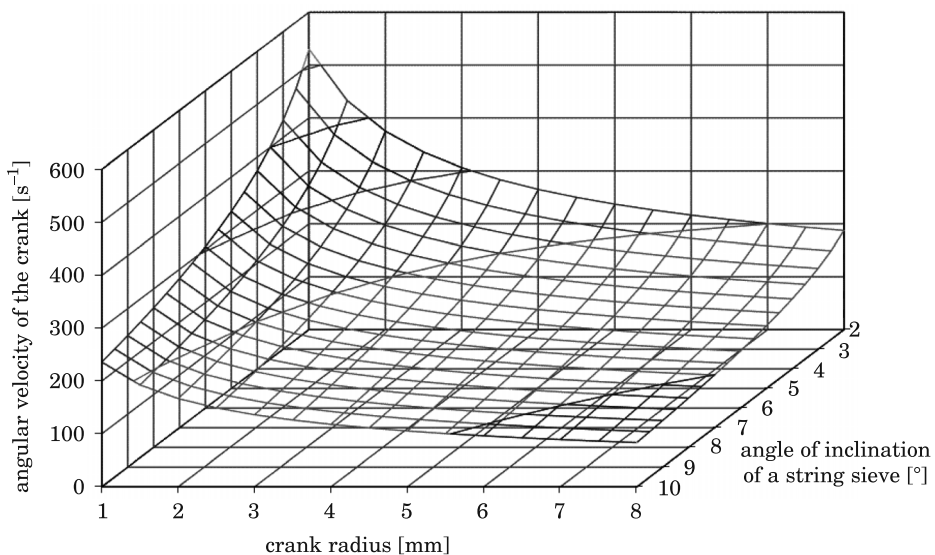

Fig. 4. Diagram illustrating changes in the minimum angular velocity of the crank which enables seeds to pass through the screen, subject to the crank radius and the angle of inclination of the sieve screen

of the string sieve should be modified accordingly. This can be achieved by motion with the use of sweeping brushes, elements that strike the screen or cause it to vibrate, or by equipping the sieve with divergent strings.

Conclusions

The following parameters affect seed movement across the working surface of a string sieve when the separator bucket is set into reciprocating motion: angular velocity of the crank, crank radius, angle of inclination of the separator screen, string diameter, seed size and the seeds' coefficient of external friction. If cereal, vetch, pea, lupine and faba bean seeds are to pass through the screen, the frequency of screen movement has to be significantly higher than that recommended for separator buckets. Thus, the string sieve modeled in this study cannot be used for cleaning and grading of the analyzed seed mixtures because seeds will be jammed between strings even when sieve parameters are set at maximum values within the recommended range. The above problem can be solved by choosing a different transmission system to power the separator bucket, using special brushes to sweep layers of seeds or by equipping the sieve with divergent strings.

References

ALTUNTAS E., DEMIRTOLA H. 2007. *Effect of moisture content on physical properties of some grain legume seeds*. N. Z. J. Crop Hortic. Sci., 35: 423–433.

COBORU 2012. *Wyniki porejestrowych doświadczeń odmianowych. Rośliny strączkowe 2011 (bobik, groch siewny, łubin wąskolistny, łubin żółty, soja)* COBORU, 89, Słupia Wielka.

DOMAGAŁA M. 1976. *Sito strunowe do przesiewania materiałów sypkich o dużym zawilgoceniu*. Urząd Patentowy PRL, opis patentowy nr 85425.

GASTON A.L., ABALONE R.M., GINER S.A. 2002. *Wheat drying kinetics. Diffusivities for sphere and ellipsoid by finite elements*. J. Food Eng., 52: 313–332.

GROCHOWICZ J. 1994. *Maszyny do czyszczenia i sortowania nasion*. Wyd. Akademia Rolnicza, Lublin.

HEBDA T., MICEK P. 2005. *Dependences between geometrical features of cereal grain*. Inżynieria Rolnicza, 6: 233–241 (article in Polish with an abstract in English).

HEBDA T., MICEK P. 2007. *Geometric features of grain for selected corn varieties*. Inżynieria Rolnicza, 5(93): 187–193 (article in Polish with an abstract in English).

KALINIEWICZ Z. 2011. *Sito strunowe*. Urząd Patentowy RP, zgłoszenie patentowe nr P.396745.

KALINIEWICZ Z. 2013a. *Analysis of frictional properties of cereal seeds*. African Journal of Agricultural Research, 8(45): 5611–5621.

KALINIEWICZ Z. 2013b. *A theoretical analysis of cereal seed screening in a string sieve*. Technical Sciences, 16(3): 234–247.

KALINIEWICZ Z. 2013c. *String sieve: design concept and parameters*. Technical Sciences, 16(2): 119–129.

KALINIEWICZ Z. 2013d. *The effect of selected physical attributes of seeds on their frictional properties*. African Journal of Agricultural Research (in press).

LEMA M., SANTALLA M., RODIÑO A.P., DE RON A.M. 2005. *Field performance of natural narrow-leafed lupin from the northwestern Spain*. Euphytica, 144: 341–351.

LEŚKIEWICZ J., KLICH P., FRANASIK K., BORÓWKA E., MORAWSKI T. 1971. *Sito strunowe szczególnie do przesiewania węgla i koksu o dużym zawilgoceniu i zanieczyszczeniach ilastych*. Urząd Patentowy PRL, opis patentowy nr 62380.

LUSZNIEWICZ A., SŁABY T. 2008. *Statystyka z pakietem komputerowym STATISTICA PL. Teoria i zastosowanie*. Wyd. C.H. Beck, Warszawa.

RABIEJ M. 2012. *Statystyka z programem Statistica*. Wyd. Helion, Gliwice.

RAWA T. 1992. *A study of the buckwheat grain clearing effectiveness*. Acta Acad. Agricult. Techn. Ols., Aedif. Mech., 22, Supplementum A (monograph in Polish with an abstract in English).

RAWA T., WIERZBICKI K., PIETKIEWICZ T. 1990. *Potential effectiveness of rape seeds cleaning according to geometrical characteristics*. Acta Acad. Agricult. Tech. Olst. Aedif. Mech., 20: 117–129 (article in Polish with an abstract in English).

RYBIŃSKI W., SZOT B., RUSINEK R., BOCIANOWSKI J. 2009. *Estimation of geometric and mechanical properties of seeds of Polish cultivars and lines representing selected species of pulse crops*. Int. Agrophys., 23: 257–267.

SADOWSKA U., ŻABIŃSKI A. 2011. *Influence of mixed sowing of yellow lupine with gymnosperm barley on the selected physical properties of seeds*. Inżynieria Rolnicza, 6(131): 187–195 (article in Polish with an abstract in English).

SKIRŁO H., SOLIK W., KRAJEWSKI K., BANASZEWSKI T., PAŁASZ M. 1989. *Sito strunowe*. Urząd Patentowy PRL, opis patentowy nr 148250.

TASER O.F., ALTUNTAS E., OZGOZ E. 2005. *Physical Properties of Hungarian and Common Vetch Seeds*. J. Applied Sci., 5(2): 323–326.

WIERZBICKI K., PIETKIEWICZ T., CHOSZCZ D., MAŃKOWSKI S. 1991. *Effectiveness of the wheat grain cleaning process with complex movement of sieve basket*. Acta Acad. Agricult. Techn. Ols., Aedif. Mech., 22: 179–189 (article in Polish with an abstract in English).

WITKOWICZ W., OSTROWSKI F., TOMICZEK M., KOŁODZIEJ H., GRZEŚ L. 1974. *Sito strunowe*. Urząd Patentowy PRL, opis patentowy nr 68591.

WITKOWICZ W., OSTROWSKI F., TOMICZEK M., KOŁODZIEJ H., GRZEŚ L. 1977. *Sito strunowe*. Urząd Patentowy PRL, opis patentowy nr 81731.

YALÇIN İ., ÖZARSLAN C. 2004. *Physical Properties of Vetch Seed*. Biosyst. Eng., 88(4): 507–512.

YALÇIN İ., ÖZARSLAN C., AKBAŞ T. 2007. *Physical properties of pea (Pisum sativum) seed*. J. Food Eng., 79: 731–735.

ŻABIŃSKI A., SADOWSKA U. 2010. *Selected physical properties of the spelt grain*. Inżynieria Rolnicza, 4(122): 309–317 (article in Polish with an abstract in English).

SINGLE-EPOCH PRECISE POSITIONING USING MODIFIED AMBIGUITY FUNCTION APPROACH

Sławomir Cellmer

Institute of Geodesy
Univeristy of Warmia and Mazury in Olsztyn

A b s t r a c t

Single-epoch positioning is a great challenge in recent research related to GNSS data processing. The Modified Ambiguity Function Approach (MAFA) method can be applied to perform this task. This method does not contain a stage of ambiguity resolution. However the final results take into account their integer nature. The functional model of the adjustment problem contains the conditions ensuring the integer nature of the ambiguities. A prerequisite for obtaining the correct solution is a mechanism ensuring appropriate convergence of the computational process. One of such mechanisms is a cascade adjustment, applying the linear combinations of the L1 and L2 signals with the integer coefficients and various wavelengths. Another method of increasing the efficiency of the MAFA method is based on the application of the integer de-correlation matrix to transform observation equations into equivalent, but better conditioned, observation equations. The next technique of improving the MAFA method is search procedure. This technique together with the de-correlation procedure allows to reduce the number of stages of the cascade adjustment and to obtain correct solution even in the case when *a priori* position is a few meters away from the actual position. This paper presents some problems related to search procedure. The results of single-epoch positioning using improved MAFA method are presented.

Introduction

The MAFA method is based on the least squares adjustment (LSA) with condition equations in the functional model of the adjustment problem (CEL-LMER et al. 2010, CELLMER 2012a). This ensures that the condition of the ambiguity 'integerness' is satisfied in the final results. The functional model for the carrier phase adjustment is relatively weak. Therefore different linear combinations (LC) of L1 and L2 GPS carrier phase observations are applied in

---

* Corespondence: Sławomir Cellmer, Instytut Geodezji, Uniwersytet Warmińsko-Mazurski, ul. Oczapowskiego 1, 10-719 Olsztyn, phone: 48 89 524 52 83, e-mail: slawomir.cellmer@uwm.edu.pl

the cascade adjustment so that the appropriate convergence of the computational process can be assured (HAN, RIZOS 1996, JUNG, ENGE 2000). Another method of improving the efficiency of the MAFA method was proposed by CELLMER (2011b). This technique exploits an integer de-correlation procedure. After transformation of the observation equations with an integer de-correlation matrix, a model of an adjustment problem turns into an equivalent model, but a better conditioned one. There are some limitations in applying the MAFA method. CELLMER (2012a) derived the necessary condition for obtaining correct solution with MAFA method. This condition describes the relationship between the accuracy of the *a priori* position and the wavelength of LC forming an observation set. The *a priori* position must be placed inside a certain region around the actual position. Therefore the approximate position in carrier phase process should be as good as possible. The accuracy of the approximate position can be increased using Network Code DGPS Positioning (BAKUŁA 2010). However this accuracy can be still insufficient for MAFA method, even if the de-correlation procedure and the cascade adjustment are applied. Therefore, the search procedure is proposed, as the technique of overcoming this problem. This procedure is based on testing the objective function values for different vectors of misclosures in the functional model of the adjustment problem. This procedure allows obtaining correct solution, even if the *a priori* position is a few meters away from the actual position. The next section presents the theoretical basis of the MAFA method followed by the description of the techniques improving its efficiency. In the third section the search procedure is presented. In the last part of the paper a numerical example, the results of the tests and some conclusions are given.

Theoretical basis of the MAFA method

The following simplified form of the observation equation for double differenced (DD) carrier phase observable is assumed (HOFMANN-WELLENHOF et al 2008, LEICK 2004, TEUNISSEN 1998):

$$\Phi + v = \frac{1}{\lambda}\, \rho(\mathbf{X_c}) + N \tag{1}$$

where:
Φ – DD carrier phase observable (in cycles)
λ – length of the carrier wave
v – residual (measurement noise)

$\mathbf{X_c}$ – receiver coordinate vector
$\rho(\mathbf{X_c})$ – DD geometrical range
N – integer number of cycles (DD initial ambiguity)

Then taking into account the integer nature of the ambiguity parameter N and assuming that the residual values are much lower than half a cycle (HOFMANN-WELLENHOF et al. 2008), the Eq. (1) can be rewritten in the following form:

$$\Phi + v - \frac{1}{\lambda}\,\rho = \text{round}\,(\Phi - \frac{1}{\lambda}\,\rho) \tag{2}$$

or

$$v = \text{round}\,(\Phi - \frac{1}{\lambda}\,\rho) - (\Phi - \frac{1}{\lambda}\,\rho) \tag{3}$$

where round is a function of rounding to the nearest integer value. The residual (3) takes into account the integer nature of ambiguities. The right side of the Eq. (3) can be expressed in the form of the following, differentiable and continuous function (CELLMER 2011b):

$$\Psi = \text{round}(s) - s = \begin{cases} -\dfrac{1}{\lambda}\ \text{arcsin}\ [\sin(\pi s)] \ \text{for}\ s \in \{s : \cos\,(\pi s) \geq 0\} \\[4mm] \dfrac{1}{\lambda}\ \text{arcsin}\ [\sin(\pi s)] \ \text{for}\ s \in \{s : \cos\,(\pi s) < 0\} \end{cases} \tag{4}$$

where s is an auxiliary variable:

$$s = \Phi - \frac{1}{\lambda}\,\rho \tag{5}$$

Each of the nonlinear observation equation for double differenced carrier phase observables is linearized. After linearization, the general formula of the residual equations can be shown in the following form (CELLMER et al. 2010):

$$\mathbf{V} = \frac{1}{\lambda}\,\mathbf{AX} + \Delta \tag{6}$$

with:

$$\mathbf{A} = \begin{bmatrix} \dfrac{\partial \rho_1}{\partial \mathrm{x}} & \dfrac{\partial \rho_1}{\partial \mathrm{y}} & \dfrac{\partial \rho_1}{\partial \mathrm{z}} \\[2ex] \dfrac{\partial \rho_2}{\partial \mathrm{x}} & \dfrac{\partial \rho_2}{\partial \mathrm{y}} & \dfrac{\partial \rho_2}{\partial \mathrm{z}} \\[1ex] \vdots & \vdots & \vdots \\[1ex] \dfrac{\partial \rho_\mathrm{n}}{\partial \mathrm{x}} & \dfrac{\partial \rho_\mathrm{n}}{\partial \mathrm{y}} & \dfrac{\partial \rho_\mathrm{n}}{\partial \mathrm{z}} \end{bmatrix} \tag{7}$$

$$\Delta = round\ (\varPhi - \frac{1}{\lambda}\ \rho) - (\ \varPhi - \frac{1}{\lambda}\ \rho) \tag{8}$$

where:

V – residual vector ($n \times 1$),
X – parameter vector (increments to a priori coordinates vector X_0),
A – design matrix ($n \times 3$),
Δ – misclosure vector ($n \times 1$),
ρ_0 – DD geometric distance vector computed using *a priori* position and satellite coordinates.

The LS solution of the formula (6) is:

$$\mathbf{X} = -\lambda(\mathbf{A^TPA})^{-1}\mathbf{A^TP}\Delta \tag{9}$$

with **P** standing for the weight matrix.

In order to assure the convergence of the computational process to the correct solution, in classic form of MAFA method, three linear combinations (LC) of L1 and L2 GPS carrier phase observables, preserving integer nature of ambiguities and long wavelengths are applied in the cascade adjustment (CELLMER et al. 2010). The efficiency of the MAFA method can be also improved using the de-correlation procedure. The ambiguities (N) are usually strongly correlated. Hence, fixing one value of ambiguity through rounding value *s* in (5) to the nearest integer as in (2), has an impact on the rest of the ambiguities. Therefore, the correlation between ambiguities should be taken into account at rounding the right side of the equation (2) or alternatively the observation equations should be transformed into the equivalent form with de-correlated ambiguities.

Let us assume that **Z** is the integer de-correlation matrix (LIU et al. 1999, TEUNISSEN 1995):

$$\mathbf{Q}_{Nz} = \mathbf{Z}\mathbf{Q}_N\mathbf{Z}^T \tag{10}$$

where:
$\mathbf{Z}$ – integer de-correlation matrix
$\mathbf{Q}_N$ – ambiguity covariance matrix
$\mathbf{Q}_{Nz}$ – diagonal transformed ambiguity covariance matrix.

By multiplying Eq. (1) with $\mathbf{Z}$, one can obtain a new equation with a new integer ambiguity vector $\mathbf{N}_z$:

$$\varPhi_z + \mathbf{V}_z = \frac{1}{\lambda}\,\rho_z(\mathbf{X}_c) + \mathbf{N}_z \tag{11}$$

The above formula can replace equation (1). Further considerations are the same but de-correlated observation equation (11) in the place of equation (1) increases the probability of obtaining the correct solution. The subsequent part of the computation process results from this equation. There are many various methods of finding the $\mathbf{Z}$ decorrelation matrix (HASSIBI, BOYD 1998, JONGE, TIBERIUS 1996, LIU et al. 1999, XU 2001). In order to find the $\mathbf{Z}$ matrix, the ambiguity covariance matrix ($\mathbf{Q}_N$) is required. This matrix can be evaluated on the basis of the system of observation equations (1) after linearization:

$$\mathbf{V} = \mathbf{A}\mathbf{X} + \mathbf{B}\mathbf{N} - \mathbf{L} \tag{12}$$

where:
$\mathbf{L}$ – misclosures (observed minus computed) vector
$\mathbf{B}$ – ambiguity functional model matrix

The covariance matrix of the unknown vector $\mathbf{X}_\Omega = [\mathbf{X}, \mathbf{N}]^T$ can be presented as:

$$\mathbf{C}_{X_\Omega} = \begin{bmatrix} \mathbf{A}^T\mathbf{P}\mathbf{A} & \mathbf{A}^T\mathbf{P}\mathbf{B} \\ \mathbf{B}^T\mathbf{P}\mathbf{A} & \mathbf{B}^T\mathbf{P}\mathbf{B} \end{bmatrix}^1 = \begin{bmatrix} \mathbf{Q}_X & \mathbf{Q}_{XN} \\ \mathbf{Q}_{NX} & \mathbf{Q}_N \end{bmatrix} \tag{13}$$

where:

$$\mathbf{Q}_N = [\mathbf{B}^T\mathbf{P}\mathbf{B} - \mathbf{B}^T\mathbf{P}\mathbf{A}(\mathbf{A}^T\mathbf{P}\mathbf{A})^{-1}\mathbf{A}^T\mathbf{P}\mathbf{B}]^{-1} \tag{14}$$

In the case of the single epoch data, matrix **B** is an identity matrix and $\mathbf{Q}_N$ computed according to formula (17), is not positive definite. It causes difficulties with the de-correlation procedure and leads to incorrect solutions. Therefore, an additional coefficient k is inserted (CELLMER 2011a, 2011b, 2012b):

$$\mathbf{Q}_{Nk} = [\mathbf{P} - k\mathbf{PA}(\mathbf{A}^T\mathbf{PA})^{-1}\mathbf{A}^T\mathbf{P}]^{-1} \qquad (15)$$

The use of the coefficient k is equivalent to the simulation of additional observations, e.g. code observations, as in the generalized least squares model presented in WIELGOSZ (2011). The matrix $\mathbf{Q}_{Nk}$ can be applied to the de-correlation procedure as an approximation of the ambiguity covariance matrix.

Search procedure in MAFA method

In (CELLMER 2012a) the necessary condition for applying MAFA method was described. This condition can be formulated as follows:

$$N = \text{round}(\varPhi - \frac{1}{\lambda}\rho_0) \qquad (16)$$

where:
N – true ambiguity
ρ_0 – DD geometric distance computed using *a priori* position coordinates.

If the above condition is not satisfied then the observation equation (2) takes the following form:

$$\varPhi + v - \frac{1}{\lambda}\rho = \text{round}(\varPhi - \frac{1}{\lambda}\rho) + N_e \qquad (17)$$

with integer N_e.

Hence in place of Eq. (3) and (4) are adequately:

$$v_e = \text{round}(\varPhi - \frac{1}{\lambda}\rho) - (\varPhi - \frac{1}{\lambda}\rho) + N_e \qquad (18)$$

and

$$\Psi_e = \mathrm{round}(s) - s = \begin{cases} -\dfrac{1}{\lambda}\ \mathrm{arcsin}\ [\sin(\pi s)] + N_e \ \text{for}\ s \in \{s : \cos(\pi s) \geq 0\} \\[3mm] \dfrac{1}{\lambda}\ \mathrm{arcsin}\ [\sin(\pi s)] + N_e \ \text{for}\ s \in \{s : \cos(\pi s) < 0\} \end{cases} \tag{19}$$

Based on linearization of the function Ψ_e, the observation equation (6) is rewritten as follows:

$$\mathbf{V} = \frac{1}{\lambda}\ \mathbf{AX} + \Delta_e \tag{20}$$

with the new misclosures vector:

$$\Delta_e = \mathrm{round}(\Phi - \frac{1}{\lambda}\ \rho_0) - (\Phi - \frac{1}{\lambda}\ \rho_0) + \mathbf{N}_e \tag{21}$$

Due to the integer values of the vector $\mathbf{N}_e$ the search procedure is necessary. The search procedure will consist of testing the values of the objective function $\mathbf{V}^T\mathbf{PV}$ for different vectors $\mathbf{N}_e$. It is proposed that the vector $\mathbf{N}_e$ will consist only of the following values -1, 0 and 1. This assumption significantly reduces of the search region. All possible vectors $\mathbf{N}_e$ can be represented by column vectors $\mathbf{e}_i$ forming matrix $\mathbf{E}$. The vectors $\mathbf{e}_i$ consists of the elements -1, 0 or 1 in all possible combinations. Generally the matrix $\mathbf{E}$ can be formed using the following recursive formula:

$$\mathbf{E}_1 = [-1 \quad 0 \quad 1]$$

$$\mathbf{E}_n = \begin{bmatrix} \mathbf{E}_1 \otimes \underset{1\times 3^{n-1}}{\mathbf{1}} \\[3mm] \underset{1\times 3}{\mathbf{1}} \otimes \mathbf{E}_{n-1} \end{bmatrix} \tag{22}$$

where:
$\underset{1\times k}{\mathbf{1}}$ – k-element row vector of ones
$\otimes$ – Kronecker product symbol
n – number of ambiguities.

The dimension of matrix $\mathbf{E}$ is $n \times m$ with the number of columns:

$$m = 3^n \tag{23}$$

The example of the matrix $\mathbf{E}$ for $n = 3$ is:

$$\mathbf{E}_3 = \begin{bmatrix} \text{-1-1-1-1-1-1-1-1-1} \, 0 \, 0 \, 0 \, 0 \, 0 \, 0 \, 0 \, 0 \, 0 \, 1 \, 1 \, 1 \, 1 \, 1 \, 1 \, 1 \, 1 \, 1 \\ \text{-1-1-1} \, 0 \, 0 \, 0 \, 1 \, 1 \, 1 \, \text{-1-1-1} \, 0 \, 0 \, 0 \, 1 \, 1 \, 1 \, \text{-1-1-1} \, 0 \, 0 \, 0 \, 1 \, 1 \, 1 \\ \text{-1} \, 0 \, 1 \, \text{-1} \, 0 \, 1 \, \text{-1} \, 0 \, 1 \, \text{-1} \, 0 \, 1 \, \text{-1} \, 0 \, 1 \, \text{-1} \, 0 \, 1 \, \text{-1} \, 0 \, 1 \, \text{-1} \, 0 \, 1 \, \text{-1} \, 0 \, 1 \end{bmatrix} \tag{24}$$

Each column of the $\mathbf{E}$ matrix is substituted into (21) for $\mathbf{N}_e$ and the criteria $\mathbf{V}^T\mathbf{P}\mathbf{V} = \min$ is tested. The value of $\mathbf{e}_i$ minimizing $\mathbf{V}^T\mathbf{P}\mathbf{V}$ is chosen to final positioning according to formula (9). Delta expression in this equation is calculated by (21) and contains the optimal value of $\mathbf{N}_e$ from the search procedure. Summarizing, the search procedure is based on the misclosure vector modifications followed by the test of the objective function value. The misclosures vector consists of the actual measurements minus predicted measurements. In consecutive tests, the different values of the predicted measurements are substituted taking into account the integer nature of the ambiguities. As it was mentioned in section 2, in classic form of the MAFA method, the three stage cascade adjustment is applied. However due to the search procedure the efficiency is increased and therefore the cascade process can be limited to two stages: only widelane L1-L2 and single L1 observations are employed in the cascade adjustment (definitely both observation sets consist of double differenced observations). The MAFA method together with the search procedure can be used for processing of the observations obtained from a single-epoch.

The processing algorithm in this case will consist of the following stages:
– *a priori* position determination (e.g. using code observations)
– forming double difference of L1, L2, geometric ranges, model matrix $\mathbf{A}$ and weight matrix $\mathbf{P}$
– de-correlation procedure
– search procedure
– final position determination (vector of the coordinates)

When using cascade adjustment two last stages are repeated for each LC. The solution obtained from L1 is assumed as the final position. However as it is shown in the next section, sometimes in the last step of cascade adjustment the criterion of $\mathbf{V}^T\mathbf{P}\mathbf{V}$ minimization can indicate on wrong solution. Therefore, it is proposed to apply search procedure only in the first step of the two-steps cascade adjustment (for L1-L2). This optimal approach was determined on the basis of tests presented in section 5.

Case study – numerical example

The test of the presented algorithm was based on the real data. This example relates to a special case – when a search procedure does not give a correct solution in the final step of cascade adjustment. Taking into account this special case, a general algorithm was modified. The input data are listed in Tables 1 and 2. In the first row of Table 1, the coordinates of an *a priori* position are placed. In the second row, there are coordinates obtained from an 8-hour static session processing using Bernese software (DACH et al. 2007). These values are presented for the purposes of comparison with the single epoch processing results. The first column of the Table 2 contains the design matrix. The second and third columns contain double differenced carrier phase observations of the signals L1 and L2. In the fourth column there are double-differenced geometric distances computed from *a priori* position.

Table 1

A priori and 'true' coordinates

	X [m]	Y [m]	Z [m]
a priori (DGPS)	3,717,669.061	1,254,116.079	5,011,896.056
True	3,717,669.167	1,254,115.775	5,011,894.647

Table 2

Input data

A	DD_L1[cycles]	DD_L2[cycles]	DD_dist [m]
0.039 0.233 -0.048	1,818,996.301	1,096,262.797	-483.100
-0.271 0.102 0.878	-7,995,014.281	-6,203,167.191	-37.579
0.494 -0.524 -0.020	7,721,422.793	5,631,992.707	1,226.360
0.368 0.746 -0.037	8,635,207.515	6,393,878.608	-1,439.328
0.814 -0.680 0.138	-10,839,038.439	-8,774,623.852	1,693.053
-0.055 -0.365 0.300	17,445,922.208	13,280,625.091	825.281

The weight matrix was obtained as an inverse of the LC double differenced carried phase covariance matrix:

$$\mathbf{P} = \mathbf{C}^{-1} \qquad (25)$$

with the following structure of matrix $\mathbf{C}$:

$$\mathbf{C} = m^2\sigma^2 \begin{bmatrix} 4 & 2 & 2 & 2 & 2 & 2 \\ 2 & 4 & 2 & 2 & 2 & 2 \\ 2 & 2 & 4 & 2 & 2 & 2 \\ 2 & 2 & 2 & 4 & 2 & 2 \\ 2 & 2 & 2 & 2 & 4 & 2 \\ 2 & 2 & 2 & 2 & 2 & 4 \end{bmatrix} \tag{26}$$

where:

σ – instrumental accuracy of the carrier phase observation ($\sigma = 0.01$ cycle)
m – LC noise, dependent on LC coefficients ($m^2 = i^2 + j^2$, where $i = 1, j = -1$ for wide lane and $i = 1, j = 0$ for L1 only).

The processing was carried out using MAFA method. A two-step cascade adjustment preceded by de-correlation process was carried out. A search procedure was also applied. The ambiguity covariance matrix was obtained using formula (15) with the coefficient $k = 0.9$. The decorrelation procedure was performed using algorithm of united ambiguity decorrelation (LIU et al, 1999) implemented by the author in Matlab for the purpose of this contribution. As a result of this procedure the following integer transformation matrix was obtained:

$$\mathbf{Z} = \begin{bmatrix} 1 & 0 & 0 & 0 & 0 & 0 \\ 0 & 0 & 0 & 0 & 0 & 1 \\ 0 & 0 & -1 & 0 & 1 & 0 \\ 0 & 0 & 1 & 0 & 0 & 0 \\ -1 & 0 & 1 & 1 & -1 & 1 \\ 1 & 1 & 0 & - & 0 & -2 \end{bmatrix} \tag{27}$$

The results of the search procedure on each stage of the cascade processing are listed in the Table 3.

Table 3

The search procedure results

LC#	Without search		With search		With search on $LC_{1,-1}$ and without search on L1	
	$\mathbf{e}_i$	$\mathbf{V^T PV}$	$\mathbf{e}_i$	$\mathbf{V^T PV}$	$\mathbf{e}_i$	$\mathbf{V^T PV}$
$LC_{1,-1}$	$[0\ 0\ 0\ 0\ 0\ 0]^T$	208.65	$[0\ 0\ 0\ 0\ 0\ -1]^T$	2.18	$[0\ 0\ 0\ 0\ 0\ -1]^T$	2.18
$LC_{1,0}$ = L1	$[0\ 0\ 0\ 0\ 0\ 0]^T$	7.11	$[0\ 1\ 1\ 0\ 1\ 1]^T$	7.11	$[0\ 0\ 0\ 0\ 0\ 0]^T$	7.93

The first column contains the name of linear combinations at each stage of cascade processing. The next two columns contain the results of computations without using search procedure. The fourth and fifth columns concern the scenario of implementing the search procedure in every step of cascade adjustment. The results in the last two columns concern the case of using search procedure only in the first step of cascade adjustment. The columns labeled '$\mathbf{e}_i$' contain the constant vector that must be added to the vector Δ in order to obtain minimum value of $\mathbf{V^T PV}$. Minimum values of $\mathbf{V^T PV}$ relating to $\mathbf{e}_i$ are listed in the columns labeled '$\mathbf{V^T PV}$'.

Table 4 contains the residuals, referenced to the 'true' coordinates at each stage of the cascade processing for three scenarios: without search procedure, with search procedure and with search procedure only on the first stage of cascade adjustment. The graphical representations of the ΔX, ΔY, ΔZ values are depicted in Fig 1. The horizontal axis on the zero level depicts the 'true' value of the coordinates. The blue, red and green lines show the residuals of the coordinates referenced to their 'true' values. In the first scenario (without search procedure) in the first step of cascade adjustment (for $LC_{1,-1}$), the $V^T PV$ value is 208.65, whereas in the second and third scenarios (with search procedure) this value equals 2.18 (for $e_i = [0\ 0\ 0\ 0\ 0\ -1]$).

Table 4

The results of elaboration

LC#	Without search			With search			With search on $LC_{1,-1}$ and without search on L1		
	ΔX	ΔY	ΔZ	ΔX	ΔY	ΔZ	ΔX	ΔY	ΔZ
DGPS	-0.107	0.304	1.410	-0.107	0.304	1.410	-0.107	0.304	1.410
$LC_{1,-1}$	0.070	0.150	0.979	0.007	-0.009	0.026	0.007	-0.009	0.026
$LC_{1,0}$ = L1	0.231	0.182	0.925	0.231	0.182	0.925	-0.008	-0.005	0.002

The residual values (Tab. 4 and Fig. 1) are much lower if using search procedure in the first step of cascade adjustment (for $LC_{1,-1}$). There was a significant improvement as a result of applying the search procedure on this stage of processing. However on final stage of cascade adjustment (for L1) the search procedure gave wrong solution. The correct solution is obtained without search procedure ($\mathbf{e}_i = [0\ 0\ 0\ 0\ 0\ 0]$, $V^T PV = 7.93$) although minimum of $V^T PV$ equals 7.11 (for $\mathbf{e}_i = [0\ 1\ 1\ 0\ 1\ 1]$). The above example shows that criterion: $\mathbf{V^T PV}$ = min can sometimes lead to incorrect solution. Especially when dealing with L1 data. Therefore it is proposed to modify the general algorithm by using search procedure only on the first stage (for $LC_{1,-1}$) of cascade adjustment. Tests presented in the next section confirm this finding.
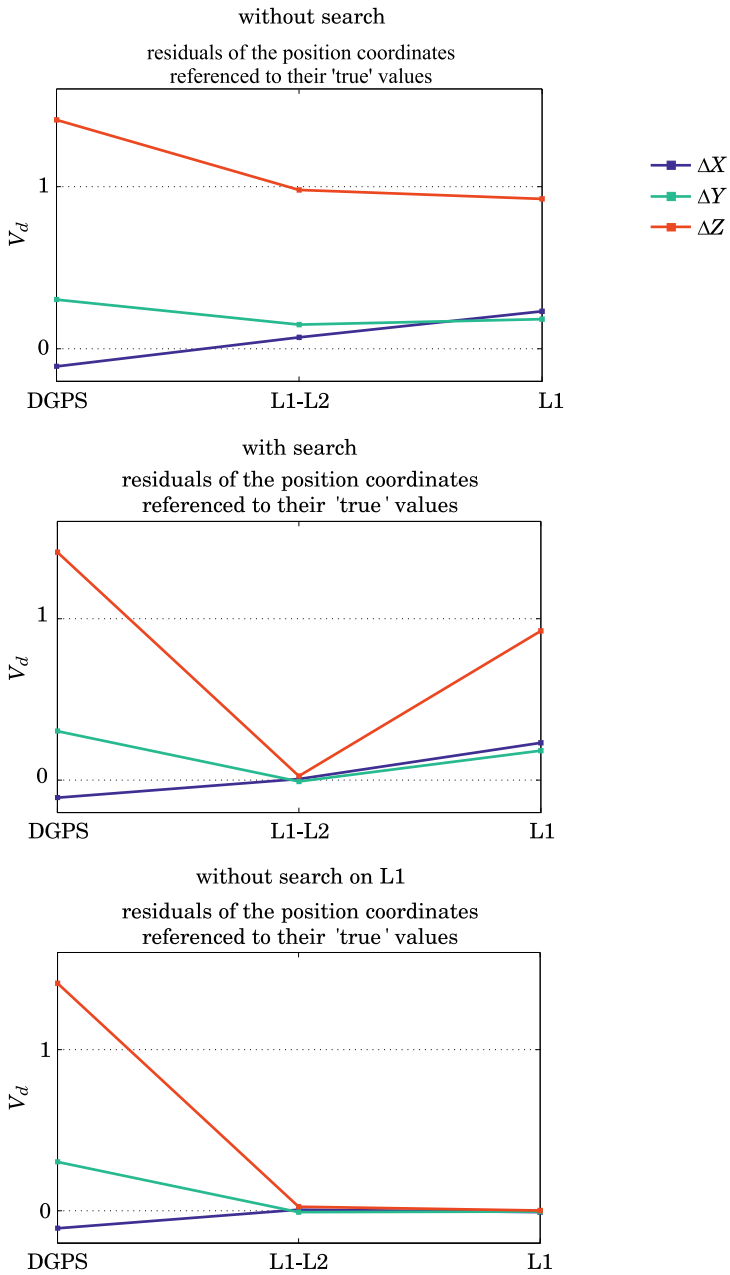
Fig. 1. Residuals of the position coordinates referenced to their 'true' values
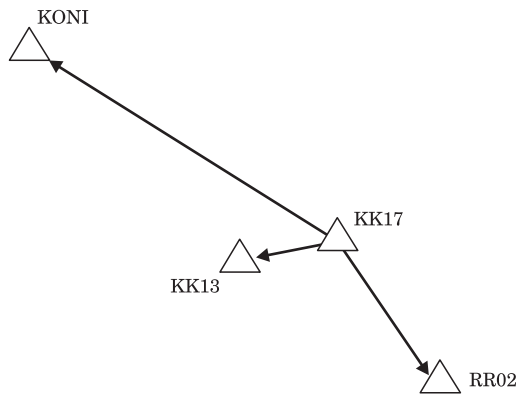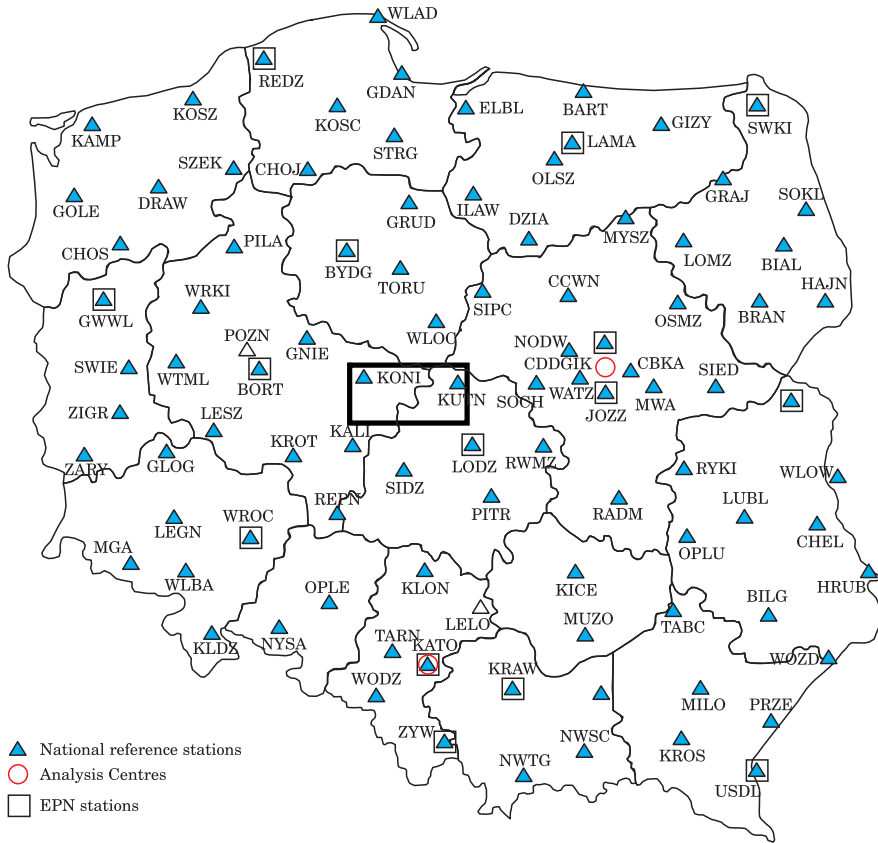
Fig. 2. The location of the test surveys http://www.asgeupos.pl/webpg/graph/dwnld/map_pl_EN.jpg

Experiment design

In order to test the efficiency of the proposed algorithm, the real GPS data of three baselines were used. Tha data come from campaign performed in order to monitor local deformation in open-pit mine 'Adamów' in Central Poland. This project is managed by Dr. Radoslaw Baryła from the Chair of Satellite Geodesy and Navigation of University of Warmia and Mazury in Olsztyn. Figure 2 depicts the location of the surveys. One GPS station of ASG-EUPOS (Polish part of European Positioning System active geodetic network) was used in test surveys ('KONI'). The surveys were performed on December 9th, 2008, on 30.7 km, 10.2 km and 2.1 km baselines, with a 30-second sampling rate. Data sets of each baseline consisted of 120 epochs. The data were processed according to the proposed approach independently for each epoch. The ambiguity covariance matrix was formed according to formula (15), as a basis for the de-correlation procedure. The 'true' coordinates were derived using Bernese software based on an 8-hour data set.

Test results

Figure 3 presents the comparison of the results of 120 single epoch data processing for different scenarios: without search procedure, with search procedure on each stage of cascade adjustment and for scenario with search procedure only on the first stage of cascade adjustment.

The horizontal lines on Fig. 3 depict the linear residuals of the position obtained independently in each epoch using MAFA method, with respect to the 'true' position. The residuals were computed as: $\sqrt{\Delta X^2 + \Delta Y^2 + \Delta Z^2}$, where ΔX, ΔY and ΔZ are components of the residuals with respect to the 'true' position. The blue lines relate to the first scenario (without search procedure), the red lines relate to second scenario (with search procedure on each stage of cascade adjustment) and the green lines relate to third scenario (search procedure only on the first stage of cascade adjustment). In most cases, *a priori* position was farther than 1m from the 'true' position. For each case the percentage of correct solutions is shown in text box. There were 20%–40% correct solutions in first scenario (without search procedure) depending on length of baseline. In second scenario the percentage of correct solutions ranged from 76% to 82%. There has been a significant improvement of the results. Further improvement can be obtained using third scenario of data processing- through applying search procedure only in the first step of cascade adjustment. In this case the percentage of correct solutions reaches even 92%. Summarizing, the number of correct single-epoch solutions using optimal scenario of data processing varied from 85% to 92%.

With search on all

Without search on L1

baseline KK17 – KONI (30.7 km)

baseline KK17 – RR02 (10.2 km)

baseline KK17 – KK13 (2.1 km)

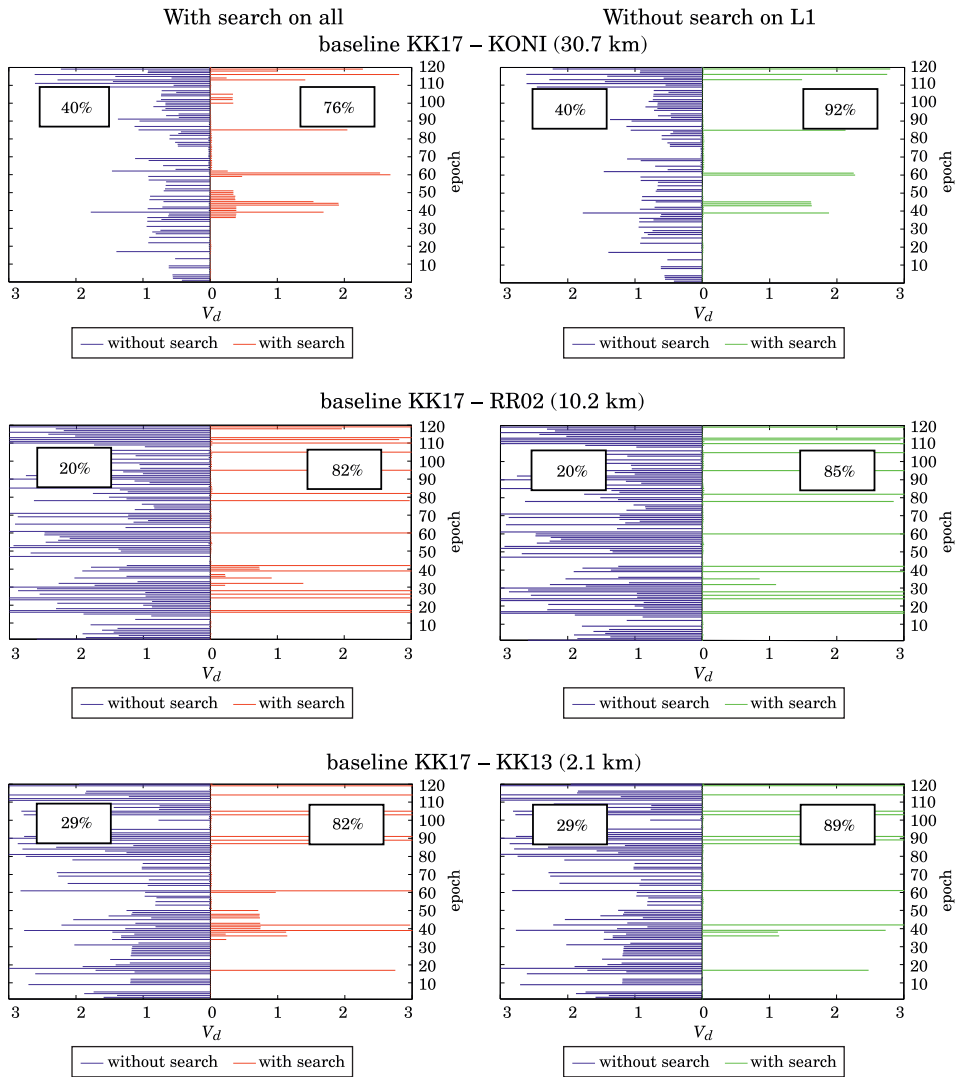Fig. 3. Linear residuals of the final position for three baselines expressed in meters

Conclusions

The MAFA method was improved with implementing a search procedure. The detailed algorithm of such procedure was elaborated and presented in this paper. The computational process allows obtaining precise position even on the basis of only single observational epoch. The results of the tests show the

usefulness of the proposed solutions. The high efficiency of the proposed algorithm was confirmed by tests performed for short and medium baselines (shorter than 30 km).

References

Bakuła M. 2010. *Network Code DGPS Positioning and Reliable Estimation of Position Accuracy*, Survey Review, 42(315): 82–91.

Cellmer S., Wielgosz P., Rzepecka Z. 2010. *Modified ambiguity function approach for GPS carrier phase positioning.* Journal of Geodesy, 84: 267–275.

Cellmer S. 2011a. *The real time precise positioning using MAFA method.* The 8th International Conference ENVIRONMENTAL ENGINEERING, selected papers, III, Vilnius, 1310–1314.

Cellmer S. 2011b. *Using the Integer Decorrelation Procedure to increase of the efficiency of the MAFA Method.* Artificial Satellites, 46(3): 103–110.

Cellmer S. 2012a. *A Graphic Representation of the Necessary Condition for the MAFA Method.* Transactions on Geoscience and Remote Sensing, 50(2): 482–488.

Cellmer S. 2012b. *On-the-fly ambiguity resolution using an estimator of the modified ambiguity covariance matrix for the GNSS positioning model based on phase data.* Artificial Satellites, 47(3): 81–90.

Dach R., Hugentobler U., Fridez P., Meindl M 2007. *BERNESE GPS Software Version 5.0.* Astronomical Institute, University of Berne.

Glenn J., Svedensen G. 2006. *Some properties of decorrelation techniques in the ambiguity space.* GPS Solut, 10: 40–44.

Hassibi A., Boyd S. 1998. *Integer parameter estimation in linear models with application to GPS.* IEEE Trans SignallProc, 46: 2938–2952.

Han S., Rizos C. 1996. *Improving the computational efficiency of the ambiguity function algorithm.* Journal of Geodesy, 70(6): 330–341.

Hofmann-Wellenhof B., Lichtenegger H., Wasle E. 2008. *GNSS-Global Navigation Satellite Systems – GPS, GLONASS, Galileo & more*, Springer-Verlag Wien.

Jung J., Enge P. 2000. *Optimization of Cascade Integer Resolution with Three Civil GPS Frequencies* Proc. ION GPS'2000, Salt Lake City, September.

Jonge P. De., Tiberius Ch. 1996. *The LAMBDA method for integer ambiguity estimation: implementation aspects* Delft Geodetic Computing Centre LGR Series.

Leick A. 2004. *GPS Satellite Surveying.* 3rd edition, John Wiley and Sons, Inc.

Liu L.T., Hsu H.T., Zhu Y.Z., Ou J.K. 1999. *A new approach to GPS ambiguity decorrelation.* Journal of Geodesy, 73: 478–490.

Teunissen P. J.G. 1995. *The least-squares ambiguity decorrelation adjustment: a method for fast GPS integer ambiguity estimation*, Journal of Geodesy, 70: 65–82.

Teunissen P.J.G., Kleusberg A. 1998. *GPS for Geodesy*, (selected papers of Intenational School lectures) Springer – Verlag, Berlin Heidelberg New York.

Wielgosz P. 2011. *Quality assessment of GPS rapid static positioning with weighted ionospheric parameters in generalized least squares.* GPS Solutions, 15(2): 89–99.

Xu P. 2001. *Random simulation and GPS decorrelation.* Journal of Geodesy, 75: 408–423.

INTERRELATIONS BETWEEN SELECTED PHYSICAL AND TECHNOLOGICAL PROPERTIES OF WHEAT GRAIN

Małgorzata Warechowska[1], *Józef Warechowski*[2], *Agnieszka Markowska*[1]

[1] Chair of Foundations of Safety
[2] Chair of Process Engineering and Equipment
University of Warmia and Mazury in Olsztyn

A b s t r a c t

The aim of this work was to determine selected physical properties of wheat grain which are of significance in transport, separation and storage processes as well as to assess the correlations between them and the technological properties of wheat.

The grain of two wheat varieties (Eta and Banti) which are popular in Poland was used as research material. The tested properties included: vitreousness, test weight, thousand kernel weight, true density, geometric parameters (thickness, width, length), static friction coefficient of wheat kernels against steel and glass, protein and gluten content and the Zeleny sedimentation value.

The grain of the investigated wheat varieties differed in most physical and technological properties. The average length, width and thickness kernels were 6.31 mm, 3.31 mm and 3.03 mm for vr. Banti and 6.05 mm, 3.33 mm, 2.97 mm for vr. Eta. The test weight ranged from 75.68 (Banti) to 78.29 $kg \cdot hl^{-1}$ (Eta), the thousand kernel weight from 36.3 (Eta) to 39.2 g (Banti) and vitreousness was from 13 (Banti) to 81% (Eta).

A correlation between the physical and technological properties of wheat was found. The vitreousness of the wheat grain was positively correlated with protein content (the correlation indices were 0.58 for Banti variety and 0.67 for Eta) and the volume was positively correlated with the true density of grain (r = -0.69 Eta, r = -0.64 Banti). The static coefficient of the friction of wheat grains of two structural materials (metal or glass) is insufficient to predict its technological properties.

Symbol list
m_1 – pycnometer mass with toluene [g],
m_2 – pycnometer mass with toluene and grain on a scale [g],
m_3 – pycnometer mass with toluene and grain in pycnometer [g],
ρ_{tl} – toluene density [$g \cdot cm^{-3}$],
ρ_g – single grain specific mass [$g \cdot cm^{-3}$],
V_g – grain volume [mm^3],
V – variability [%],

---

* Corespondence: Małgorzata Warechowska, Katedra Podstaw Bezpieczeństwa, Uniwersytet Warmińsko-Mazurski, ul. Heweliusza 10, 10-719 Olsztyn, phone/fax: +48 89 524 56 13

L   – length [mm],
W   – width [mm],
T   – thickness [mm],
TW – test weight [kg · hl⁻³],
TKW– thousand kernel weight [g],
KV   – kernel virtuousness [%],
PC   – protein content [%],
TD   – true density [g · cm⁻³],
GC   – gluten content [%],
SV   – Zeleny sedimentation value [ml].

Introduction

In transport, the separation and storage processes of the physical properties of grain mass and single kernels are of great significance. Knowledge of important physical properties such as mass density, test weight, internal angle of friction and static coefficient of friction is necessary to design various separating, handling, storing systems (HORABIK 2001). The static coefficient of friction is used to determine the angle at which chutes must be positioned in order to achieve a consistent flow of materials through the chute. Single grain properties, such as shape, linear sizes and volume, should also be considered for optimizing technological processes (GRUNDAS 2004, KHEIRALIPOUR et al. 2008, MOHSENIN 1986). Grain geometrical properties are of special significance during the separation and removal of impurities. Cereal transport, purification, drying and storage are operations in which grain quality changes may occur (MARKOWSKI et al. 2006, AL-MAHASNEH, RABABAH 2007, MARKOWSKI et al. 2007, SYPUŁA, DADRZYŃSKA 2008).

Grain quality is characterized based on indicators of storage durability and technological value such as: moisture, falling number, gluten and protein content and the Zeleny sedimentation value (DELWICHE 1998, RACHOŃ et al. 2011). Since grain processing requires increasingly stringent standards for raw material quality, it has become imperative to identify the correlations between physical and technological properties to develop better methods for grain quality assessment (ZAPOTOCZNY 2009). Knowledge of these correlations may find application in designing and monitoring technological processes in the cereal-milling industry (DZIKI, LASKOWSKI 2005).

The physical properties of wheat grain at different moisture levels were tested by TABATABAEEFAR (2003), AL-MAHASNEH, RABABAH (2007), KARIMI et al. (2009). An increasing moisture content was found to increase axial dimensions, mass of 1000 kernels, kernel volume and static friction coefficient, while decreasing bulk density, true density and porosity.

The correlation between the physical and technological properties of cereal grain was tested by DZIKI, LASKOWSKI (2002), who found a significant correla-

tion between the test weight and grain shape factor. The correlations between physical and technological properties were also investigated by Różyło, Las-kowski (2007a, 2007b), who found correlations between hardness index and grain squeeze strength for durability threshold and Zeleny sedimentation value, protein and gluten content. The protein content of the grain was significantly correlated to the hardness of the grain. Thus, vitreous kernels are usually harder and have a higher protein content than the non-vitreous (starchy) kernels (Symons et al. 2003). A positive correlation between hardness index and protein content was also observed by Różyło et al. (2003) and Konopka et al. (2005).

Wheat grain physical properties are essential in transport, separation and storage processes. These properties include specific density, bulk density and friction angle against construction materials. Knowledge of the correlations between physical and technological properties of wheat grain is important for designing and optimizing the processing stages. There is insufficient information on this subject in the literature.

The aim of the study was to determine selected physical and technological properties of wheat grain and investigate the correlations between them.

Materials and Methods

The kernels of spring wheat varieties (Eta and Banti) used in this study were procured from the Experimental Station of the University of Warmia and Mazury in Olsztyn, in north- eastern Poland (Tomaszkowo; 53°73'N 20°41'E).

The sample was cleaned and pooled together to obtain approximately 20 kg samples of each variety. The initial moisture content of seeds was determined by ICC Standard No. 110/1. The physical properties of wheat grain were determined with a moisture content in the range of 8.2–9.9%. All measurements were taken using at least 30 replications.

Thousand kernel weight (TKW) was measured for each variety using an electronic kernel counter (Kernel Counter LN S 50A, UNITRA CEMI) and an electronic balance WPE 120 Radwag (PN-68/R-74017). The grain test weight was also determined (PN-ISO 7971-2:1998). The vitreousness of grain was evaluated based on an analysis of the cross-sections of kernels and expressed as the percentage of vitreous kernels in a sample of 50 elements. The partially vitreous kernels were classified as semi-vitreous kernels and their number in the sample was multiplied by 0.5 (PN-70/R-74008). The static friction coefficient was determined with respect to different surfaces: steel and glass. The sample was then placed on a slab and the inclination angle was slowly increased. At the moment of movement, the angle was read from the scale and

the friction coefficient was calculated according to the following formula (SHARMA et al. 2011):

$$\mu = \tan(\alpha) \tag{1}$$

where μ is the coefficient of friction and α is the angle of tilt in degrees.

The kernels were measured along the three principal axial dimensions, i.e. length (L), width (W) and thickness (T), using an electronic caliper (Limit company) ($\Delta = \pm 0.05$ mm). True density and volume were measured for singular kernels using a 25 cm³ volume pycnometer and an analytical balance (AS 110/C/2 Radwag). The true density was determined using the toluene displacement method in order to avoid absorption of water during the experiment (JHA 1999, COSKUNER, KARABABA 2007). The true density and volume measurements were taken at 20°C. The results of measurements of pycnometer mass with toluene (m_1), pycnometer mass with toluene and grain on a weighing pan (m_2), and pycnometer mass with toluene and grain in pycnometer (m_3) were used to calculate the grain true density according to the following formula (2):

$$\rho_z = \frac{m_2 - m_1}{m_2 - m_3} \tag{2}$$

Grain volume was calculated as:

$$V = \frac{m_2 - m_3}{\rho_{tl}} \tag{3}$$

Kernel density measurement was performed in 100 replications for each variety and the technological properties of the grain were also determined. Protein and gluten content and Zeleny sedimentation value measurements were taken with the near-infrared method (NIR) on an Inframatic 8100 apparatus.

Statistical analysis of the results was performed and a variation analysis was made with STATISTICA for Windows v. 10 (StatSoft Inc.) software. The significance of differences was determined with a Tukey test. Linear correlation coefficients were calculated along with the variability coefficient as a standard deviation and the average value quotient. Statistical hypothesis were tested at the significance level $\alpha = 0.05$.

Results and Discussion

The kernels of each wheat variety differed significantly for most of the physical and technological properties (Table 1). The test weight, an important parameter of wheat technological value, was significantly correlated with wheat variety.

Table 1

Physical and technological properties of spring wheat grain

Feature		BANTI				ETA			
		mean	min.	max	V [%]	mean	min.	max	V [%]
TW [kg · hl⁻¹]		75.68[a]	74.4	76.8	0.8	78.29[b]	76.8	80.0	1.0
Static friction coefficient of wheat kernels [–]	steel	0.42[a]	0.40	0.47	3.1	0.43[b]	0.41	0.46	2,2
	glass	0.27[a]	0.25	0.29	2.7	0.28[b]	0.26	0.30	2.4
TKW [g]		39.2[b]	35.75	45.64	4.7	36.3[a]	33.42	37.96	2.8
KV [%]		13[a]	7	20	23.4	81[b]	61	90	8.9
L [mm]		6.31[b]	5.7	7.15	5.9	6.05[a]	5.5	6.7	4.1
W [mm]		3.31[a]	2.80	3.80	8.2	3.33[a]	2.85	3.85	6.3
T [mm]		3.03[a]	2.55	3.65	7.9	2.97[a]	2.60	3.25	5.1
V_g [mm³]		36.8[a]	22.7	57.8	26.2	34.8[a]	23.0	57.7	24.5
TD [g · cm⁻³]		1.250[a]	1.038	1.731	16.8	1.281[a]	1.040	1.739	17.9
PC [%]		13.1[a]	12.3	13.9	4.0	13.6[b]	11.5	14.6	5.9
GC [%]		27[a]	25	28	2.5	28[b]	23	30	4.5
SV [ml]		19[a]	10	28	27.6	42[b]	26	61	20.0

a, b – differences of values in lines marked with the same letters are insignificant at $\alpha = 0.05$.

The static coefficient of friction is important for designing storage bins, hoppers, pneumatic conveying systems, threshers, forage harvesters, etc. (SHARMA et al. 2011). The static coefficient of friction, which affects the design of the processing machine, was determined based on two different contacting materials (steel sheet, glass). The static coefficient of friction is higher for steel sheet than for glass. It was demonstrated that the static coefficient of friction of wheat kernels on two surfaces was higher for wheat Eta variety (0.43 steel sheet; 0.28 glass). KHEIRALIPOUR et al. (2008) showed that this coefficient of wheat grains increased linearly against the surface of three structural materials (0.33–0.4 for glass, 0.46–0.55 for plywood and 0.34–0.54 for galvanized iron).

Thousand kernel weight is one of the basic indices of sowing potential and commodity quality of cereals and indicates the ripeness of grain. The statistical evaluation indicated the statistically significant influence of the variety and

a Banti vr. (39.2) had the highest thousand kernel weight of all the analyzed varieties.

The average length, width and thickness kernels were 6.31 mm, 3.31 mm and 3.03 mm for vr. Banti and 6.05 mm, 3.33 mm, 2.97 mm for vr. Eta. Significant differences were observed in kernel length between wheat varieties. The true density value of wheat vr. Eta (1.281 g · cm³) was higher than that of wheat vr. Banti (1.250 g · cm⁻³). Grain was characterized by a high variability of volume ($V = 24.5\%$ for Eta and 26.2% for Banti vr.) and Zeleny sedimentation value (respectively $V = 20\%$ and 27.6%).

Only such geometrical parameters as width, thickness and volume were comparable for each variety. There were no significant differences in the true density of kernels between the analyzed wheat varieties.

An analysis of the obtained results found a correlation between the physical and technological properties of wheat grain. The vitreousness of the investigated samples was between 13% and 81%. This property is dependent on protein content (Table 2). The correlation indices were 0.58 for Banti vr. and 0.67 for Eta vr. A significant positive correlation of grain protein content with vitreousness was reported by EL-KHAYAT et al. (2003), EL-KHAYAT et al. (2006), MARTINEZ et al. (2005), FIGIEL et al. (2011), RÓŻYŁO, LASKOWSKI (2007a). It was found that wheat of higher vitreousness also had a higher protein content.

The influence of protein content on other physical properties was not as clear as in the case of virtuousness. There were weak negative correlations between protein content and the test weight of wheat ($r = -0.39$), but only for the Eta variety. A significant negative correlation between grain protein content and test weight was reported by MATSUO and DEXTER (1980) and RHARRABTI et al. (2003), while a positive correlation was reported by SCHULER et al. (1995). A significant positive correlation was observed between grain protein content and the static coefficient of friction of wheat kernels on glass ($r = 0.54$) for vr. Banti. For vitreous variety (Eta), as in other studies (RÓŻYŁO and LASKOWSKI 2007a), a significant correlation between virtuousness and gluten content was observed ($r = 0.50$).

The relationship between Zeleny sedimentation value and grain physical properties is unclear for all varieties. A correlation between Zeleny sedimentation value and the static coefficient of friction of wheat kernels on glass ($r = -0.55$) and vitreousness for the Banti variety ($r = -0.61$) was observed. For Eta vr., a correlation between sedimentation volume and test weight ($r = 0.50$) and thousand kernel weight ($r = 0.39$) was observed.

The correlations between the physical properties of investigated grain wheat types are shown in Table 2. A statistical analysis of the results showed a significant correlation between test weight and the static friction coefficient of wheat kernels on glass. The correlation coefficients were $r = -0.46$ and

Table 2

Values of linear correlation coefficients between physical and technological properties of wheat

Variety	Feature			PC	GC	SV	Static friction coefficient of wheat kernels		TKW	KV	TD	W	T	V_g
							steel	glass						
Banti	TW			-0.18	-0.02	0.17	-0.20	-0.46*	0.73*	-0.38*	-0.36			
	Static friction coefficient of wheat kernels	steel		-0.02	0.02	-0.05		0.23	-0.06	0.05	-0.02			
		glass		0.54*	0.25	-0.55*			-0.55*	0.56*	0.13			
	TKW			-0.27	-0.16	0.19				-0.35	-0.44*			
	KV			0.58*	0.14	-0.61*					0.15			
	TD			0.06	0.05	0.11						0.06	-0.13	-0.64*
	L										-0.05	0.58*	0.68*	0.59*
	W												0.56*	0.51*
	T													0.66*
Eta	TW			-0.39*	0.01	0.50*	0.13	-0.56*	0.42*	-0.26	0.17			
	Static friction coefficient of wheat kernels	steel		0.09	0.27	0.31		-0.07	-0.16	0.45*	0.25			
		glass		0.19	-0.11	-0.33			-0.50*	0.19	0.05			
	TKW			-0.28	0.01	0.39*				-0.41*	-0.13			
	KV			0.67*	0.50*	-0.15					0.12			
	TD			-0.11	-0.04	0.22						0.06	-0.04	-0.69*
	L										0.05	0.16	0.41*	0.34
	W												0.39*	0.16
	T													0.38*

* Significant correlation coefficients at $p < 0.05$

r = -0.56 for Banti and Eta varieties, respectively. With the increase in test weight, the static coefficient of friction on glass decreased. The basic factors that affect the test weight of wheat are kernel size and shape and kernel density (POMERANZ 1964). Positive correlations between test weight and thousand kernel weight were also observed. Stronger correlations were demonstrated for a variety of larger grains (r = 0.73). A correlation between thousand kernel weight and static coefficient of friction for glass was also found (the correlation coefficients were -0.55 and -0.50 for Banti and Eta varieties, respectively).

A comparison of the physical properties for investigated cereal grains indicates that correlation coefficients values are relatively small, which is not good for determining regression equations with a high degree of explained variability.

A correlation between volume and true density of grain (r = -0.69 Eta, r = -0.64 Banti) was also found (Table 2) as well as between basic linear sizes of wheat grain. These correlations were not as significant as those reported by other authors (HEBDA, MICEK 2005, 2007). The strongest correlation was calculated for grain length and thickness (r = 0.68 and r = 0.41 for vr. Banti and vr. Eta respectively). HEBDA and MICEK (2005) found the strongest correlation between the length and width of the grains.

Conclusions

The studied wheat varieties differed in most physical and technological properties. An analysis of the obtained results found correlations between the physical features and technological properties of the grain:

1. Banti variety wheat had significantly longer grains than Eta variety wheat.

2. Grain vitreousness is positively correlated with grain protein content.

3. The static friction coefficients for glass and steel are not useful for determining grain technological properties.

4. Test weight increased linearly with a thousand kernel weight increase. Stronger correlations were found for a variety of larger grains.

5. The higher the volume of wheat grain for Banti and Eta varieties is, the lower the true density will be.

References

AL-MAHASNEH M.A., RABABAH T.M. 2007. *Effect of moisture content on some physical properties of green wheat.* Journal of Food Engineering, 79: 1467–1473.

COSKUNER Y., KARABABA E. 2007. *Physical properties of coriander seeds (Coriandrum sativum L.).* Journal of Food Engineering, 80: 408–416.

DELWICHE S.R. 1998. *Protein Content of Single Kernels of Wheat by Near-Infrared Reflectance Spectroscopy.* Journal of Cereal Science, 27: 241–254.

DZIKI D., LASKOWSKI J. 2002. *Wpływ wielkości ziarna na wybrane właściwości pszenicy.* Inżynieria Rolnicza, 5: 337–344.

DZIKI D., LASKOWSKI J. 2005. *Wheat kernel physical properties and milling process.* Acta Agrophysica, 6(1): 59–71.

EL-KHAYAT H.G., SAMAAN J., BRENNAN C.S. 2003. *Evaluation of vitreous and starchy Syrian durum (Triticum durum) wheat grains: the effect of amylose content on starch characteristics and flour pasting properties.* Starch, 55: 358–365.

EL-KHAYAT H.G., SAMAAN J., MANTHEY F.A, FULLER M. P., BRENNAN C.S. 2006. *Durum wheat quality I: some physical and chemical characteristics of Syrian durum wheat genotypes.* International Journal of Food Science and Technology, 41 (Sup. 2): 22–29.

FIGIEL A., SPYCHAJ R., GIL Z., BOJARCZUK J. 2011. *Właściwości mechaniczne ziarna polskiej pszenicy twardej.* Inżynieria Rolnicza, 9(134): 23–30.

GRUNDAS S. 2004. *Charakterystyka właściwości fizycznych ziarniaków w kłosach pszenicy zwyczajnej triticum aestivum L.* Acta Agrophysica, 102(2).

HEBDA T., MICEK P. 2005. *Zależności pomiędzy właściwościami geometrycznymi ziarna zbóż.* Inżynieria Rolnicza, 6: 233–241.

HEBDA T., MICEK P. 2007. *Cechy geometryczne ziarna wybranych odmian zbóż.* Inżynieria Rolnicza, 5(93): 187–193.

HORABIK J. 2001. *Charakterystyka właściwości fizycznych roślinnych materiałów sypkich istotnych w procesach składowania.* Acta Agrophysica, 54.

ICC Standard No. 110/1: *Determination of Moisture Content of Cereals and Cereal Products.*

JHA S.N. 1999. *Physical and hygroscopic properties of Makhana.* Journal of Agricultural Engineering Research, 72: 145–150.

KARIMI M., KHEIRALIPOUR K., TABATABAEEFAR A., KHOUBAKHT G.M., NADERI M., HEIDARBEIGI K. 2009. *The Effect of Moisture Content on Physical Properties of Wheat.* Pakistan Journal of Nutrition 8(1): 90–95.

KHEIRALIPOUR K., KARIMI M., TABATABAEEFAR A., NADERI M., KHOUBAKHT G., HEIDARBEIGI K. 2008. *Moisture-Depend Physical Properties of Wheat (Triticum aestivum L.).* Journal of Agricultural Technology 53: 53–64.

KONOPKA I., ROTKIEWICZ D., TAŃSKA M. 2005. *Wheat endosperm hardness.* Part II. *Relationships to content and composition of flour lipids.* European Food Research and Technology, 220: 20–24.

MARKOWSKI M., KONOPKA I., CYDZIK R., KOZIROK W. 2006. *The effect of air temperature on the kinetics of drying and the quality of dried malting barley.* Annual Review of Agricultural Engineering, 5(1): 41–49.

MARKOWSKI M., SOBIESKI W., KONOPKA I., TAŃSKA M., BIAŁOBRZEWSKI I. 2007. *Drying Characteristics of Barley Grain Dried in a Spouted-Bed and Combined IR-Convection Dryers.* Drying Technology, 25(10): 1621–1632.

MARTINEZ M.C., RUIZ M., CARRILLO J.M. 2005. *Effects of different prolamin alleles on durum wheat quality properties.* Journal of Cereal Science, 41: 123–131.

MATSUO R.R., DEXTER J.E. 1980. *Relationship between some durum wheat physical characteristics and semolina milling properties.* Canadian Journal of Plant Science, 60(1): 49–53.

MOHSENIN N.N. 1986. *Physical Properties of Plant and Animal Materials*. 2nd ed. Gordon and Breach Science Publishers, New York.

PN-ISO 7971-2:1998. *Ziarno zbóż. Oznaczanie gęstości w stanie zsypnym zwanej „masą hektolitra".*

PN-70/R-74008. *Ziarno zbóż. Oznaczanie ziarn szklistych.*

PN-68/R-74017. *Ziarno zbóż i nasiona strączkowe jadalne. Oznaczanie masy 1000 ziarn.*

POMERANZ Y. 1964. *Wheat Chemistry and Technology*, St. Paul, Minnesota. American Association of Cereal Chemists.

RACHOŃ L., SZUMIŁO G., STANKOWSKI S. 2011. *Porównanie wybranych wskaźników wartości technologicznej pszenicy zwyczajnej (triticum aestivum ssp. vulgare), twardej (triticumdurum) i orkiszowej (triticum aestivum ssp. spelta).* Fragmenta Agronomica, 28(4): 52–59.

RHARRABTI Y., VILLEGASB D., ROYOB C., MARTOS-NÚÑEZA V., GARCÍA DEL MORAL L.F. 2003. *Durum wheat quality in Mediterranean environments.* II. *Influence of climatic variables and relationships between quality parameters.* Field Crops Research, 80: 133–140.

RÓŻYŁO R., LASKOWSKI J., GRUNDAS S. 2003. *Badania zależności indeksu twardości i energochłonności rozdrabniania od zawartości białka w pszenicy.* Acta Agrophysica, 2(1): 173–178.

RÓŻYŁO R., LASKOWSKI J. 2007a. *Analiza zależności pomiędzy fizycznymi i technologicznymi właściwościami ziarna pszenicy jarej.* Acta Agrophysica, 9(2): 459–470.

RÓŻYŁO R., LASKOWSKI J. 2007b. *Wpływ właściwości pszenicy jarej na wodochłonność mąki.* Acta Agrophysica, 9(3): 755–765.

SCHULER S.F., BACON R.K., FINNEY P.L., GBUR E.E. 1995. *Relationship of test weight and kernel properties to milling and baking quality in soft winter wheat.* Crop Science, 35(4): 949–953.

SHARMA V., DAS L., PRADHAN R.C., NAIK S.N., BHATNAGAR N., KUREEL R.S. 2011. *Physical properties of tung seed: an industrial oil yielding crop.* Industrial Crops and Products, 33(2): 440–444.

SYMONS S.J., VAN SCHEPDAEL L., DEXTER J.E. 2003. *Measurement of hard vitreous kernels in durum wheat by machine vision.* Cereal Chemistry, 80: 511–517.

SYPUŁA M., DADRZYŃSKA A. 2008. *Wpływ czasu przechowywania ziarna pszenicy na zmianę jego cech jakościowych.* Inżynieria Rolnicza, 1(99): 371–376.

TABATABAEEFAR A. 2003. *Moisture-dependent physical properties of wheat.* International Agrophysics, 17: 207–211.

ZAPOTOCZNY P. 2009. *Dyskryminacja odmian ziarna pszenicy na podstawie cech geometrycznych.* Inżynieria Rolnicza, 5(114): 319–328.

ESTIMATION OF COVARIANCE PARAMETERS FOR GNSS/LEVELING GEOID DATA BY LEAVE-ONE-OUT VALIDATION

Wojciech Jarmołowski

Department of Satellite Geodesy and Navigation
University of Warmia and Mazury in Olsztyn

A b s t r a c t

The article describes the estimation of covariance parameters in Least Squares Collocation (LSC) by Leave-One-Out (LOO) validation, which is often considered as a kind of cross validation (CV). Two examples of GNSS/leveling (GNSS/lev) geoid data, characterized by different area extent and resolution are applied in the numerical test. A special attention is focused on the noise, which is not correlated in this case. The noise variance is set to be homogeneous for all points. Two parameters in three covariance models are analyzed via LOO, together with a priori noise standard deviation, which is a third parameter.

The LOO validation finds individual parameters for different applied functions i.e. different correlation lengths and a priori noise standard deviations. Diverse standard deviations of a priori noise found for individual datasets illustrate a relevance of applying LOO in LSC. Two examples of data representing different spatial resolutions require individual noise covariance matrices to obtain optimal LSC results in terms of RMS in LOO validation. The computation of appropriate a priori noise variance is however difficult via typical covariance function fitting, especially in the case of sparse GNSS/leveling geoid data. Therefore LOO validation may be helpful in describing how the a priori noise parameter may affect LSC result and a posteriori error.

List of abbreviations

LSC   – least squares collocation
LOO   – leave-one-out validation
ECF   – empirical covariance function
CV   – cross-validation
GNSS/lev – GNSS/leveling geoid height

* Corespondence: Wojciech Jarmołowski, Katedra Geodezji Satelitarnej i Nawigacji, Uniwersytet Warmińsko-Mazurski, ul. Heweliusza 5, 10-724 Olsztyn, Poland, Phone: + 48 89 523 47 64, Fax + 48 89 523 47 23, e-mail: wojciech.jarmolowski@uwm.edu.pl

SSH   – sea surface heights
C_0 – signal variance parameter in covariance model
δn – a priori noise standard deviation in covariance model
CL   – correlation length in covariance model
CG   – Gaussian covariance model
CGM2   – Gauss-Markov second order covariance model
CGM3   – Gauss-Markov third order covariance model
RMS   – root mean square
RMSL   – root mean square in leave-one-out validation

Introduction

GNSS/leveling (GNSS/lev) data provide an independent source of geoid height information, aside from the gravity data. Both sources may be used to calculate the same functional of disturbing potential with comparable accuracy. However, the spatial resolution of GNSS/lev is usually worse than gravity data sampling. Therefore a special attention is focused in the article on the relation of the horizontal data distribution with the modeling accuracy. GNSS/lev data constitute irreplaceable source of geoid information, used most frequently for an assessment of local gravimetric models (DARBEHESHTI, FEATHERSTONE 2010, ILIFFE et al. 2003, SMITH, MILBERT 1999), global geopotential models (ŁYSZKOWICZ 2009) or also models based on satellite gradiometry (GODAH, KRYŃSKI 2011). GNSS/lev is also frequently used in the combination with gravity or other data in local geoid or quasigeoid modeling (OSADA et al. 2005, TROJANOWICZ 2012). GNSS/lev data provide the information on the local relation between leveling heights and geometric ellipsoidal heights, which is especially useful before the unification of height systems at the global scale. The combination of GNSS with the locally matched geoid is still a common practice in height determination with GNSS (DAWIDOWICZ 2012). The combination of GNSS and leveling heights may be sometimes used alone, as the only source of geoid information, which is compatible with the local height system. This is also applicable in surveying, for dense data and small areas.

Many authors use Least Squares Collocation (LSC) for modeling of the GNSS/lev data or residuals of GNSS/lev and other data (DARBEHESHTI, FEATHERSTONE 2009, DENKER 1998, SMITH, MILBERT 1999). Some authors analyze the efficiency of other methods for GNSS/lev geoid modeling, but use LSC for the validation purposes (KAVZOGLU, SAKA 2005). LSC is also frequently applied in the investigations closely related to geoid or heights in general, i.e.: sea surface heights (SSH) derived from the satellite altimetry

(ANDERSEN, KNUDSEN 1998), vertical crustal movements (EL-FIKY et al. 1997, KOWALCZYK et al. 2010), gravity anomalies (CATALAO, SEVILLA 2009) or deflections of the vertical (ŁYSZKOWICZ 2010a, ŁYSZKOWICZ 2010b). The spectrum of LSC applications is wide, which may be caused by the fact that the covariance in LSC may be modeled in detail and a posteriori error estimates may be calculated. A very frequent method of the covariance estimation is the selection of the analytical model based on the empirical covariance function (ECF) values (HOFMANN-WELLENHOF, MORITZ 2005, MORITZ 1980). There are many practical examples of different numerical techniques of fitting the analytical model into empirical covariance values (ARABELOS, TSCHERNING 2003, DARBEHESHTI, FEATHERSTONE 2009, SMITH, MILBERT 1999). The planar covariance models are often investigated as well, as the spherical models. The standard deviation of a priori noise (δn) is hard to determine using ECF, however YOU, HWANG (2006) have noted its significant role among the covariance parameters. They have also found that different parameters may have an influence on the prediction error in terms of cross-validation (CV) error. The problem of the parameter estimation occurs in the context of combined geoid modeling (FOTOPOULOS et al. 2003) and in the regularization of gravity field from satellite gradiometry (KUSCHE, KLEES 2002). DARBEHESHTI and FEATHERSTONE (2009) apply the non-stationarity for better representation of the local covariance. Among different considerations, the most closely related research has been found in JEKELI, GARCIA (2002), in MARCHENKO et al. (2003) and in MORITZ (1980). They investigate similar problem of optimal covariance matrix by applying Tikhonov regularization parameter. In this paper the problem is treated numerically using a kind of CV. LOO provides some additional observations, which introduces a look from some other side than it is presented in the mentioned works.

The most probable covariance parameters are investigated in this work and a special emphasis is placed on spatially sparse data distribution, which is common in e.g. vertical movements data (EL-FIKY et al. 1997) or deflections of the vertical (ŁYSZKOWICZ 2010a, ŁYSZKOWICZ 2010b). Two datasets of GNSS/lev are used in the numerical test: sparse regional data and significantly denser local data. Three typical, planar covariance models are applied to compare estimates of the same parameters applied in different functions. Two covariance function parameters: correlated signal variance (C_0) and correlation length (CL) are analyzed in the work, together with δn parameter. The method used for the empirical assessment of the parameters is a frequently used form of CV, named leave-one-out validation (LOO) (ARLOT, CELISSE 2010, KOHAVI 1995, KUSCHE, KLEES 2002).

LOO validation applied in LSC

The scalar quantity distributed in 2D space may be represented by the addition of deterministic part and residuals of the signal (MORITZ 1980, RAO, TOUTENBURG 1995). In our case we have:

$$\mathbf{N} = \mathbf{X}\boldsymbol{\beta} + \mathbf{N}^r \tag{1}$$

where $\mathbf{N}$ is the vector of observed geoid heights, $\boldsymbol{\beta}$ is the vector of unknown trend parameters and $\mathbf{X}$ is the design matrix of the trend. Different forms of the deterministic part of the signal are often used in practice (GREBENITCHARSKY et al. 2005, OSADA et al. 2005). Deterministic part of the signal is commonly called trend in many papers. This part of the signal approximates large-scale features of the stochastic field, commonly known as long-wavelength part of the signal in the spectral analysis. The trend removal extracts local properties of the data, occuring at higher spatial resolutions. The matrix $\mathbf{X}$ used for detrending of the data in the case of current test reads:

$$\mathbf{X} = \begin{bmatrix} 1 & \varphi_1 & \lambda_1 & \varphi_1{}^2 & \lambda_1{}^2 & \varphi_1\lambda_1 \\ \dots & \dots & \dots & \dots & \dots & \dots \\ 1 & \varphi_n & \lambda_n & \varphi_n{}^2 & \lambda_n{}^2 & \varphi_n\lambda_n \end{bmatrix} \tag{2}$$

where n is the number of the observations. Such parametric form of the trend is based on the data distribution and is sufficient to obtain the residuals, which have expected value close to zero and can be modeled efficiently by the covariance function. The so-called projection matrix $\mathbf{P}$ is used for data detrending (RAO, TOUTENBURG 1995):

$$\mathbf{P} = \mathbf{I}_n - \mathbf{X}(\mathbf{X}^T \mathbf{X})^{-1} \mathbf{X}^T \tag{3}$$

Some authors have reported that a linear dependency in the matrix $\mathbf{P}$ exists for the number of rows equal to the rank of $\mathbf{X}$ (KITANIDIS 1983, RAO, TOUTENBURG 1995). If we denote the rank of the matrix $\mathbf{X}$ by p, we may remove p rows from $\mathbf{P}$ matrix. Since p number has no significance in relation to the whole set here, we compute $\boldsymbol{\Lambda}$ matrix by removing last p rows from $\mathbf{P}$. The residuals can be computed, as follows:

$$\mathbf{N}^r = \boldsymbol{\Lambda}\mathbf{N} \tag{4}$$

where $\boldsymbol{\Lambda} = \mathbf{P}_{(n-p)\times n}$. The LSC equation for detrended GNSS/lev data reads:

$$\tilde{\mathbf{N}}^r = \mathbf{C}_P^T \cdot (\mathbf{C} + \mathbf{D})^{-1} \cdot \mathbf{N}^r \tag{5}$$

where $\tilde{\mathbf{N}}^r$ is the vector of predicted, residual values. $\mathbf{C}$ is the covariance matrix of the data signal, $\mathbf{C}_P$ is the covariance matrix between predicted points and the data and $\mathbf{D}$ represents the noise covariance matrix. In this case, when we investigate average estimates of a priori noise, the noise is assumed to be homogeneous and uncorrelated, i.e.:

$$\mathbf{D} = \delta n^2 \cdot \mathbf{I}_n \tag{6}$$

where δn represents a priori noise standard deviation, homogeneous for all points in the example test. The studies can be extended to individual data noise values, however this implies weighting and therefore more detail information on the data noise is needed.

Three planar covariance models are applied in the numerical experiment. The choice of the models was arbitrary in some sense, but on the other hand, these models appear in the literature in the same context or even with the same or similar data related to the height system problems. The models are: Gaussian model (DARBEHESHTI, FEATHERSTONE 2009, YOU, HWANG 2006), Gauss-Markov second order model (ANDERSEN, KNUDSEN 1998, ILIFFE et al. 2003, STRYKOWSKI, FORSBERG 1998) and Gauss-Markov third order model (GREBENITCHARSKY et al. 2005, KAVZOGLU, SAKA 2005). The functional covariance models are described by Eq. (7) – Gaussian (CG), Eq. (8) – Gauss-Markov second order (CGM2) and Eq. (9) – Gauss-Markov third order model (CGM3).

$$\mathrm{CG}(C_0,\ CL,\ s) = C_0 \cdot \exp\left(\frac{-s^2}{CL^2}\right) \tag{7}$$

$$\mathrm{CGM2}(C_0,\ CL,\ s) = C_0 \left(1 + \frac{s}{CL}\right) \cdot \exp\left(\frac{-s}{CL}\right) \tag{8}$$

$$\mathrm{CGM3}(C_0,\ CL,\ s) = C_0 \left(1 + \frac{s}{CL} + \frac{s^2}{3 \cdot CL^2}\right) \cdot \exp\left(\frac{-s}{CL}\right) \tag{9}$$

Although spherical distance is a typical variable in the spherical covariance models e.g. Tscherning-Rapp model (ARABELOS, TSCHERNING 2003, HOFMANN-WELLENHOF, MORITZ 2005), it is adopted here to work as a variable in the planar models (Eqs 7–9). This choice is based on the assumption of no advantage coming from cartographic projection, since the area of the regional data is large and the distortion can be significant. The variable distance s is

therefore calculated using the spherical distance formula (Eq. 12), also in the ECF and $s = \psi$ in the article.

The collocation formula (Eq. 5) is applied in CV test by LOO (Eq. 10). This method is quite frequently applied in the literature (DARBEHESHTI, FEATHERSTONE 2009, KUSCHE, KLEES 2002), but other, often similar kind of CV may be also efficient. The formula of root mean square (RMS) in LOO (RMSL) may be written as:

$$\text{RMSL}((C_0,\ CL,\ \delta n)\mid(\tilde{\mathbf{N}}^r_{n\times 1},\ \mathbf{N}^r_{n\times 1})) = \sqrt{\frac{\sum\limits_{i=1}^{n}(\tilde{N}^r_i - N^r_i)^2}{n}}\ \mid N^r_i \notin \mathbf{N}^r_{(n\text{-}1)\times 1} \quad (10)$$

The vector $\tilde{\mathbf{N}}^r$ estimated using Eq. (5) is compared to $\mathbf{N}^r$ in terms of RMS and this is repeated for every set of covariance parameters. The vector of the residuals $\mathbf{N}^r$ is replaced by the vector $\mathbf{N}^r_{(n\text{-}1)\times 1}$ in the Eq.(5), i.e. the analyzed point i is omitted in the vector as well as in the matrices $\mathbf{C_P}$, $\mathbf{C}$ and $\mathbf{D}$. RMSL is a measure of prediction precision with variable parameters. Additionally the estimates of a posteriori error are provided in the numerical part of the article. Assuming now that $\mathbf{C_P}$ is the vector of covariances limited to one point only, the error of the prediction is (HOFMANN-WELLENHOF, MORITZ 2005):

$$m_P^2 = C_0 - \mathbf{C}_P^T \cdot (\mathbf{C} + \mathbf{D})^{-1} \cdot \mathbf{C}_P \quad (11)$$

The estimation of covariance parameters by LOO validation is preceded and supported by ECF estimation. ECF provides an initial assessment of the residual data and an approximation of C_0 and CL. These initial values support a search of the parameters in LOO estimation and may be posteriorly compared with LOO results. ECF may be calculated by well-known formula (HOFMANN-WELLENHOF, MORITZ 2005):

$$\forall(i,j)\ \mid \cos\psi = \cos\theta_i\ \cos\theta_j + \sin\theta_i\ \sin\theta_j\ \cos(\lambda_i - \lambda_j)$$

$$\text{EC}(\psi\mid\mathbf{N}^r) = \frac{\sum\limits_{i,j}^{k} N^r_i N^r_j}{k} \quad (12)$$

The spherical distance is used as a variable and $\theta_i = \pi/2 - \varphi_i$. The products of residuals are grouped using rings of constant width, which is determined by the sampling interval of the ECF. Average products form the ECF, which is
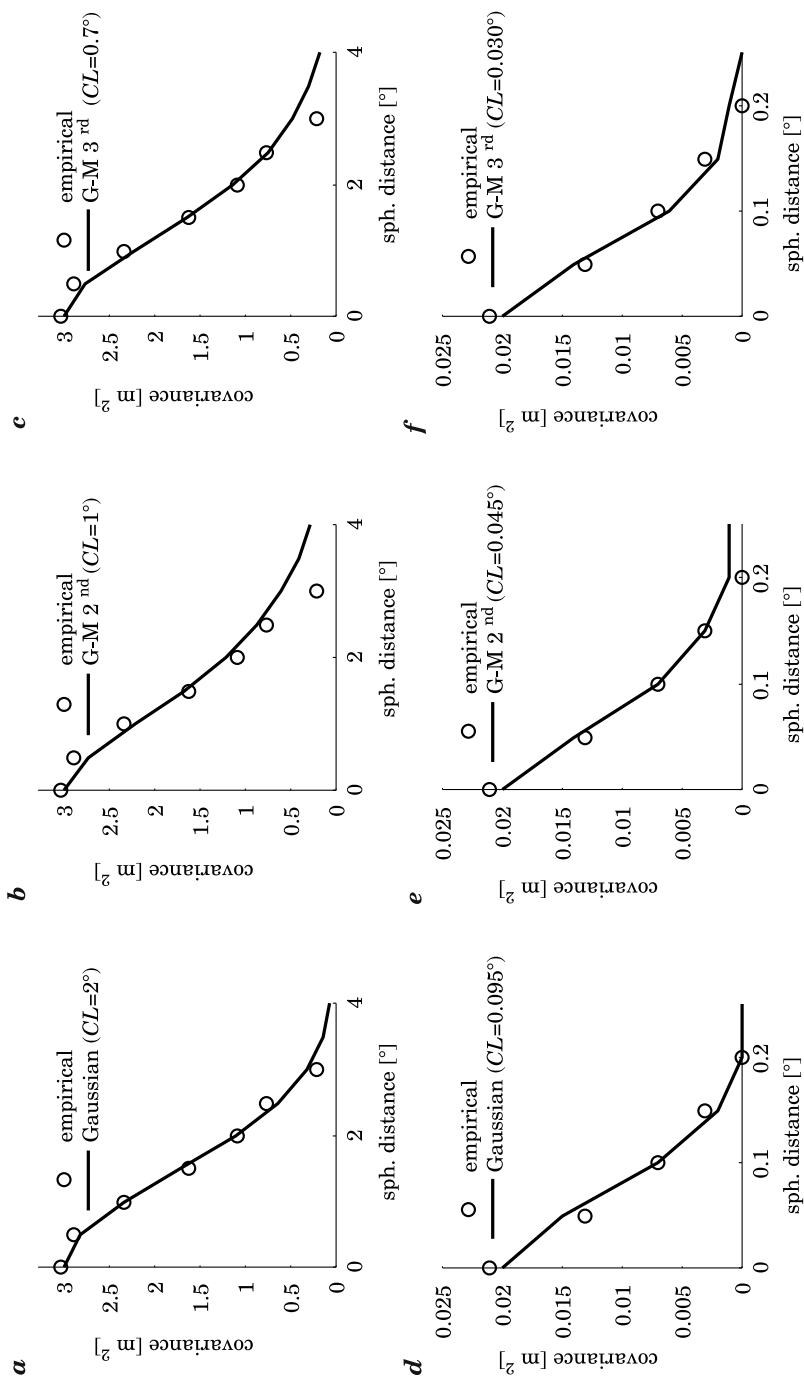
Fig. 1. ECFs of residuals and analytical covariance models fitted graphically disregarding δn: a – regional CG, b – regional CGM2, c – regional CGM3, d – local CG, e – local CGM2, f – local CGM3

shown in Figure 1. Analytical covariance models (Eqs 7–9) are approximately fitted to ECF by graphical manipulation of C_0 and CL, which are roughly determined this way.

Data assessment and numerical experiment

The data are acquired from the National Geodetic Survey website. GNSS/lev geoid heights are located in the area of the North America. Two subsets are selected from the data and the first set is slightly reduced to obtain homogeneous horizontal distribution (Fig. 2c). The first set of GNSS/lev geoid heights (Fig. 2a) covers a large area in the western part of the continent and therefore will be named regional dataset in further considerations. The second dataset (Fig. 2b) represents much smaller area in Texas and consequently
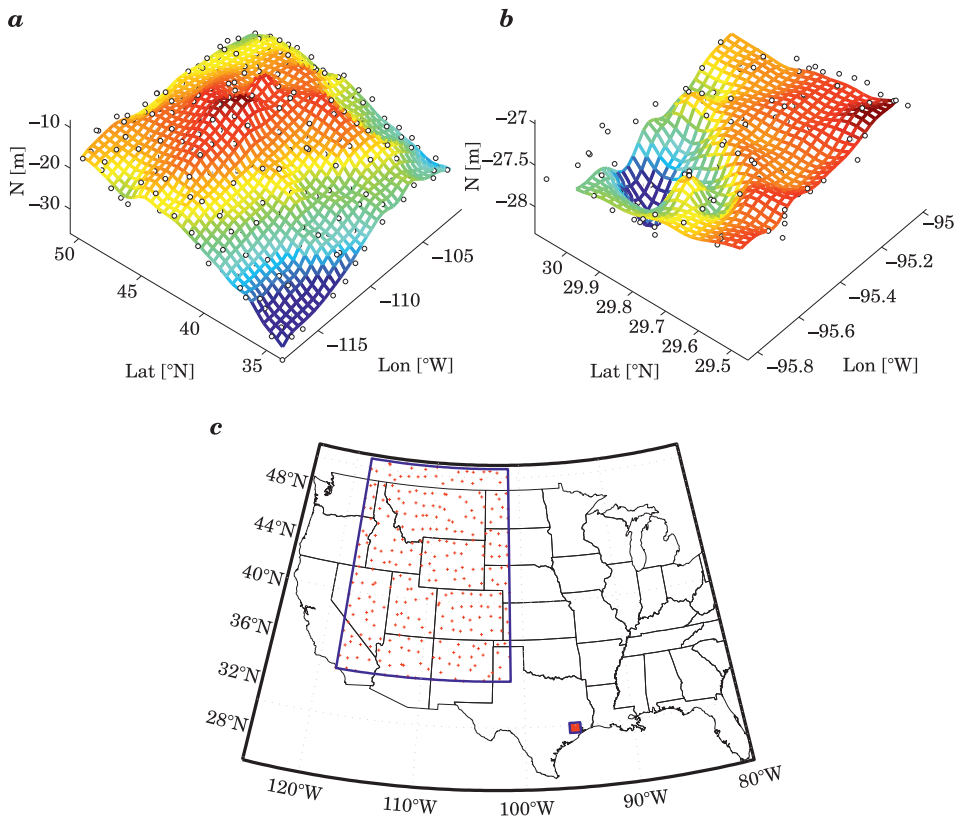

Fig. 2. Selected GNSS/lev samples representing regional and local GNSS/leveling geoid data: *a* – regional geoid (meters), *b* – local geoid (meters)

Table 1

Basic statistics of regional and local data samples (meters)

	Regional (287 points)	Reg. residual	Local (139 points)	Loc. residual
Min.	-36.01	-3.71	-28.32	-0.66
Max.	-8.14	5.04	-26.95	0.27
Mean	-18.60	0.00	-27.41	0.00
Median	18.02	-0.04	-27.35	0.01
RMS	19.26	1.74	27.41	0.14
Std dev.	5.01	1.74	0.26	0.14

is named local dataset. The regional data are reduced to have very sparse distribution with average data spacing about 1° in latitude and similarly in longitude. The local data are denser, i.e. around 0.05° in latitude and longitude. Moreover, the local data are slightly more irregularly spaced than the regional data. There are no evident outlying observations in the datasets, therefore larger observed errors are assumed as random ones.

Numerical calculations were performed using ellipsoidal coordinates, starting from the data detrending (Eq. 2–4). Both datasets were reduced by the polynomial trend of the second order (Eq. 2). ECF is computed for both residual datasets, according to the Eq. (12). The sampling interval of ECF represented by the interval of ψ cannot be significantly smaller than average minimum distance between the data points. Otherwise, we would search for the covariances at the distances that occur only occasionally between data points and the estimation accuracy will be poor for ECF at small distances. Three functional models are graphically compared to ECF values (Eq. 12) and different CL parameter is found for each covariance model (Fig. 1). At this moment C_0 is assumed to be equal to the variance of the residuals and constant for all covariance models. ECF estimation is an additional, separate tool for the covariance parameters estimation and it is used for the further comparisons with LOO estimation. It should be noted, that δn is not estimated by the fitting of analytical model. The values of the empirical covariance may strongly depend on the sampling interval. Therefore one should be careful in assessing δn by fitting the analytical model into the empirical covariance samples, which have arbitrarily chosen interval. Some authors find a priori noise empirically, e.g. iteratively searching for the consistency between a priori noise variance and RMS in CV (SMITH, MILBERT 1999). Some others use a priori noise based on the observational accuracy (DENKER 1998). The proposed method is based on the minimum RMSL in the space of three covariance parameters.

Besides the ECF computation for initial assessment of the parameters, an additional data are prepared for the comparisons and discussion. Geoid height

residuals are computed using the harmonic expansion of EGM2008 geopotential model. The two applied terrestrial datasets represent significantly different area sizes and spatial resolutions. The spatial resolution of the local data is around 5–10 km, which may be approximately comparable with the resolution of EGM2008 geopotential model with its maximum harmonic expansion degree (PAVLIS et al. 2012). The spatial resolution of regional data is around 100 km, which corresponds approximately to 180 degree and order of the harmonic expansion. Therefore the residual geoid signal is calculated using EGM2008 coefficients for the area of regional data (Fig. 3). These residuals represent the spectrum of the geoid between 180 and 2190 degree and order and show significant variance in the area of regional data. The measurement accuracy of GNSS/lev data is usually at the centimeter level and therefore is insignificant in relation to the signal in Figure 3, which can be lost in LSC due to limited resolution. The corresponding residuals for the local data are not computed,
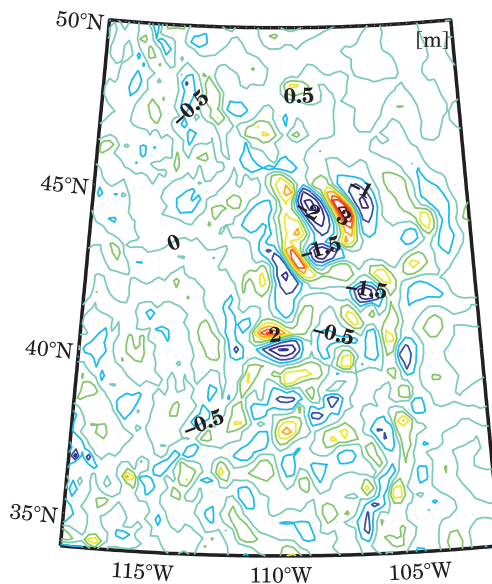

Fig. 3. Residual geoid from EGM2008 model equal $N_{2190} - N_{180}$ (area of regional dataset)

because there are no degrees in EGM2008 supplying more than local data resolution. On the other hand, geoid height residuals at the frequency higher than $0.05°$ may have the variance comparable to or less than GNSS/lev measurement error (RAPP 1973).

Two sets of residual data are interpolated with use of three above mentioned covariance models. LOO is performed as an iterative LSC process, which
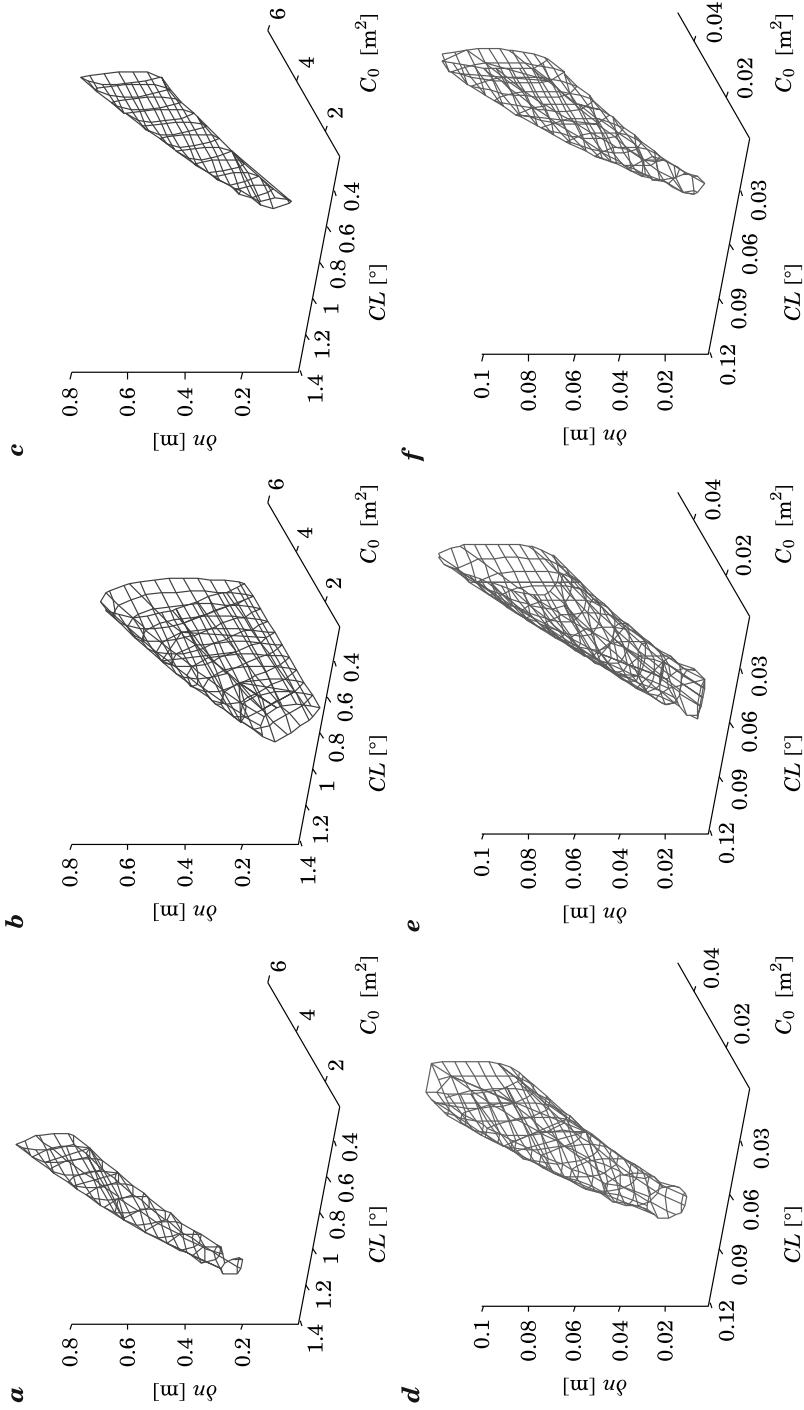
Fig. 4. Surfaces of equal RMSL in space of three covariance parameters: *a* – regional CG, RMSL = 0.784 m, *b* – regional CGM2, RMSL = 0.754 m, *c* – regional CGM3, RMSL = 0.761 m, *d* – local CG, RMSL = 0.089 m, *e* – local CGM2, RMSL = 0.086 m, *f* – local CGM3, RMSL = 0.087 m

uses variable covariance parameters. The estimate of geoid height for each point excludes this point from the dataset (Eq. 10). The LSC prediction is made with $3°$ distance limit for each regional $\tilde{N}_i^r$. Respective distance limit for the local data is $0.2°$. These distances are assessed from Figure 1, by finding the maximum distances of the correlated residuals. LOO process is applied and the predictions are compared to the measured data by RMSL calculation. The analysis of three covariance parameters is performed in their 3D space (Fig. 4). The minimum RMSL is a measure of optimum prediction possible for the chosen data and covariance model. This minimum RMSL indicates covariance parameters enabling the prediction that fits best the data in the least squares sense. Figure 4 describes regions in 3D space of three parameters, which have RMSL smaller than individually specified values. These values are computed by adding 0.001 m to the global RMSL minimum in every case. One may note that these regions have elongated shapes. This means that various parameter sets may provide similar LSC results if properly combined. *CL* parameter has a tendency to be more constant than δn, when C_0 is increasing. More specifically, δn rises with the increase of C_0, which may indicate a correlation between the parameters.

Figure 5 presents the cross-sections of subfigures from Figure 4. The sections are realized for C_0 parameter equal 3 m^2 for regional data and 0.02 m^2 for local geoid heights. These values are variances of the residuals, which are often used to approximate C_0. The sections show the problem in more detail and indicate the regions of the parameters, where the prediction has decreased accuracy. The choice of too small *CL* may strongly affect accuracy of the prediction as well as small δn.

CL parameter is different in particular covariance models, which is a confirmation of the previous observations (Fig. 1). *CL* values in Figure 5 are usually smaller than their respective estimates in Figure 1. This is especially noticeable in the case of regional data (Figs. 5 *a–c*). The parameter δn that represents a priori noise is similar for all covariance models used and large in the case of regional data (Fig. 5 *a–c*). The predictions, where δn is closer to GNSS/lev data accuracy are poor, especially in case of CG (Fig. 5*a*) and CGM3 (Fig. 5*c*).

Figure 3 describes a part of the geoid signal that represents some details of the geoid height between 180 and 2160 degree and order of the harmonic expansion. These spectra may be present in GNSS/lev data due to the centimeter accuracy of GPS and leveling, however, the spatial resolution of the regional data is not sufficient to interpolate them. The information about the correlation of this higher frequency signal may be impossible to gain from data with 100 km spacing. This signal may be treated as a noise, since the sampling is here insufficient to find it as a correlated signal.
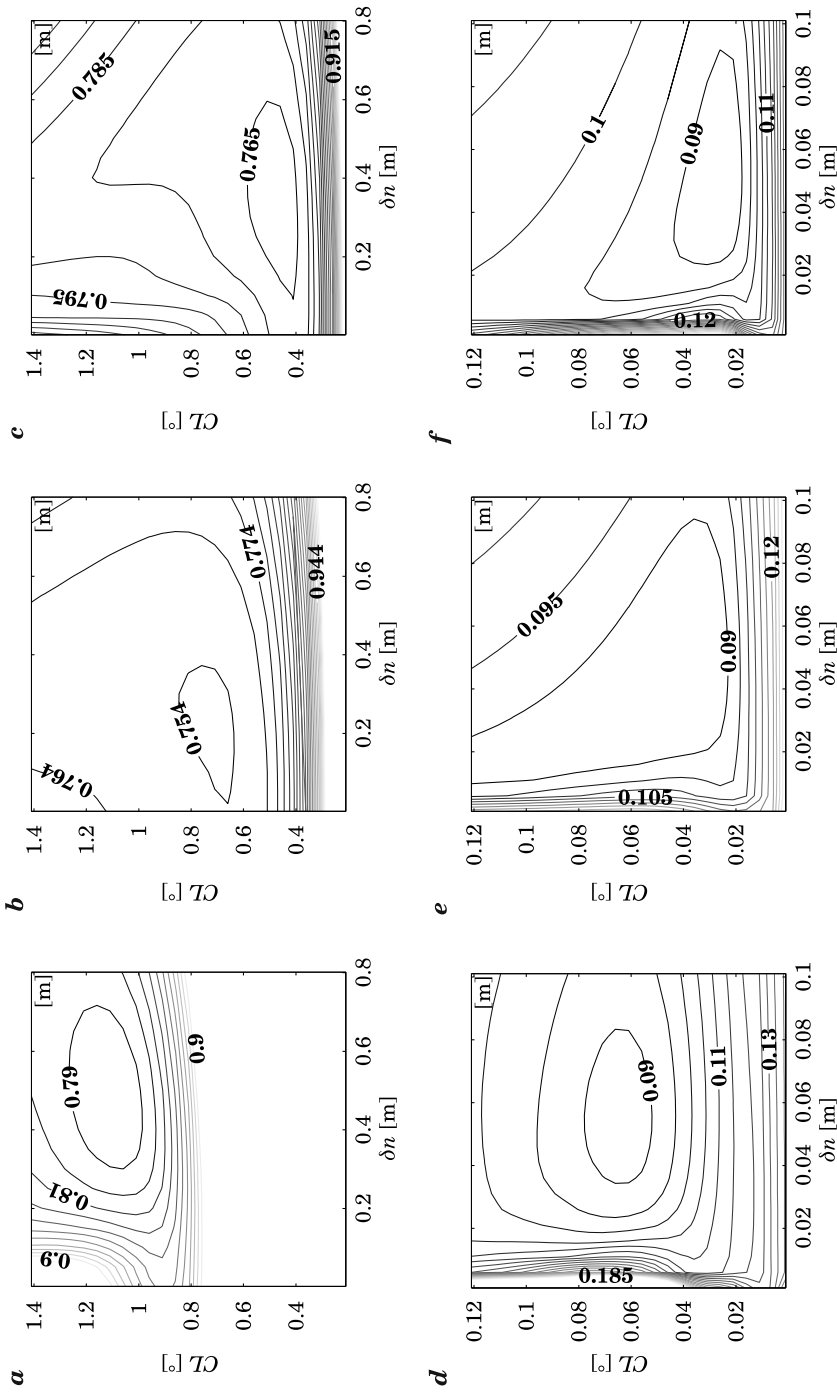
Fig. 5. RMSL for C_0 parameter equal to variance of residuals (i.e. 3 m² and 0.02 m²): a – regional, CG, C_0 = 3 m², b – regional, CGM2, C_0 = 3 m², c – regional, CGM3, C_0 = 3 m², d – local, CG, C_0 = 0.02 m², e – local, CGM2, C_0 = 0.02 m², f = local, CGM3, C_0 = 0.02 m²
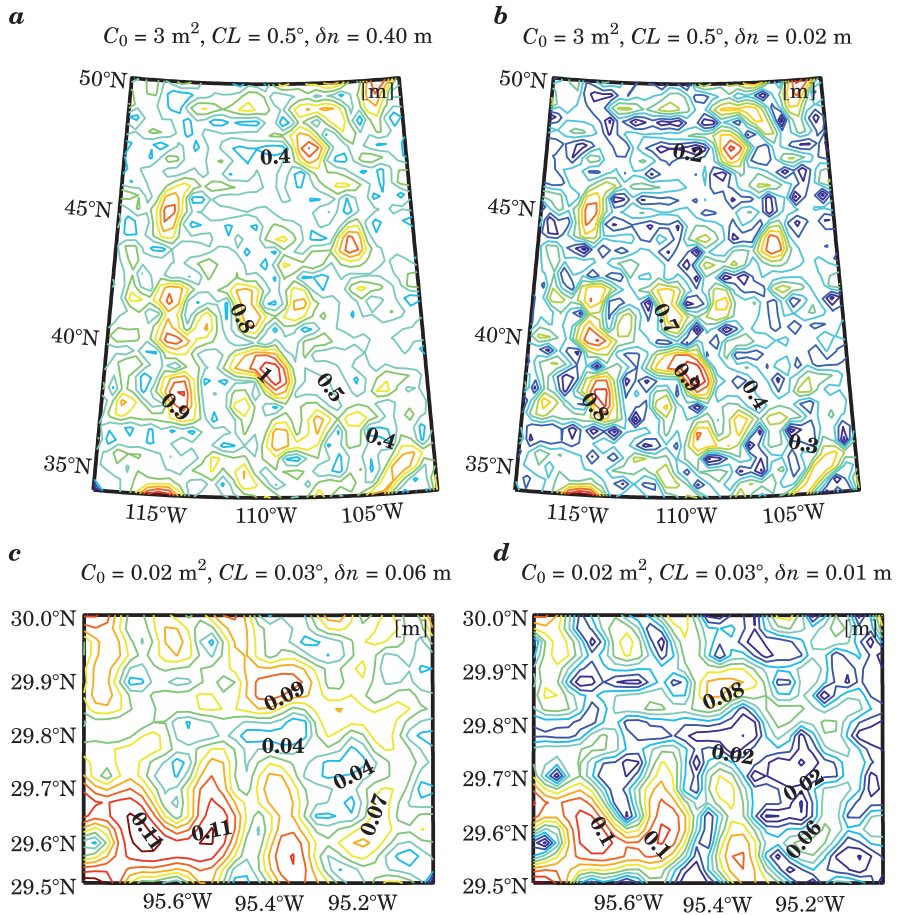
Fig. 6. A posteriori standard deviations for optimal parameters found by LOO and when only noise variances are decreased (CGM3 model): *a* – a posteriori st. dev. for regional geoid, *b* – a posteriori st. dev. for regional geoid, *c* – a posteriori st. dev. for local geoid, *d* – a posteriori st. dev. for local geoid

Additional problem that may be considered here is the a posteriori error, which is usually used in the assessment of LSC accuracy. It is strongly related with a priori noise, however remaining covariance parameters may have also significant influence on LSC error. SANSÓ et al. (1999) and DARBEHESHTI, FEATHERSTONE (2009) report that a posteriori error estimate may be even more affected by the changes of parameters than the LSC result. Figure 6 presents standard deviations of LSC prediction computed from Eq. 11 with optimal parameters (Fig. 5) and with the same C_0 and CL, but smaller δn values used. The underestimated a posteriori standard deviations may be found in Figure 6*b* and 6*d*.

Conclusions

CV methods like e.g. LOO are useful tools for finding covariance parameters that enable optimal prediction with arbitrarily selected covariance model. In some cases, wrong covariance parameters may give significantly worse result and some ranges of the parameters are especially inappropriate. A posteriori LSC error may even stronger depend on the parameters, especially on δn. The parameter δn should represent the noise existing in the observations, therefore applying smaller parameter can provide too optimistic accuracy estimate. It is suspected from analyses that δn depends not only on the measurement error. Limited spatial resolution of the data may exclude higher frequency signal from the correlated data part. Consequently, this part of the signal, which exists in the data due to the high accuracy of the measurement, can be assessed as uncorrelated. Such occurrence is very hard to detect when the data spatial resolution corresponds in a measure to its accuracy. This is quite frequent in practice, however, the case similar to regional data used in this paper may also be found.

Observed LSC properties are essentially consistent with mentioned works, where Tikhonov regularization is applied. In this work, the actual covariance parameters have been estimated instead of the regularization parameter. The paper reveals probable influence of data spatial resolution on the noise covariance matrix. However, the data resolution may be not sole variable influencing a priori noise. Some additional tests have to be performed to explain this in detail.

Acknowledgements

References

ANDERSEN O.B., KNUDSEN P. 1998. *Global marine gravity field from the ERS-1 and Geosat geodetic mission altimetry*. J. Geophys. Res., 103(C4): 8129–8137.

ARABELOS D., TSCHERNING C.C. 2003. *Globally covering a-priori regional gravity covariance models*. Adv. Geosci., 1: 143–147, DOI:10.5194/adgeo-1-143-2003.

ARLOT S., CELISSE A. 2010. *A survey of cross-validation procedures for model selection*. Stat. Surv., 4: 40–79, DOI: 10.1214/09-SS054.

CATALAO J., SEVILLA M.J. 2009. *Mapping the geoid for Iberia and the Macaronesian Islands using 430 multi-sensor gravity data and the GRACE geopotential model*. J Geod., 48(1): 6–15. DOI: 10.1016/j.jog.2009.03.001.

DARBEHESHTI N., FEATHERSTONE W.E. 2009. *Non-stationary covariance function modelling in 2D least-squares collocation*. J Geod., 83(6): 495–508. DOI:10.1007/s00190-008-0267-0

DARBEHESHTI N., FEATHERSTONE W.E. 2010. *Tuning a gravimetric quasigeoid to GPSlevelling by non-stationary least-squares collocation*. J. Geod., 84 (7): 419–431.

DAWIDOWICZ K. 2012. *GNSS satellite levelling using the ASG-EUPOS system services*, Techn. Sc., 15(1): 35–48.

DENKER H. 1998. *Evaluation and Improvement of the EGG97 Quasigeoid Model for Europe by GPS and Leveling Data*. In: *Proceed. Continental Workshop on the Geoid in Europe*. Eds. M. Vermeer, J. Adam. Budapest, Hungary, March 10–14, Reports of the Finnish Geodetic Institute, 98(4): 53–61, Masala.

EL-FIKY G.S., KATO T., FUJII Y. 1997. *Distribution of vertical crustal movement rates in the Tohoku district, Japan, predicted by least-squares collocation*. J. Geod., 71(7): 432–442.

FOTOPOULOS G., KOTSAKIS C., SIDERIS M.G. 2003. *How accurately can we determine orthometric height differences from GPS and geoid data?* J. Surv. Eng., 129: 1–10.

GODAH W., KRYŃSKI J. 2011. *Validation of GOCE gravity field models over Poland using the EGM2008 and GPS/levelling data.* Geoinformation Issues, 3, 1(3): 5–17.

GREBENITCHARSKY R.S., RANGELOVA E.V., SIDERIS M.G. 2005. *Transformation between gravimetric and GPS/levelling-derived geoids using additional gravity information*. J. Geodyn., 39(5): 527–544.

HOFMANN-WELLENHOF B., MORITZ H. 2005. *Physical Geodesy.* Springer, New York.

ILIFFE J.C., ZIEBART M., CROSS P.A., FORSBERG R., STRYKOWSKI G., TSCHERNING C.C. 2003. *OGSM02: A new model for converting GPS-derived heights to local height datums in Great Britain and Ireland*. Surv. Rev., 37(290): 276–293.

JEKELI C., GARCIA R. 2002. *Local geoid determination with in situ geopotential data obtained from satellite-to-satellite tracking data*. In: *Gravity, Geoid and Geodynamics 2000*. Ed. M.G. Sideris. Springer, Berlin, p. 123–128.

KAVZOGLU T., SAKA M.H. 2005. *Modeling local GPS/levelling geoid undulations using artificial neural networks*. J. Geod., 78: 520–527. DOI 10.1007/s00190-004-0420-3.

KITANIDIS P.K. 1983. *Statistical estimation of polynomial generalized covariance functions and hydrologic applications*. Water Resour. Res., 19(4): 909–921.

KOHAVI R. 1995. *A study of cross-validation and bootstrap for accuracy estimation and model selection*. Proceedings of the 14th International Joint Conference on Artificial Intelligence. Montreal, Canada, 2: 1137–1143.

KOWALCZYK K., RAPIŃSKI J., MRÓZ M. 2010. *Analysis of vertical movements modelling through various interpolation techniques*. Acta Geodyn. Geomater., 7, 4(160): 1–11.

KUSCHE J., KLEES R. 2002. *Regularization of gravity field estimation from satellite gravity gradients*. J Geod 76: 359–368.

ŁYSZKOWICZ A. 2010a. *Refined astrogravimetric geoid in Poland*. Part I. Geomatics and Environmental Engineering, 4(1): 57–67.

ŁYSZKOWICZ A. 2010b. *Refined astrogravimetric geoid in Poland*. Part II. Geomatics and Environmental Engineering, 4(2): 63–73.

ŁYSZKOWICZ A. 2009. *Assessment of accuracy of EGM08 model over the area of Poland.* Technical Sciences, 12: 118-134, DOI 10.2478/v10022-009-0011-x.

MARCHENKO A., TARTACHYNSKA Z., YAKIMOVICH A., ZABLOTSKYJ F. 2003. *Gravity anomalies and geoid heights derived from ERS-1,ERS-2, and Topex/Poseidon altimetry in the Antarctic peninsula area.* Proceedings of the 5th International Antarctic Geodesy Symposium AGS'03, September 15-17, Lviv, Ukraine, SCAR Report No. 23, http://www.scar.org/publications/reports/23/

MORITZ H. 1980. *Advanced Physical Geodesy.* Herbert Wichmann Verlag, Karlsruhe.

OSADA E., KRYŃSKI J., OWCZAREK M. 2005. *A robust method of quasigeoid modelling in Poland based on GPS/levelling data with support of gravity data.* Geodesy and Cartography, 54(3): 99–117.

PAVLIS N.K., HOLMES S.A., KENYON S.C., FACTOR J.F. 2012. *The development and evaluation of Earth Gravitational Model (EGM2008)*, J. Geophys. Res., 117, B04406, DOI:10.1029/2011JB008916.

RAO C.R., TOUTENBURG H. 1995. *Linear Models: Least Squares and Alternatives*. New York: Springer-Verlag, pp. 352.

RAPP R.H. 1973. *Geoid information by wavelength*. Bull. Geod., 110(1): 405–411.

SANSÓ F., VENUTI G., TSCHERNING C.C. 1999. *A theorem of insensitivity of the collocation solution to variations of the metric of the interpolation space*. In: *Geodesy Beyond 2000*. Ed. K.P. Schwarz. The Challenges of the First Decade, International Association of Geodesy Symposia, 121: 233–240, Springer, Berlin.

SMITH D.A., MILBERT D.G. 1999. *The GEOID96 high-resolution geoid height model for the United States*. J. Geod., 73(5): 219–236.

STRYKOWSKI G., FORSBERG R. 1998. *Operational merging of satellite airborne and surface gravity data by draping techniques*. In: *Geodesy on the Move*. Eds. R. Forsberg, M. Feissl, R. Dietrich. Springer, Berlin, p. 207–212.

TROJANOWICZ M. 2012. *Local modelling of quasigeoid heights with the use of the gravity inverse method – case study for the area of Poland*. Acta Geodyn. Geomater., 9, 1(165): 5–18.

YOU R.J., HWANG H.W. 2006. *Coordinate transformation between two geodetic datums of Taiwan by least-squares collocation*. J. Surv. Eng.-ASCE, 132(2): 64–70.

DESCRIBING OF GENERALIZED DRYING KINETICS WITH APPLICATION OF EXPERIMENT DESIGN METHOD

German Efremov

Department of Mathematical Modeling
Moscow State Open University, Moscow

A b s t r a c t

The purpose of this article is an application of experiment design method for describing of generalized drying kinetics. Generalized kinetic equation for the first drying period as the linear dependence of the material moisture content vs. drying time and temperature is obtained. For determination of generalized kinetic equation the limited number of experimental data (only two moisture contents of a material for two temperatures of drying agent) is needed. The comparison of calculations of generalized kinetic equation with experimental data for convection drying of sludge and for convectional drying of cotton fabric in the first drying period are fulfilled. The mathematical modification of the two-period model of drying kinetics over the entire drying process is obtained. This modified model permits to avoid of the determination of a characteristic drying time. The comparison of drying kinetic calculations with experimental data for convection drying of sludge in the first and second drying periods for four temperatures using of experiment design method was fulfilled. As follows from calculations, the experimental data of sludge correspond well to the lines obtained through the factorial design which means that this method can successfully be used to determine constant drying rates, total kinetics and the influence of temperature in drying process.

Nomenclature

E – Dimensionless drying time
N_0 – Initial drying rate
t – Drying air temperature
X_0 – Initial moisture content (dry basis)
$X(\Theta)$ – Moisture content (dry basis)
X_{eq} – Equilibrium moisture content

* Corespondence: German Efremov, Department of Mathematical Modeling, Moscow State Open University, Moscow, 107996, Russia, e-mail: g1e@nm.ru

Greek letters

θ – Drying time

θ_f – Total (final) drying time

σ – Characteristic drying time

Introduction

For the description of drying kinetics it is required to establish an appropriate mathematical model and to find numerical values for the model parameters. Drying of different materials is almost always treated empirically in the primary literature, usually by regression on experimental data or by empirical equations, par example, in exponential form (so-called Page model) (CHEN, SCHMIDT 1990, PERKIN 1990, KEMP et al. 2001, MUJUMDAR 2007). Several equations available in the literature for explaining drying behavior of different products have been used (FROLOV 1987, CHEN, SCHMIDT 1990, PERKIN 1990, EFREMOV 1998, 2000, 2001, 2002, KEMP et al. 2001, CHEN et al. 2002, BENALI, KUDRA 2002, REYES et al. 2004, MUJUMDAR 2007).

Another approach to determine the drying kinetics includes the using of experiment design method (BOX et al. 2005, EFREMOV, KUDRA 2011, EFREMOV 2012, MONTGOMERY 2012). As an initial model, the results of experiment often serve that represent a set of the several measurements executed according to a certain plan. In the elementary case this plan is built on the description of conditions to perform measurements that is the set of values of entrance parameters (factors).

In statistics, a full factorial experiment is an experiment whose design consists of two or more factors, each with discrete possible values or ;levels;, and whose experimental units take on all possible combinations of these levels across all such factors (BOX et al. 2005, MONTGOMERY 2012). Such an experiment allows studying the effect of each factor on the response variable, as well as the effects of interactions between factors on the response variable.

In this study an application of experiment design method for describing of drying kinetics of sludge and cotton fabric is considered. Generalized kinetic equation for the first drying period as the linear dependence of the material moisture content vs. drying time and temperature is obtained. For determination of coefficients of this equation the limited number of experimental data (only two moisture contents of a material for two temperatures of drying agent) is needed. The comparisons of calculations of generalized kinetic equation with experimental data for convection drying of sludge and for convectional drying of cotton fabric in the first drying period are considered. The mathematical modification of the two-period model of drying kinetics

(EFREMOV 1998, 2000, 2002, CHEN et al. 2002) over the entire drying process is also proposed.

The comparison of drying kinetic calculations with experimental data for convection drying in the first and second drying periods for four temperatures using experiment design method was fulfilled. The comparison of calculations with experiments shows that the deviations of calculations from experience did not exceed 3.8%.

Materials and Methods

Kinetics of drying

Drying kinetics in the first period is described by linear dependence of the volume-averaged moisture content of a material X from time of the process θ (FROLOV 1987, CHEN, SCHMIDT 1990, PERKIN 1990, EFREMOV 1998, 2000, 2001, 2002, KEMP et al. 2001, CHEN et al. 2002, BENALI, KUDRA 2002, REYES et al. 2004, MUJUMDAR 2007). Linear dependence of moisture content is successfully applied to describe convective and microwave drying of hygroscopic (CHEN, SCHMIDT 1990) and non hygroscopic (PERKIN 1990) capillary-porous materials, such as polymer pellets, glass beads and alumina spheres. Linear drying kinetics in the first period is used also for description of drying of fine-dispersed macro porous materials (FROLOV 1987). The proposed two-period model (EFREMOV 1998, 2000, 2002) is suitable when drying takes place in both constant rate (first) and falling rate (second) periods of drying. Though the model was developed for convective drying of capillary-porous materials such as leather, paper, cotton, fibre and peat (EFREMOV 2000) it was successfully applied to describe drying of organic materials (EFREMOV 1998, 2002, CHEN et al. 2002, BENALI, KUDRA 2002). Two-period model was obtained as summation of two solutions of diffusion process (isotropic flat material with uniform distribution of initial moisture content – EFREMOV 2000). First solution of the diffusion process was obtained on the basis of constant initial drying rate N_0 and the second solution was obtained in the form of function of integral of errors with modification for volume-averaged moisture content (EFREMOV 1998, 2000). This two-period model in form of ration of time-dependant and initial volume-averaged moisture content is describing by the following equation (EFREMOV 1998, 2000, 2001, 2002, CHEN et al. 2002, BENALI, KUDRA 2002, REYES et al. 2004):

$$\frac{X(\theta)}{X_0} = \left(1 - N_0 \, \frac{\theta}{X_0}\right) + \frac{N_0 \, \sigma \sqrt{\pi}}{2X_0} \, \mathrm{erfc} \left(\frac{\theta_f - \theta}{\sigma}\right) \tag{1}$$

where: X is the volume-averaged moisture content (kg/kg, db), X_0 – the initial moisture content, θ – time of drying, θ_f – the elapsed time of drying, σ – the characteristic drying time which is constant for given process conditions.

The first term in Equation (1) represents the relatively long first drying period characterized by a constant drying intensity $N_0 = dX/d\theta$. The second term reflects the macroscale nonstationary diffusive moisture transport in a drying material, obtained by applying the Laplace transform method to the equation of isotropic diffusion with boundary conditions in the form of a constant concentration on the material surface (FROLOV 1987, EFREMOV 1998, 2000, REYES et al. 2004). Accepting that the moisture content at the end of drying approaches an equilibrium value X_{eq}, equation (1) becomes

$$\frac{X_{eq}}{X_0} = \left(1 - N_0 \frac{\theta}{X_0}\right) + \frac{N_0\,\sigma\sqrt{\pi}}{2X_0} \tag{2}$$

Hence from Equation (2) the characteristic drying time is

$$\sigma = \frac{2}{\sqrt{\pi}}\left(\theta_f - \frac{X_0 - X_{eq}}{N_0}\right) \tag{3}$$

Using of equation (3) leads to the following mathematical modification of the two-period model (1):

$$\frac{X(\theta)}{X_0} = 1 - \frac{N_0}{X_0} \cdot \left[\theta - \left(\theta_f - \frac{X_0 - X_{eq}}{N_0}\right) \cdot \operatorname{erfc}\left(\frac{N_0\sqrt{\pi}}{2} \cdot \frac{\theta_f - \theta}{N_0 \cdot \theta_f - X_0 + X_{eq}}\right)\right] \tag{4}$$

The drying kinetics can be generalized using the following dimensionless equation (EFREMOV 2001):

$$K = \frac{X - X_{eq}}{\sigma N_0} = \frac{\theta_f - \theta}{\sigma} - \frac{\sqrt{\pi}}{2}\operatorname{erf}\left(\frac{\theta_f - \theta}{\sigma}\right) = E - \frac{\sqrt{\pi}}{2}\operatorname{erf}(E) \tag{5}$$

where: $E = (\theta_f - \theta)/\sigma$ represents the dimensionless drying time.

Usually initial and equilibrium moisture content, elapsed time of drying are the experimentally determined drying parameters. The main problem is determination of N_0 – the constant drying rate in the first period of drying as a function of drying time θ and process temperature t.
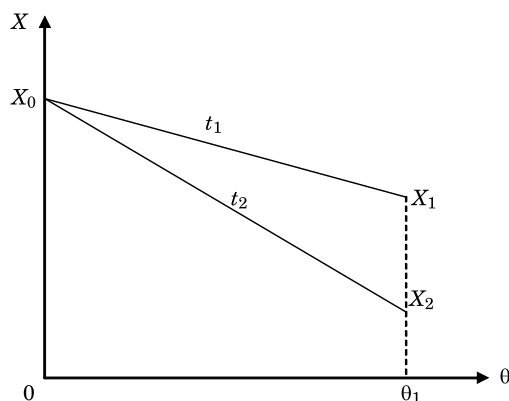
Fig. 1. Dependence of average moisture content of a material X from time θ in the first period of drying for two temperatures

Drying kinetics in the first period is described by linear dependence of moisture content of a material X from time of the process θ (FROLOV 1987, CHEN, SCHMIDT 1990, PERKIN 1990, EFREMOV 1998, 2000, 2001, 2002, KEMP et al. 2001, CHEN et al. 2002, BENALI, KUDRA 2002, REYES et al. 2004, MUJUMDAR 2007). In Figure 1 the example of such dependence for drying agent of two temperatures $t1$ and $t2$ is submitted. The lines of drying kinetics pass from the point of total initial moisture content $X0$ (at $\theta0 = 0$) up to points corresponding of final values $X1$ and $X2$, appropriate to the minimal and maximal values of temperature of the drying agent $t1$ and $t2$ in experiment (Fig. 1).

Experiment design method

For mathematical description of the dependence of moisture content from time and temperature of the process can be used experiment design method (BOX et al. 2005, MONTGOMERY 2012). To obtain the mathematical description of such model the plan of first order can be used. For the vast majority of factorial experiments, each factor has only two levels. For example, with two factors each taking two levels, a full factorial experiment would have four treatment combinations in total, and is usually called a 2×2 (or 2^2) factorial design. Three factors, each assuming two levels give 2×3 (or 2^3) factorial design which generates 8 combinations and so on. If the number of combinations in a full factorial design is too high to be logistically feasible, a fractional factorial design may be used, in which some of the possible combinations (usually at least half) are omitted.

For an illustration of this process, the estimation of parameters is interesting from the practical point of view, the calculation of temperature dependence for the first period of drying can be considered also.

Let's consider at first the solution in a general view. The process of convective drying of a material at constant drying rate depends mainly on external mass transfer and it can be described by temperature of hot air t and time of process θ.

The necessary number of full factorial experiment would have four combinations $2^2 = 4$. The drying kinetics are describing by changing of moisture content from initial value X_0 (at $\theta_0 = 0$) up to final values X_1 and X_2, appropriate to the minimal and maximal values of temperature of the drying agent t_1 and t_2 (Fig. 1).

The matrix of full factorial experiment planning for coded variable of two factors in view of their double interaction (Box et al. 2005, Montgomery 2012). To save space, the points in a two-level factorial experiment are often abbreviated with strings of plus (+) and minus (–) signs. The strings have as many symbols as factors, and their values dictate the level of each factor; conventionally, "–" for the first (or low) level, and "+" for the second (or high) level. The plan of this two-level factorial experiment is presented entered in the Table 1. Parameter y represents the current material moisture content X; x_1 and x_2 are two coded variables of entrance parameters (factors) – temperature of hot air t and drying time θ; b_0, b_1, b_2 and b_{12} are the coefficients of regression equation (6). The value of temperature at the centre of the plan we shall designate t_0, interval of a temperature variation δ_1, accordingly the values for time of the process – θ_0 and δ_2.

Table 1

Matrix of full factorial experiment for coded variable of two factors

x_0	x_1	x_2	$x_1 \cdot x_2$	y
+	–	–	+	y_0
+	+	–	–	y_0
+	–	+	–	y_1
+	+	+	+	y_2

The appropriate regression equation has the following form:

$$y = b_0 + b_1 x_1 + b_2 x_2 + b_{12} x_1 x_2 \qquad (6)$$

The coefficients of the regression equation (6) can be calculated from the formula (Efremov 2001, 2012, Efremov, Kudra 2011, Box et al. 2005)

$$b_i = \frac{\sum\limits_{1}^{4} x_i y_j}{4} \tag{7}$$

Then, the coefficients of regression in view of given matrices of planning (Table 1)

$$b_0 = \frac{y_0 + y_0 + y_1 + y_2}{4}, \; b_1 = \frac{-y_1 + y_2}{4}, \; b_2 = \frac{-y_0 - y_0 + y_1 + y_2}{4}, \; b_{12} = \frac{-y_1 + y_2}{4} \tag{8}$$

Let's substitute values of the coefficients in the regression equation (6)

$$4y = (y_0 + y_0 + y_1 + y_2) + (y_1 + y_2)x_1 + (-y_0 - y_0 + y_1 + y_2)x_2 + (-y_1 + y_2)x_1 x_2 \tag{9}$$

The transitions from coded variables to initial parameters are

$$x_1 = \frac{t - t_0}{\delta_1}, \; x_2 = \frac{\theta - \theta_0}{\delta_2}, \; y_0 = X_0, \; y_1 = X_1, \; y_2 = X_2, \; \theta_0 = \delta_2 \tag{10}$$

After transformations, finally the generalized kinetic equation for the first drying period can be obtained

$$X = X_0 - \frac{2X_0 - X_1 - X_2}{4} \cdot \frac{\theta}{\delta_2} - \frac{X_1 - X_2}{4} \cdot \frac{t - t_0}{\delta_1} \cdot \frac{\theta}{\delta_2} \tag{11}$$

It is necessary to note, that the influence of temperature on a drying process is taken into account only by the last member of double interaction of the influencing factors because the second term of right side of equation (6) equals to 0.

The first two experiments (Table 1) correspond to initial condition of a material ($\theta = 0$ and moisture content X_0). The plan of a two-level full factorial experiment indicates that it is necessary to carry out only 2 experiments (X_1 and X_2) to determine the linear dependence of the material moisture content vs. drying time and temperature.

Results and Discussion

The 2^2 factorial experiment is exemplified in this paper for the process of convection drying of sludge from a municipal sewage treatment plant in a laboratory drying tunnel with parallel airflow at different temperatures and at constant air velocity 0.65 m/s (REYES et al. 2004, EFREMOV, KUDRA 2011. The initial sludge had a paste-like consistency with 72.6% wb moisture content, equivalent to 2.65 kg water/kg dry matter (REYES et al. 2004). The experiments were performed in a standard drying tunnel with a cross section 0.2×0.2 m. The samples were held on sets of 0.1×0.1 m metal boxes with rim height $L = 0.005$ m.

As drying of sludge depends on two main parameters, namely temperature of hot air t and drying time θ, the equation of regression was using in the form (6), where y represents the current material moisture content X; x_1 and x_2 are two coded variables of entrance parameters (factors) – temperature of hot air t and drying time θ; b_0, b_1, b_2 and b_{12} are the coefficients of regression equation (6).

In this process the change of temperature t (variable x_1) is in an interval 80-112° and the change of time θ (variable x_2) is from 0 up to 80 minutes.

Value of air temperature at the centre of the plan was designated t_0, interval of a variation δ_1, accordingly for time of process – θ_0 and δ_2. The initial data for this drying process are shown in Table 2.

Table 2

The initial data for convective drying of sludge

Variable, x	Min. (–)	Max (+)	Center	Interval (δ)
x_1 – temperature t, °C	80	112	96	16
x_2 – time θ, min	0	80	40	40

The plan of two-level factorial experiment for convective drying of sludge is presented in Table 3. The first two experiments correspond to initial condition of a material ($\theta = 0$ and moisture content X_0). The plan indicates that it is necessary to carry out only 2 experiments to determine moisture content at the same temperature at time $\theta = 80$ minutes. As a result of the experiments, the appropriate values of moisture content are equal to 1.31 and 0.49. All values of moisture content are in a matrix of planning of full factorial experiment for convective drying of sludge (Table 3).

Matrix of full factorial experiment for convective drying of sludge

x_0	x_1	x_2	$x_1 \cdot x_2$	y
+	–	–	+	2.65
+	+	–	–	2.65
+	–	+	–	1.31
+	+	+	+	0.49

After substitution data of moisture content (Table 3), the generalized equation for the first drying period (11) is

$$X = X_0 + 0.009125 \cdot \theta - 0.0003203 \cdot \theta \cdot t \qquad (12)$$

The drying rate can be calculated by differentiation of equation (12) with respect to time θ:

$$N_0 = \frac{dX}{d\theta} = 0.009125 - 0.0003203 \cdot t \qquad (13)$$

Figure 2 shows the comparison of calculations using equation (12) with experimental data for convection drying of sludge in the 1-st drying period for four temperatures (REYES et al. 2004). The straight lines are drawn through three black points that mark the values determined according to the full factorial experimental plan for these calculations. Method can successfully be used to determine the influence of temperature from limited number of experimental data. The plan of a two-level factorial experiment indicates that it is necessary to carry out only 2 experiments to determine the linear dependence of the material moisture content vs. drying time.

Designation of experimental points in Figure 2 and 3

Temperature t, ºC	80	90	100	112	80 (plan)
Run No (BENALI, KUDRA 2002)	9	1	10	5	
Symbol	○	◊	+	□	●

As follows from Figure 2, the experimental data correspond well to the lines obtained through the factorial design which means that this method can successfully be used to determine constant drying rates from limited number of experimental data.
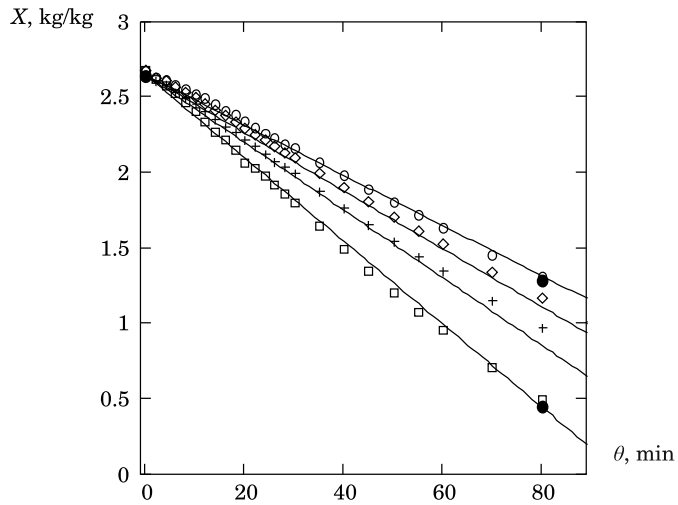
Fig. 2. Comparison of calculations of moisture content X vs. drying time θ using equation (11) with experiments on convection drying of sludge in the first period (Reyes et al. 2004) for four temperatures (Table 4)
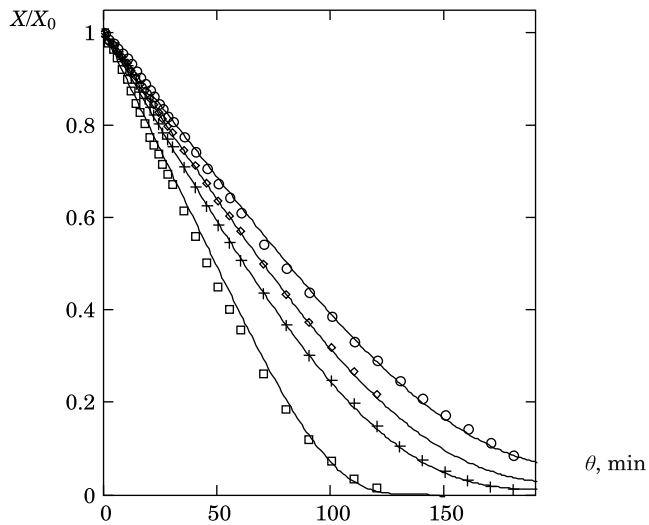

Fig. 3. Comparison of calculations using two-period model (4) with experiments
Source: Reyes et al. (2004).

Using the equation (13) for drying rate N_0 in the first drying period the calculation of moisture content for two-period model (4) may be fulfilled. Table 5 compiles the calculated values of drying parameters σ, N_0 and θ_f for two-period model whereas Figure 3 compares the results of calculations

according to equation (4) with experimental data. For all run the equilibrium moisture content X_{eq} = 0.03 kg/kg. For clarity reasons only 4 curves for runs No 1, 5, 9 and 10 are shown in the Figures 2 and 3, but equally good fit was obtained for other experimental data (BENALI, KUDRA 2002).

Table 5

Experimental and calculated parameters for the two-period model (Drying kinetics of sludge)

Run No [10]	t, ºC	N_0, 1/min	σ, min	θ_f, min
9	80	0.017	97	235
1	90	0.020	101	220
10	100	0.023	96.1	200
5	112	0.027	42.1	135

Good match of experimental points and model solution corresponds to sludge tests in Figure 3. It indicates that two-period equation (4) can be used to predict drying kinetics with possible extrapolation for different temperatures and air velocities.

Analogical calculations and comparison with experiments were fulfilled for convectional drying of cotton fabric for first and second periods in temperature interval 480–83ºC and at change of time θ from 0 up to 18 minutes (EFREMOV 2012). The initial data for convective drying of cotton fabric are shown in Table 6.

Table 6

The initial data for convective drying of cotton fabric

Variable, x	Min. (−)	Max (+)	Center	Interval (δ)
x_1 – temperature t, ºC	48	83	65.5	17.5
x_2 – time θ, min	0	18	9	9

The initial moisture content of cotton fabric was equivalent to w_0 = 1.09 kg water/kg dry matter. Accordingly of matrix of full factorial experiment (Table 3) the first two experiments correspond to initial condition of a material (θ = 0 and moisture content X_0). The matrix indicates that it is necessary to carry out only 2 experiments to determine moisture content at temperature 48 and 83ºS and time θ = 18 minutes. As a result of the experiments, the appropriate values of moisture content were equal to 0.65 and 0.1. After substitution data of moisture content, the generalized equation for the first drying period (11) of cotton fabric is

$$X = X_0 + 0.01746 \cdot \theta - 0.000873 \cdot t \cdot \theta \qquad (14)$$

Comparison of calculations with experiments (FILONENKO 1939) was fulfilled for four temperatures: 48ºC, 56.3ºC, 70ºC and 83.5ºC (Table 7, Figure 4). The deviations of calculations from experience did not exceed 3.8%.
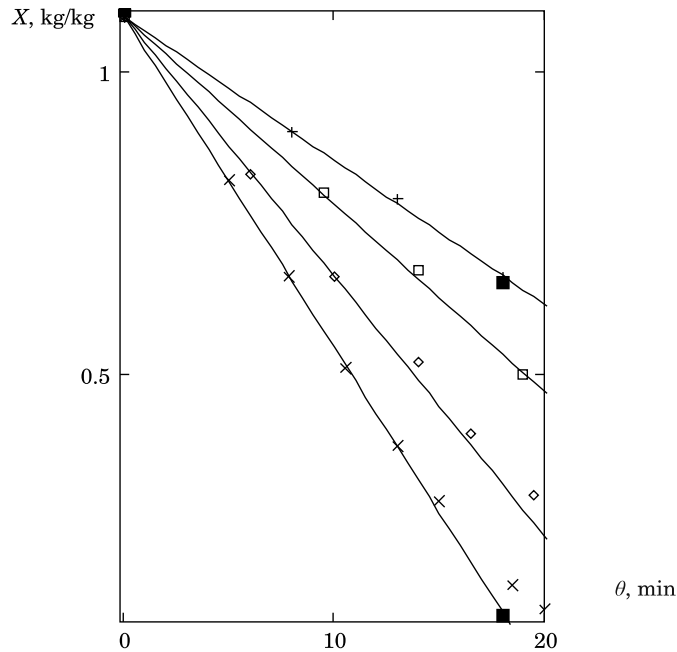

Fig. 4. Comparison of calculations of moisture content *X* vs. drying time *θ* using equation (14) with experiments on convection drying of cotton fabric (FILONENKO 1939) for four temperatures (Table 7)

Table 7

Designation of experimental points (FILONENKO 1939) in Figure 4

Temperature *t*, ºC	48	56.3	70	83.5
Symbol	+	□	◊	×

Using the characteristic drying parameters listed in Table 5, the dimensionless number *K* (Equation 5) was calculated and plotted against the *E* parameter. Good match of the experimental points and the model solution in Fig. 4 indicates that generalized equation (5) can be used to predict drying kinetics with possible extrapolation for other temperatures and air velocities.
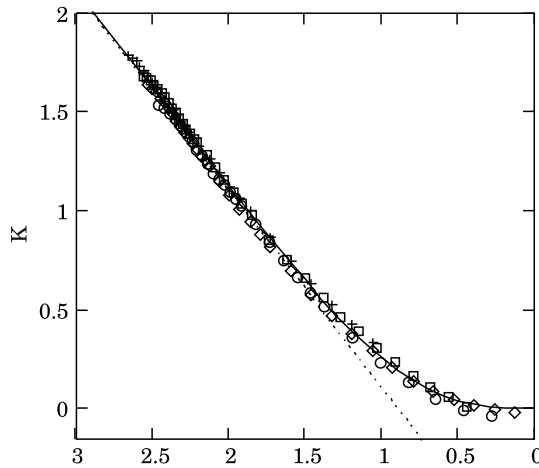
Fig. 5. Generalized drying curve for two-period model

It is necessary to note, that the obtained generalized kinetic equation (11) for the first drying period may be used for different types of drying and kind of materials. The drying rate N_0 for the first drying period can always be calculated by differentiation of the generalized equation with respect to time θ. Using the equation for drying rate N_0 in the first drying period the calculation of moisture content for two-period model may be fulfilled. The application of obtained mathematical modification of two-period model allows to avoid the application in calculations of the characteristic drying time which is constant for given process conditions.

Conclusion

The experiment design method (BOX et al. 2001, MONTGOMERY 2012) is a progressive method in application for convection drying in the first drying period and for two-period drying model. The comparison of calculations with experimental data for convection drying of sludge and cotton fabric for four temperatures using of experiment design method is fulfilled. As follows from calculations, the experimental data correspond well to the lines obtained through the factorial design which means that this method can successfully be used to determine drying kinetics for different types of drying and materials and to determine the influence of temperature from limited number of experimental data. The plan of a two-level factorial experiment indicates that it is necessary to carry out only 2 experiments to determine the linear dependence of the material moisture content vs. drying time.

References

Benali M., Kudra T. 2002. *Thermal dewatering of diluted organic suspensions: process mechanism and drying kinetics*. Drying Technology, 20: 935–951.

Box G.E., Hunter W.G., Hunter J.S. 2005. *Statistics for Experimenters: Design, Innovation, and Discovery*. John Wiley & Sons, New York, USA, p. 675.

Chen G., Yue P.L., Mujumdar A.S. 2002. *Sludge dewatering and drying*. Drying Technology, 20: 883–916.

Chen P., Schmidt P.S. 1990. *An integral model for drying of hygroscopic materials with dielectric heating*. Drying Technology, 8: 907–930.

Efremov G. 1998. *Analytical solution of equation of diffusion for process of convective drying of flat materials*. Proceeding of 11th International Drying Symposium (Drying'98), pp. 2121–2128.

Efremov G.I. 2000. *Generalized kinetics of drying of fibre materials*. Fibre Chemistry, 32: 430–436.

Efremov G.I. 2001. *Macrokinetics of Transfer Processes*. MSTU Press, Moscow, Russia, p. 289.

Efremov G.I. 2002. *Generalized kinetics for external drying task*. Proceeding of 13th International Drying Symposium (IDS-2002), pp. 563–570.

Efremov G.I. 2012. *Finding the temperature dependence for the first period of drying by the method of planning an experiment*. Proceeding of XIV Minsk International Heat and Mass Transfer Forum, pp. 2–22.

Efremov G., Kudra T. 2011. *Application of experiment design method for determination of drying kinetics*. Proceeding of 11th International Congress on Engineering and Food (ICEF-11), pp. 491–492.

Filonenko G.K. 1939. *Kinetics of Drying Process*. Moscow, p. 138.

Frolov V.F. 1987. *Modeling of Drying of Disperse Materials*, "Chemistry" Press, Leningrad, Russia, p. 207.

Kemp I.C., Fyhr C.B., Laurent S., Roques M.A., Groenewold C.E., Tsotsas E., Sereno A.A., Bonazzi C.B., Bimbenet J-J., Kind M. 2001. *Methods for processing experimental drying kinetics data*. Drying Technology, 19: 15–34.

Montgomery D.C. 2012. *Design and Analysis of Experiments*. John Wiley & Sons, New York, USA, p. 752.

Mujumdar A.S. 2007. *Handbook of Industrial Drying*. Marcel Dekker Inc., New York, United States, p. 1423.

Perkin R.M. 1990. *Simplified modelling for the drying of a non hygroscopic capillary porous body using a combination of dielectric and convective heating*. Drying Technology, 8: 931–951.

Reyes A., Eckholt M., Troncoso F., Efremov G. 2004. *Drying kinetics of sludge from a wastewater treatment plant*. Drying Technology, 9: 2135–2150.

SULPHUR CONCRETE'S TECHNOLOGY
AND ITS APPLICATION TO THE BUILDING INDUSTRY

Natalia Ciak[1], Jolanta Harasymiuk[2]

[1] The Chair of Building Construction and Building Physics
[2] The Chair of Engineering Materials and Building Processes
University of Warmia and Mazury in Olsztyn

A b s t r a c t

This article is a scientific – review piece of work which purpose is to popularize the common knowledge of sulphur concrete – the material that has become more and more popular not only in countries with established market economy. In the article there are presented key phases of scientific studies concerning technology of the sulphur concrete, concrete modified with sulphur and its application in building industry. There is also presented methodology of sample preparations, technology of production and its main technical properties.

Introduction

Science and practice have been always searching for new materials and solutions characterised by durability and good strength properties that would become an alternative for materials demanding huge energetic costs. Very often we come to the conclusion that the "new one" is a modern version of well known "old one". That is what happens in the case of the sulphur concrete. It was in the previous century that many researchers (FARAŃSKI 1999, LOOV, VROOM, WARD 1974, MALHOTRA 1979, ORŁOWSKI 1992) proved that in order to obtain composite resistant to chemical aggression, the sulphur can be used as a bond. This article is to draw the attention to the most distinguished advantages and disadvantages of this material, its application and the technology of production assuring designed, required properties.

---

* Corespondence: Natalia Ciak, Katedra Budownictwa Ogólnego i Fizyki Budowli, ul. Heweliusza 4, 10-724 Olsztyn, phone: 48 89 523 45 76, e-mail: n.ciak@uwm.edu.pl

Main features of the sulphur concrete

Growing interests in sulphur usefulness as a bond in the sulphur concrete is led by huge amount of this raw material (it occurs as a natural raw material and is also created as a waste from the fuel desulphurisation process), and by proved advantages of created composite (CZARNECKI, WYSOKIŃSKI 1994, KUŚ, ROGAL 2004, Patent PL *Sposób utylizacji niebezpiecznych odpadów, zwłaszcza popiołów ze spalarni* 2003). The advantages include e.g.:
  – relatively high strength obtained in short time,
  – resistance to most of the aggressive agents,
  – waterproof,
  – utilisation possibility of most of the harmful substances including radio-active wastes (Patent PL *Sposób utylizacji niebezpiecznych odpadów, zwłaszcza popiołów ze spalarni* 2003),
  – recycling possibility.
In spite of many advantages of the sulphur concrete, it should not be treated as a substitute for cement concrete, but in particular cases as an alternative. Such an approach can be justified by some of the faults of the material (CZARNECKI, WYSOKIŃSKI 1994) such as:
  – high energy consumption during the production process,
  – limited thermal resistance (the sulphur concrete is a thermoplastic material),
  – a need for stable, high temperature during the production process.

Development of the sulphur concrete's technology

The interests in concrete and materials modified with sulphur, its properties and the technology have been heading towards two directions. The first one concentrated on sulphur bonds, mastics, and concrete based on sulphur as a thermoplastic bonding material. The second one was devoted to the use of melted sulphur for saturation of cement concrete manufactures in order to enhance their physical and mechanical properties, but mostly to increase its corrosive durability. All of the actions focused into these two directions can be divided into four stages.

The first stage, from the second half of XIX century till the forties of XX century, included the study of properties of the mastics and concrete modified with sulphur and their reasonable application in the building industry. Unfortunately high costs of sulphur these days was not conductive for scientific and practical publications of this subject.

In the second stage, from the forties to the early seventies of XX century,

there was a commercial idea created of the sulphur concrete applications. There were also intense researches conducted over the ways of improving the sulphur properties, that were based on the latest scientific publications about the chemistry of the sulphur (development of the inorganic chemistry of polymers). Simultaneously, industrial polymeric sulphur modification was introduced into various fields, what led to creating effective building materials using such technology. Research centres that were leading the way in the subject were located in the USA, Canada and Russia (former the Soviet Union).

Third stage, dated from the late seventies was characterised by putting into practice the production of building materials, especially concrete. Those days (1975) the S*ulfurcrete Produducts Inc.* company for the first time created the sulphur concrete. In the eighties sulphur concrete became one of the building materials used in construction of many parts of motorways and industrial floors that were built in the USA.

In the fourth stage, starting from the late nineties till now, production of the sulphur concrete, its improvements and composition patents are being created (Patent PL 197205, Patent PL *Sposób utylizacji niebezpiecznych odpadów, zwłaszcza popiołów ze spalarni* 2003, Patent RU 2154602, Patent RU 2166487, Patent RU 2167120, Patent RU 2239834, Patent USA 4256489) as well as technology of production used by different companies, usually located in the USA, Canada (*SULROCK, CHEMPRUF, SULPOL, STARCRETE*), Russia and Poland.

Since 1998, a company "SIARKOPOL" from Tarnobrzeg has started to put the usage of the sulphur concrete into building practice. Now a "MAR-BEL" company is using their own patented solutions for manufacturing composites such as: *SULCEM, SULTECH, SULBET* (Mysłowski 2005, Richter 2006).

Manufacturing and usage of the sulphur concrete

Process of the sulphur concrete manufacture is based on the "hot" technology. In which all the mixed components are heated until 140–150°C. The sulphur used in the sulphur concrete production can be mixed with any type of traditional aggregate. Dosage should be optimized according to practical criteria as well as the mechanical properties (Gracja, Vazguez, Carmona 2004). Optimal amount for sulphur mortar is about 30% of the bond while for the sulphur concrete is about 15% of the bond. The sulphur matrix with the percentage of mineral extender is 5% for mortar and 10% for concrete (on sulphur mass basis).

Mineral aggregate is very important in the sulphur concrete. The concrete mixture should consist of thick and fine aggregate as well as the extenders
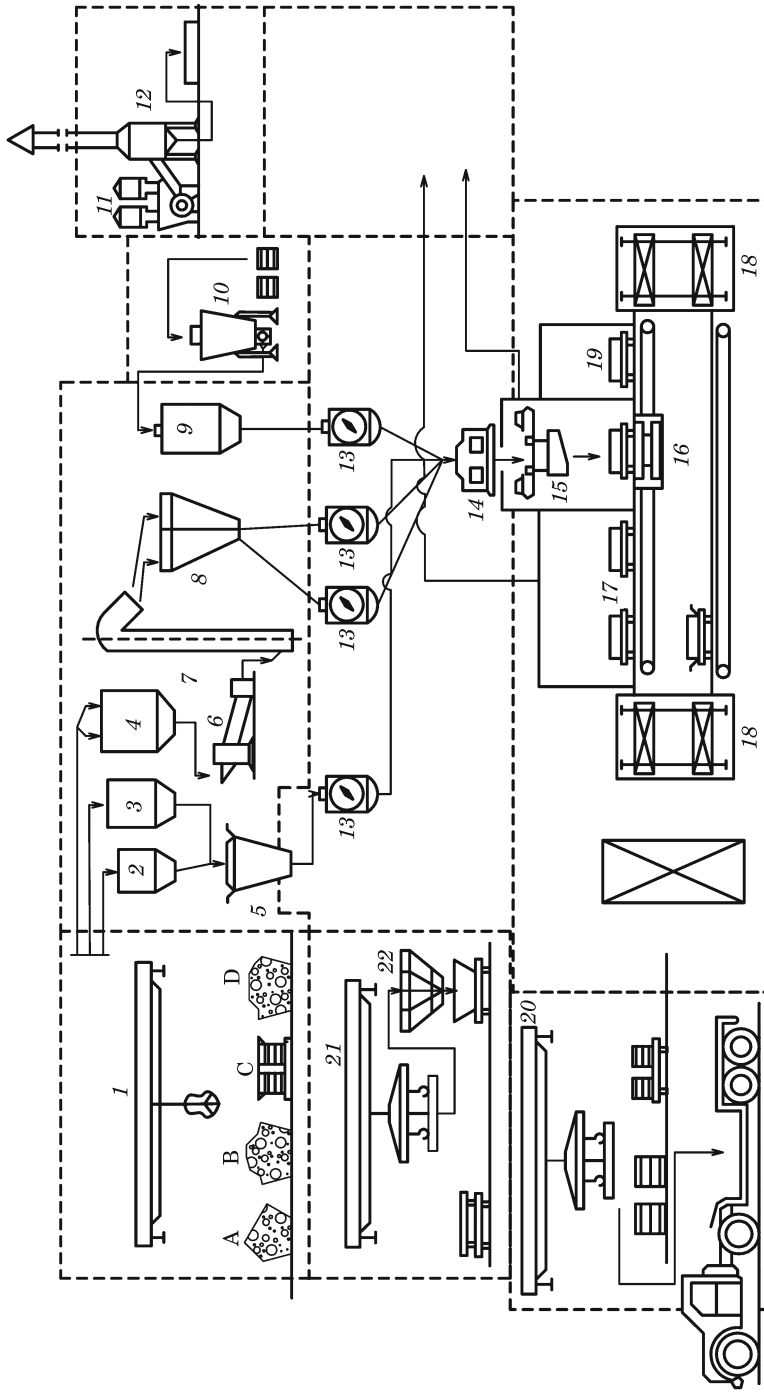
Fig. 1. Technological scheme for sulphur concrete manufactures production: *A* – gravel, *B* – sand, *C* – additives, *D* – sulphur, *1* – compounds storehouse, *2, 3, 4* – tanks (silos), *5* – sulphur modification reactor, *6* – rotary dryer, *7* – feeder, *8* – sand and gravel's silo, *9* – extender's silo, *10* – extender's feeder, *11* – cyclone, *12* – filter, *13* – feeder, *14* – mixer with heater, *15* – forming device, *16* – vibration station, *17, 18* – mobile forms, *19* – chamber for heating up the forms, *20* – storehouse for finished manufactures, *21, 22* – recycling station

Source: Ciak (2007a).

```
┌─────────────┐  ┌─────────────┐  ┌─────────────┐  ┌─────────────────────┐
│  Chemical   │  │  Technical  │  │   Extender  │  │  Aggregate: quartz  │
│    dope     │  │   sulphur   │  │             │  │    sand, gravel     │
└─────────────┘  └─────────────┘  └─────────────┘  └─────────────────────┘
```

**Components' dosage
due to its weight**

Drying the components
until the constants mass · · · · · · Metal forms

Melting the sulphur
and mixing the heated

Moulding and thickening
the samples · · · · · · Dryer for heating up
the forms

Cooling and hardening
of the samples

Dismoulding the samples · · · · · · Cleaning the forms
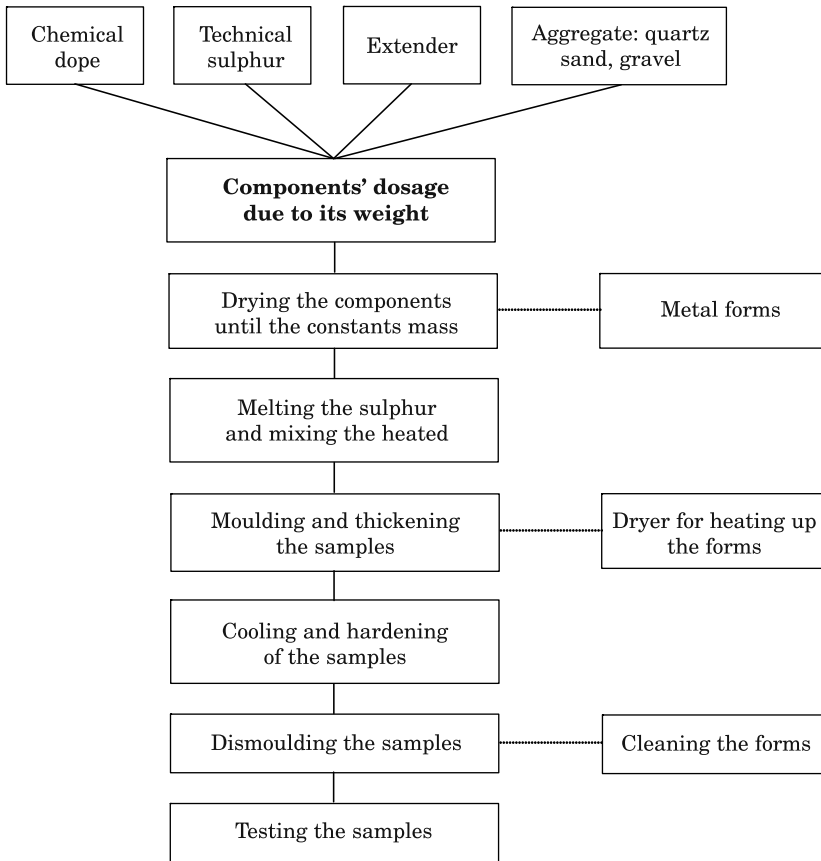
Testing the samples

Fig. 2. Technological scheme of sulphur concrete sample preparation for laboratory usage
Source: own researches.

(GILLOT, JORDAN, LOOV 1980). Gravel and other mineral materials bigger than
4 mm in diameter can be assumed as a thick aggregate while sand and other
mineral materials in the range of 150 µm to 4 mm will be assumed as a fine
aggregate. The extenders can be in the shape of volatile ashes, quartz dust,
minced chalk and others mineral materials smaller than 150 µm. The exten-
ders' presence reduces the pores, that emerge during the sulphur contraction
where the sulphur due to the hardening process, changes its volume. One
should notice that getting a proper, designed form of plastic mass is only
possible when the mixture is characterised by defined plasticity adjusted by the
exact amount of fine and thick aggregate and the extenders. Excessive amount
of them usually leads to worsening the moulding process.

Process of sulphur concrete production is based on the sulphur's properties of changing its viscosity with the change of the temperature (in 119–122ºC sulphur completely turns from the solid into the liquid).

The technology of the sulphur concrete is very similar to the technology of the asphalt concrete. The sulphur concrete production process is presented in the figure 1.

It consists of following steps:
– heating up the mixture until 150ºC,
– melting of modified sulphur and mixing the components,
– moulding samples into metal moulds which were initially heated to the same temperature as the mixture,
– cooling the samples to the ambient temperature.

In University of Warmia and Mazury in Olsztyn there has been conducted researches of sulphur concrete's resistance to chemical and microbiological aggression. In order to prepare the sulphur concrete in a laboratory (scheme for preparation of samples process is presented in the Figure 2), there was constructed a reactor in which the samples were prepared (Fig. 3). The researches results proved usefulness of application of the sulphur concrete in
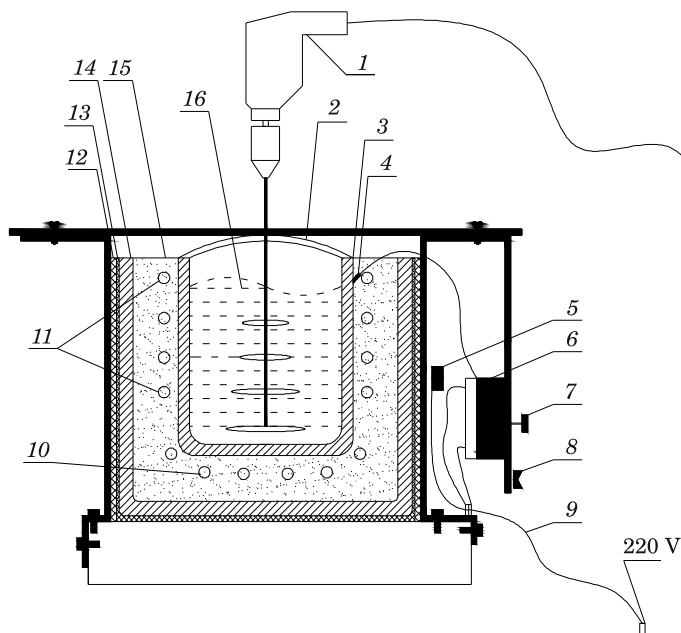

Fig. 3. Lab reactor scheme for sulphur bond and mastics preparation: *1* – mixer wit adjustable speed, *2* – heat-insulating cover, *3* – aluminium mixer, *4* – temperature meter, *5* – short circuit pin, *6* – thermostat, *7* – temperature controller, *8* – power switch, *9* – voltage 220 V, *10* – electrical spiral (1 pc.), *11* – electrical spiral (2 pcs.), *12* – thermal insulation in aluminium foil of 6 mm, *13* – asbestos sheet, *14* – metal container, *15* – fire insulation, *16* – sulphur
Source: own researches.

Table 1

Comparison of averaged, selected properties of sulphur concrete and the cement concrete*

Properties	Unit	Sulphur concrete	Cement concrete
Density	kg/m^3	2400	2200
Compressive strength	MPa	60–115	15–60
Bending strength	MPa	10–16	6–7
Modulus of elasticity	GPa	35–50	25–28
Contraction	mm/m	0.5–1.0	0.6
Linear coefficient of thermal expansibility	10^{-6}/K	8–12	8–10
Porosity	%	1–4	9–15
Absorptivity	%	0–1	5
Frost resistance	cycles	500	50
Minimal period for forming an element	Hour	0.1–0.4	48
Minimal period for nominal strength	hours	2–24	28 days
Corrosive durability in aggressive surroundings	–	resistant	partly resistant
Bond content	%	10–15	20–30

* Notice: In the sulphur concrete contraction occurs only during the hardening process and cooling the mixture within 2–24 hours.
Source: own researches on the basis of: CIAK (2007a,ń), and information data from MARBET®WIL company, for sulphur concrete SULTECH®.

building roads, drainage systems, industrial and harbour engineering, and agriculture. Comparison of selected sulphur concrete's features with the cement concrete's ones are presented in table 1.

On the basis of (Patent PL 197206, ŻAKIEWICZ 1996), the sulphur concrete can be used for anti-radiation protective shields.

The use of sulphur concrete for manufactures production gives an opportunity to create new, effective material solutions creating new standard in building elements. Among the most popular manufactures are:

– tanks for various substances, cesspits, drains;

– sewerage pipes, drainages, sewerage channels, weights for electric traction lines (MAĆKOWSKI 2009);

– telecommunications drains, elements reinforcing the wharf and harbour constructions; (CZARNECKI, WYSOKIŃSKI 1994);

– surfaces of landing strips, roadwork's elements (SERUGA, SMAGA 2006).

As shown above, sulphur concrete can be applied both for non-reinforced elements (weights, channels, drainage elements) and for reinforced elements (tanks, plates). To the wide range of usage we can also add its usefulness in renovations works (coatings with fiber extenders) and restoration works (CIAK 2005, CZARNECKI, WYSOKIŃSKI 1994).

Fig. 4. Exemplary manufactures made with the sulphur concrete – photographs by Andrzej Drożdżal, present manufactures produced by Marbet-Wil Company: *a* – sulphur bond, *b* – sulphur concrete granulate consisting of harmful waste destabilised with the use of Sultech® technology, *c* – linear drainage AQUADREN® *d* – weights for electric traction lines, *e* – channel drainage S520, *f* – channel drainage S520 put along the railway tracks

In the figure 4 there are presented chosen manufactures made with the sulphur concrete.

Assessing the sulphur concrete by the mechanical and chemical properties and by comparing it to the cement concrete's properties one can state that the variety of the sulphur concrete usage is quite broad. What is more the production is almost waste less and the product itself can be recycled.

Conclusions

The sulphur concrete are characterised by high resistance to biological and chemical corrosion. In some cases its mechanical and physical properties can even transcend the properties of traditional concrete so can it can be assumed as a better solution for some building constructions. It should be expected that the interests in the sulphur concrete and its development within next several years should not deteriorate.

References

BŁASIAK I., ŁUSZCZYK L. ŻWIMK S., DOJKA M. 1988. *Zastosowanie siarki modyfikowanej do wyrobu betonów siarkowych.* Chemik, 41 (9): 243.

CIAK N. 2007a. *Analiz vlijania sostava żidkich agresivnych sred na korrozjonnuju stojkost' cementnych betonom propitannych rasplavom siery).* Stroitelstvo i technogennaja bezopasnost'. Sbornik naucznych trudov. Vypusk 22 Symferopol, p. 50–53.

CIAK N. 2007b. *Chimiczeskaja i mikrobiologiczeskaja stojkost' betonov, modificirovannych sieroj.* Diss. Simferopol, p. 191.

CZARNECKI L., WYSOKIŃSKI L. 1994. *Beton siarkowy – nowy materiał konstrukcyjny w budownictwie morskim.* Inżynieria Morska i Geotechnika, 5: 262–266.

FARAŃSKI R.J. 1999. *Tworzywa siarkobetonowe.* Materiały Budowlane, 6: 78.

GILLOT J.E., JORDAN I.J., LOOV R.E. 1980. *Sulphur concretes, mortars and the like.* United States Patent (4.188.230).

GRACJA V., VAZGUEZ E., CARMONA S. 2004. *Utilization of by-produced sulfur for the manufacture of unmodified sulfur concrete.* International RILEM Conference on the Use of Recycled Materials in Buildings and Structures, International RILEM Conference on the Use of Recycled Materials in Buildings and Structures, RILEM PROCEEDINGS PRO; 1–2, 40: 1054–1066.

KUŚ M., ROGAL S. 2004. *Zastosowanie przemysłowe siarkobetonu.* Autostrady, 3.

LOOV R.E., VROOM A.H., WARD M.A. 1974. *Sulfur concrete-a new construction material.* PCI Journal/January-February, p. 86–95.

MAĆKOWSKI R. 2005. *Zastosowania chemoodpornych betonów siarkowych.* Ochrona przed korozją, 4: 134–136.

MALHOTRA V.M. 1979. *Sulphur Concrete and Sulphur Infiltrated Concrete.* Properties, Applications and Limitations, Canada Centre for Mineral and Energy Technology, Mineral Sciences in Ottawa, Ont. Canmet Report, 79–28: 26.

MYSŁOWSKI W. 2004. *Lepsze, trwalsze i nie droższe od dotychczasowych technologiei wyroby firmy MARBET®-WIL.* Autostrady, 5: 36–37.

ORŁOWSKI J. 1992. *Betony, modyficirovannyje sieroj.* Dys. dra tech. nauk: 05.23.05, Charkov, HGTUSA, p. 529.

Patent 2002. PL 197205. *Elektroizolacyjny materiał budowlany.*

Patent 2003. PL 205151 B1. *Sposób utylizacji niebezpiecznych odpadów, zwłaszcza popiołów ze spalarni.*

Patent 2004. PL 196856. *Mieszanka spoiwa siarkowego zawierającego polimer siarki.*

Patent 2008. PL 197206. *Antyradiacyjny materiał budowlany.*

ANALYSIS OF CONVECTIONAL DRYING PROCESS OF PEACH

Ewa Golisz[1], Małgorzata Jaros[1], Monika Kalicka

Faculty of Production Engineering
Warsaw University of Life Sciences

A b s t r a c t

In this study the convectional drying process of peach were investigated. Peaches were cut longitudinally into eight similar pieces and were dried in a laboratory air-drier with forced horizontal air flow. Drying experiments were carried out at temperatures of 50, 60, 70ºC and for two air velocities: 1.0 and 1.2 m/s. The results are shown graphically on the charts. It was found that a greater effect on increasing the rate of drying is the drying air temperature than the increase in flow velocity. The verification of theoretical models of the first and second drying period indicates that the drying process of peach is determined by internal conditions of heat and mass transfer, therefore to describe the drying process were used models of the second period of drying. Global relative error calculated for the whole process was less than 5%.

Introduction

Drying is one of the basic way of preserving food. It involves the removal of water from the product by its evaporation. With this method, water (80-90%) is discharged from the fresh product and a large amount of nutrients are preserved. Drying of agricultural products is one of the oldest and most important methods of food preservation which allows for market surplus management.

Peaches (*Prunus persica* L.), by apricots and nectarines, are the richest source of vitamins and minerals. Therefore they should be eaten throughout the year fresh or dried. Raw peaches and apricots in more than 86% consist of water. In warm countries (India, Iran, Turkey) the most commonly used

---

* Corespondence: Ewa Golisz, Zakład Podstaw Nauk Technicznych, Szkoła Główna Goispodarstwa Wiejskiego, ul. Nowoursynowska 164, 02-787 Warszawa, phone: 48 22 593 46 14, e-mail: ewa.golisz@sggw.pl

method of drying these fruits is sun drying, which requires little capital, simple equipment and low energy input (TOGRUL, PEHLIVAN 2004, KINGSLY et al. 2007). To achieve consistent quality dried product industrial dryers should be used. The drying kinetics of food is a complex phenomenon and requires simple representations to predict the drying behaviour, and for optimizing the drying parameters.

In literature there are lot of studies on drying kinetics of fruits e.g.: apricot (SARSILMAZ et al. 2000, TOGRUL, PEHLIVAN 2002, 2003, DOYMAZ 2004, IGUAL et al. 2012); bananas (DANDAMRONGRAK et al. 2003); melon, papaya (Pereira et al. 2006); grapes (YALDIZ et al. 2001), plum (GOYAL et al., 2007) and some studies on drying peach. TOGRUL and PEHLIVAN (2004) modelled thin layer drying kinetics of peach under open-air sun drying process. WANG and SHENG (2006) studied microwave and far-infrared dehydration characteristics and two-stage drying process involving far-infrared following microwave drying on peach. SAHARI et al. (2006) investigated physicochemical properties of sliced peach during osmotic pre-treatment and dehydration, the optimum condition of the dehydration and sensory evaluation of dried products. KINGSLY et al. (2007) investigated the effect of pre-treatments (potassium meta. bisulphite and ascorbic acid) and drying air temperature (55 and 65°C) on drying behaviour of peach slices. GERMER et al. (2010) evaluated the influence of temperature and concentration of the sucrose syrup on the pre-osmotic dehydration of peaches. However, there is little detailed information on drying kinetics and modelling of drying process of peach. Since drying is an energy-intensive process, its optimization is extremely important for both environmental and economic reasons. In order to optimize drying process, it is necessary to develop its mathematical model to predict the process course. Such model should take into account drying kinetics model that is versatile and has strong theoretical basis.

The objective of this study was to identify the conditions governing of the heat and mass exchange in the convection drying process of peach, using models of the kinetics drying. The external conditions of the heat and mass exchange are dominant from the initial moisture content to the critical one, which in the case of peach is not known. Therefore, the second objective of this study was to indicate the critical moisture content symbolically separated first and second drying period.

Materials and methods

Fresh peaches (Reliance variety) were purchased from local market in Warsaw, Poland. The initial moisture content of fresh samples was 6.7 kg H_2O/kg db (dry basis). For each drying experiment fruits of similar size and

shape and initial mass of 800g were cut longitudinally into eight similar pieces, pips removed. Samples were dried in a laboratory air-drier with forced horizontal air flow. Moisture loss was measured at 15–30 min intervals during experiments with accuracy of ±0.01 g (Radwag WPX 4500). Drying experiments were carried out at temperatures of 50, 60, 70ºC and for two air velocities: 1.0 and 1.2 m/s. Originally in the methods of research planned air velocity were 1 and 1.5 m/s, however, due to technical conditions in the drying tunnel managed to get the velocity maximum 1.2 m/s, therefore such measurements were made and the relevant results were presented. Drying of peach started at the initial moisture content and continued, until moisture content reached equilibrium value (till was no large variation in the moisture lost). Experiments were replicated three times to minimise error, then mean values was used. For each experimental setup a relative humidity of the ambient air was controlled and a series of mass measurements were conducted. Mass of dry solid was determined with accuracy of 0.01 g for each individual sample by oven drying at 105ºC for 24 h (PN-A-75101-03:1990).

Results and discussion

Drying kinetics

The effect of temperature and air velocity on moisture content changes during drying of peach pieces is shown on Figure 1. Figure 2 shows the effect of air velocity on the drying rate of peach at a fixed temperature.

Air velocity had less effect on the drying time than the drying temperature. It may be concluded that the surface of the fruit dried faster and drying rate is determined by the external water exchange to a lesser extent than by the internal one. The air velocity in the range 1-1.2 m/s has any effect on the drying time for air temperature 50ºC but this effect is visible with increasing temperature. Further studies including temperature measurements of dried material would be valuable.

Mathematical modelling

According to the theory, in the initial drying phase, drying rate of the material with high initial moisture content should be determined by external conditions of water exchange. It means that water exchange takes place only on the surface of the dried material. The heat supplied to the body is consumed for the evaporation of water from its surface, and the surface temperature
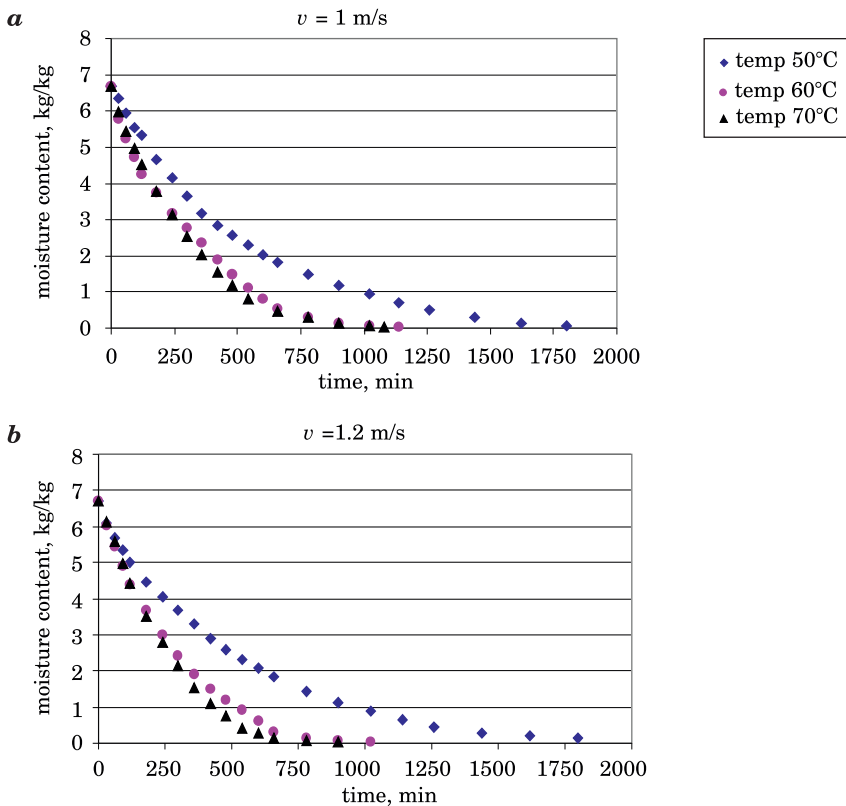
Fig. 1. Drying kinetics depending on temperature at a fixed velocity: *a* – velocity 1.0 m/s, *b* – 1.2 m/s

of the dried material is approximately equal to the wet bulb temperature. According to the theory of convectional drying of agricultural products this kind of water exchange is called the first drying period (PABIS 1982). During this period the drying rate of solid surface is constant. First drying period ends when the water molecules are vaporized from the surface. The moisture content at this point is called the critical moisture content. This period is always present in products with high initial moisture content such as fruits and vegetables and also peach.

Decreasing drying rate is characteristic for the second drying period. The temperature of dried material increases, water from inner layers changes its state to vapour and moves to the sample surface. This phenomenon is called inner diffusion and its rate is lower than water evaporation on the sample surface. The second drying period ends when the moisture content reaches the equilibrium and remains constant.
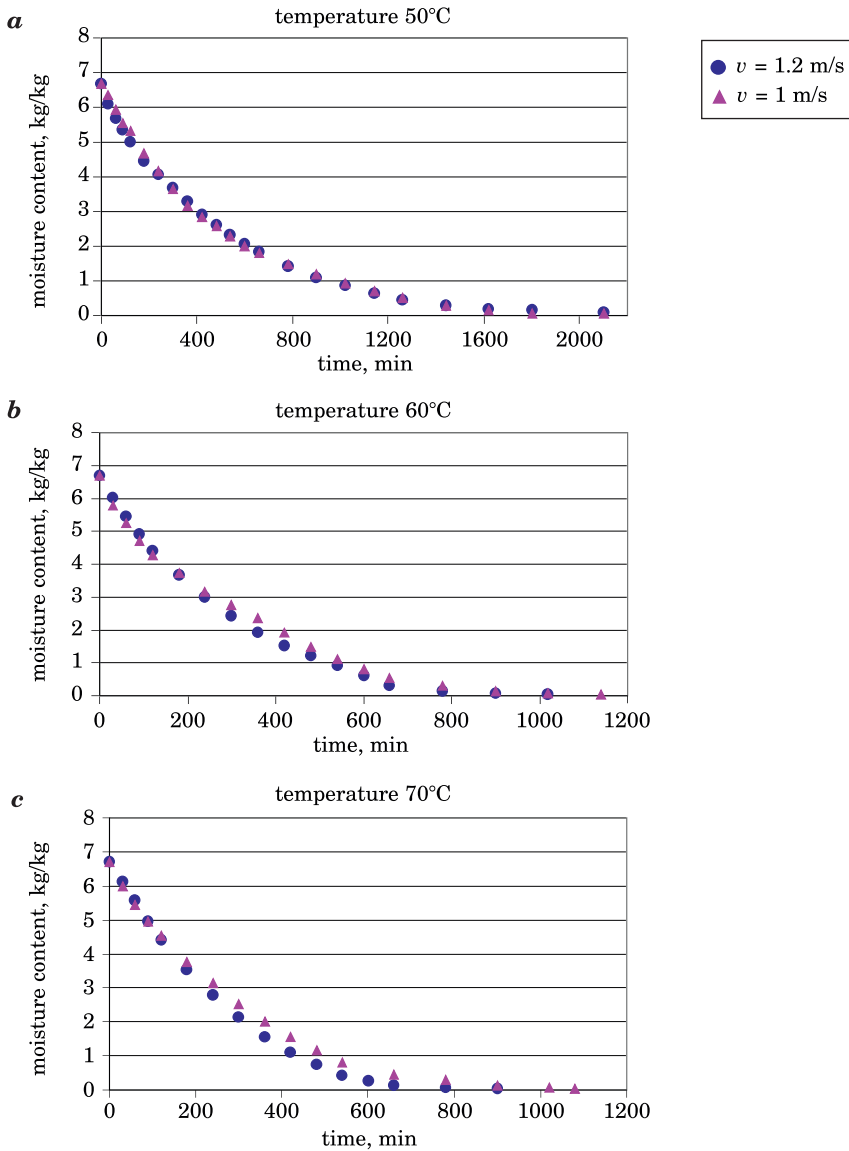
Fig. 2 Drying kinetics depending on hot-air velocity at a fixed temperature: a – 50ºC temperature, b – 60ºC, c – 70ºC

Drying kinetics in this study according to PABIS (1994, 1999), was modelled by means of: first drying period equation in terms of shrinkage (Eq. 1).

$$u_I(\tau) = u_0\left[\frac{1}{1-b}\left(1 - \frac{1-b}{Nu_0}k_0\tau\right)^N - \frac{b}{1-b}\right] \tag{1}$$

where:
u_0 – initial moisture content [kg/kg]
k_0 – coefficient of initial speed of drying [1/min]
τ – time of drying [min]
N – correction factor, the rate of anisotropic changes [–]
b – maximum rate of shrinkage, [–]
V_s – volume of dry basis [m^3]
V_0 – initial volume of the material [m^3]
and second drying period equation (Eq. 2), which is a simplified diffusion equation of mean moisture content $u(\tau)$:

$$u_{II}(\tau) = u_r + (u_0 - u_r)\ e^{-Kr} \tag{2}$$

where:
$K = f(a_m, x, \tau)$ – factor depending on the shape of the dried sample [–]
u_r – equilibrium moisture content [kg/kg]
a_m – mass diffusion coefficient [m^2/s]
x – characteristic dimension [m]

Verification of models described by Eq. 1 and Eq. 2 leads to the conclusion about the type of conditions governing the drying process.

Determination of critical moisture content occurrence is contractual. This moment corresponds to change from external mass transfer dominance to internal one. Drying rate in the first period is then equal to the rate of drying in the second period (PABIS 1999). This allows to estimate the value of the coefficient of drying rate in second period (K from Eq. 2):

$$K = \frac{k_0}{u_{cr} - u_r}\left(1 - \frac{1 - b}{Nu_0}\ k_0\tau_{cr}\right)^{N-1} \tag{3}$$

Since critical moisture content was unknown in this study, therefore three different moisture contents were assumed:

1. $u_{cr} = 2$ kg H$_2$O/kg db – according to JAROS (1999) it was assumed that such critical moisture content of fruits and vegetables separates the first "surface" and the second "diffusive" drying period

2. $u_{cr} = 4$ kg H$_2$O/kg db – intermediate value between $u_{cr} = 2$ and $u_0 = 6,7$ kg/kg

3. $u_{cr} = u_0$ – assuming that the process runs only in the second period of drying.

Coefficients k_0 and N were selected for each model in order to minimize its errors.

Fig. 3. Models of moisture content changes during the 1st and the 2nd drying period and error plots for assumed critical moisture content u_{cr} = 2 kg/kg, temperature 50°C and air velocity v = 1.2 m/s
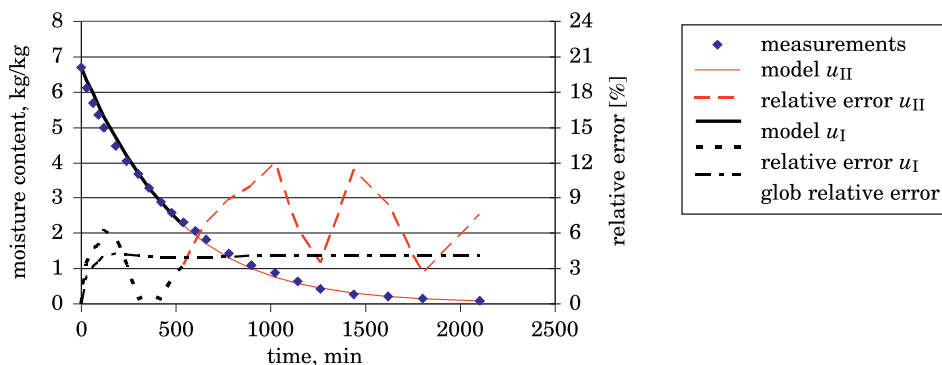

Fig. 4. Models of moisture content changes during the 1st and the 2nd drying period and error plots for assumed critical moisture content u_{cr} = 4 kg/kg and temperature 50°C, air velocity v = 1.2 m/s
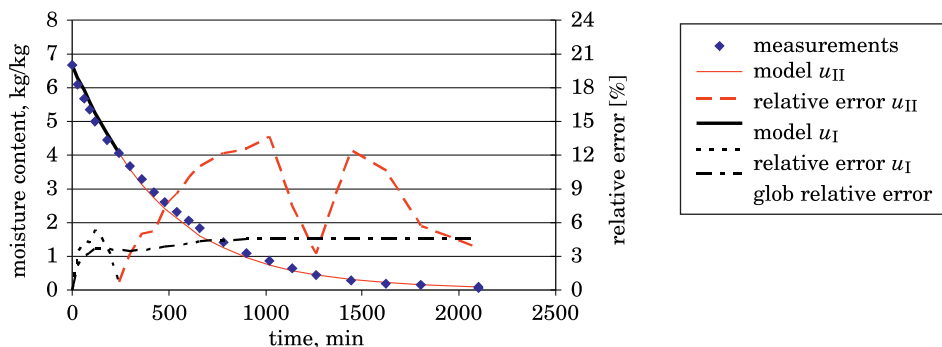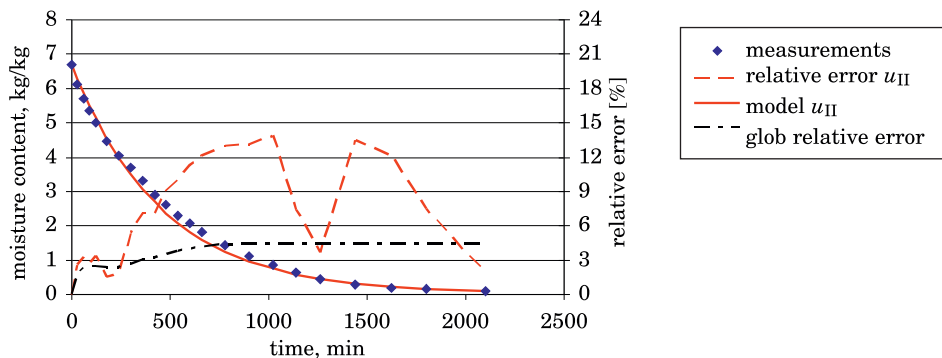

Fig. 5. Models of moisture content changes during the 1st and the 2nd drying period and error plots for assumed critical moisture content $u_{cr} = u_0$, temperature 50°C, air velocity v =1.2 m/s

Modelling results of moisture content changes of drying peach presented in figures 3–5, for exemplary temperature 50°C and air velocity v = 1.2 m/s. Results include original data and those obtained by means of mathematical modelling.

Analyzing the graphs in Figures 3–4 can be seen, the relative errors model u_I for the assumed critical moisture content of 2 and 4 kg/kg (drying time 500 and 250 min) were higher than for model u_{II} (Figure 5). Thus, assumption that the process of drying peach in the initial period is determined by external mass transfer conditions was not confirmed.

It is possible to use empirical models to describe the kinetics of the second drying period. In the literature some models of moisture content changes which do not arise directly from the theory of heat and mass transfer were also reported. Such models are based on specific solution of diffusion equation for convective drying of solids. To describe falling drying rates in literature have been widely used semi-theoretical models, for example: the Newton, the Henderson and Pabis, the Logarithmic and the Page models. These models are generally derived by simplifying general series solutions of Fick's second law and considering a direct relationship between the average moisture content and the drying time. They neglect the fundamentals of the drying process and their parameters have no physical meaning (SIMAL et al. 2005). Despite this, Pages's model (PAGE'S 1949) has been used to describe the drying kinetics of various agricultural materials, such as fruits: grapes (DOYMAZ, PALA 2002), apricots (BOZKIR 2006), strawberry, apple (CONTRERAS et al. 2008), kiwi (SIMAL et al. 2005) in convective and microwave-convective drying.

Also in this work drying kinetics was modelled by means of Page's model (Eq. 4):

$$U = \frac{u(\tau) - u_r}{(u_0 - u_r)} = \exp(-k^n) \tag{4}$$

Results obtained by means of Page's model in exemplary temperature 50°C are shown in figure 6.

As seen in Figure 6 Page's model does not better fit experimental drying kinetics data in the falling rate period than theoretical model (Eq. 2). Because it is empirical model which does not arise directly from the theory of heat and mass transfer therefore it was considered that in the case of peach, the Page's model was not well suited to describe the kinetics of drying. In this work was focused on theoretical models described by equations 1 and 2.

Model coefficients (N, k_0) were chosen so that the relative error of the 1st drying period model was about 5% and of 2nd drying period does not exceed 15%. The global relative error calculated for the whole process should have been less than 5% (Eq. 5):

$$\delta_g = \sqrt{\frac{\sum\limits_{i=1}^{n} [u_{\exp \cdot i} - u_{\mathrm{mod} \cdot i}]^2}{\sum\limits_{i=1}^{n} u_{\exp \cdot i}}} \cdot 100\% \qquad (5)$$

where $u_{\exp}$ and u_{mod} – moisture content measured and calculated from model.
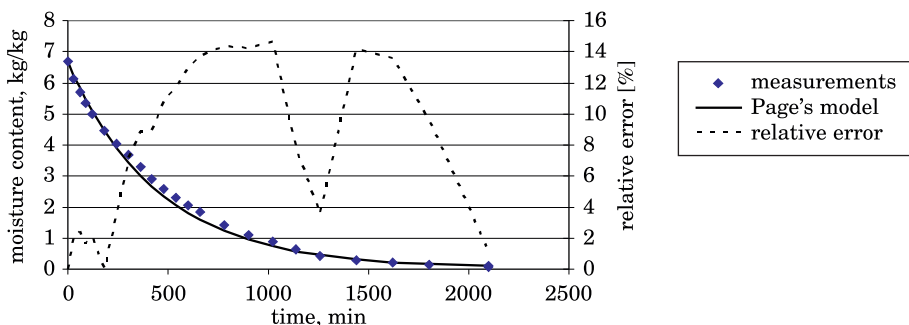

Fig. 6. The Page's model of moisture content changes and error plot, at temperature 50ºC, air velocity $v = 1.2$ m/s

Absolute errors of every model were of 0.2 kg H_2O/kg db. Table 1 presents coefficients *N*, k_0 and *K* for all cases.

Table 1

Coefficients *N*, k_0 and *K* in mathematical models (Eq. 1 and 2)

Critical moisture content	Coefficient	50ºC		60ºC		70ºC	
		1 m/s	1.2 m/s	1 m/s	1.2 m/s	1 m/s	1.2 m/s
$u_{cr} = 2$ kg/kg	N	10	15	20	8	6,2	6
	k_0	0.01205	0.0124	0.0196	0.0208	0.021	0.023
$u_{cr} = 4$ kg/kg	N	3.9	6.4	6	8	8	2
	k_0	0.0125	0.0131	0.0195	0.022	0.0215	0.022
$u_{cr} = u_0$	k_0	0.0145	0.0145	0.0219	0.0245	0.024	0.026
	K	0.00218	0.00218	0.00329	0.00368	0.00361	0.00392

There can not be seen logical relationship between the coefficient *N* and the parameters of the drying process. However, the coefficient k_0 of the initial drying rate is logically correct, that is larger for higher temperature and drying air velocity.

Conclusions

The effect of temperature and velocity on thin-layer drying of peach slices in a tunnel dryer was investigated. Increase in drying air temperature decreased the drying time. Velocity has less effect on drying rate than temperature.

The critical moisture content in drying process of peach was not identified. The verification of theoretical models of the first and second drying period indicates that in the drying process of peach can not take into account the first drying period, which means that external conditions of mass exchange does not significantly influence the process of the drying. The reason of this fact can be quick formation on the cross-sectional area of the fruit layer of the crystallized sugar and then the caramelization, which prevents wetting the surface by water transported in the form of liquid from inside the fruit.

The drying process of peach occurred in the falling rate period and is determined by internal conditions of heat and mass transfer. Full verification of the theoretical model requires conducting apart from the empirical verification, also the logical verification, for example the analysis and interpretation of physical numerical coefficients in the model, therefore work needs to be continued.

References

Bozkir O. 2006. *Thin layer drying and mathematical modeling for washed dry apricots*. Journal of Food Engineering, 77(1): 146-151.

Contreras C., Martin-Esparza M.E., Chiralt A., Martinez-Navarrete N. 2008. *Influence of microwave application on convective drying: Effects on drying kinetics, and optical and mechanical properties of apple and strawberry*. Journal of Food Engineering, 88: 55–64.

Dandamrongrak R., Mason R., Young G. 2003. *The effect of pretreatments on the drying rate and quality of dried bananas*. International Journal of Food Science and Technology, 38: 877–882.

Doymaz I., Pala M. 2002. *The effects of dipping pretreatments on air-drying rates of the seedless grapes*. Journal of Food Engineering, 52: 413–417.

Doymaz I. 2004. *Effect of pre-treatments using potassium metabisulphite and alkaline ethyl oleate on the drying kinetics of apricots*. Biosystems Engineering, 89: 281–287.

Germer S.P.M., Queiroz M.R., Aguirre J.M., Berbari S.A.G., Anjos V. 2010. *Process variables in the osmotic dehydration of sliced peaches*. Ciência e Tecnologia de Alimentos. 30(4): 940–948. Online: http://dx.doi.org/10.1590/S0101-20612010000400016 (access: 31.07.2013).

Goyal R.K., Kingsly A.R.P., Manikantan M.R,. Ilyasa S.M. 2007. *Mathematical modelling of thin layer drying kinetics of plum in a tunnel dryer*. Journal of Food Engineering 79: 176–180.

Igual M., Garcia-Martinez E., Martin-Esparza M.E., Martinez-Navarrete N. 2012**.** *Effect of processing on the drying kinetics and functional value of dried apricot*. Food Research International 47: 284–290

Jaros M. 1999. *Kinetyka suszenia warzyw*. Rozprawa habilitacyjna. WAR Lublin.

Kingsly R.P., Goyal R.K., Manikantan M.R., Ilyas S.M. 2007. *Effects of pretreatments and drying air temperature on drying behaviour of peach slice*. International Journal of Food Science & Technology, 42(1): 65–69.

Pabis S. 1982. *Teoria konwekcyjnego suszenia produktów rolniczych*. PWRiL, Warszawa.

Pabis S. 1994. *Uogólniony model kinetyki suszenia warzyw i owoców w pierwszym okresie*. Zeszyty Problemowe Postępów Nauk Rolniczych, 417: 15–34.

Pabis S. 1999. *Koncepcja teorii konwekcyjnego suszenia warzyw*. In: *Konwekcyjne suszenie warzyw-teoria i praktyka*. Ed. S. Pabis, p. 9–31.

Page G. 1949. *Factors influencing the maximum rates of air-drying shelled corn in thin layers*. M.S. Thesis. Lafayette, IN: Purdze University.

Pereira L.M., Ferrari C.C., Mastrantonio S.D.S., Rodrigues A.C.C., Hubinger M.D. 2006. *Kinetic aspects, texture, and colour evaluation of some tropical fruits during osmotic dehydration*. Drying Technology, 24(4): 475–484.

Sahari M.A., Souti M., Emam-Jomeh Z. 2006. *Improving the dehydration of dried peach by osmotic method*. Journal of Food Technology, 4(3): 189–193.

Sarsilmaz C., Yaldiz C., Pehlivan D. 2000. *Drying of apricots in a rotary column cylindrical dryer (RCCD) supported with solar energy*. Renewable Energy, 21: 117–127.

Simal S., Femenia A., Garau M.C., Rossello C. 2005. *Use of exponential, Page's and difusional models to simulate the drying kinetics of kiwi fruit*. Journal of Food Engineering, 60: 323–328.

Togrul I.T., Pehlivan D. 2002. *Mathematical modelling of solar drying of apricots in thin layers*. Journal of Food Engineering, 55: 209–216.

Togrul I.T., Pehlivan D. 2003. *Modelling of drying kinetics of single apricot*. Journal of Food Engineering, 58: 23–32.

Togrul I.T., Pehlivan D. 2004. *Modelling of thin layer drying kinetics of some fruits dunder open-air sun drying process*. Journal of Food Engineering, 65: 413–425.

Yaldiz O., Ertekin C., Uzun H.I. 2001. *Mathematical modeling of thin layer solar drying of sultana grapes*. Energy – An International Journal, 26: 457–465.

Wang J., Sheng K. 2006. *Far-infrared and microwave drying of peach LWT*. Food Science and Technology**,** 39(3): 247–255.

PN-A-75101-03:1990. *Przetwory owocowe i warzywne. Przygotowanie próbek i metody badań fizykochemicznych. Oznaczanie zawartości suchej masy metodą wagową.*

Technical Sciences

Reviewers of Years – book 2013

Monika Aniszewska

Raffael Argiolu

Ndubisi Aviara

Ivan W. Barabash

Janusz Bogusz

Andrzej Borkowski

Jarosław Bosy

Stefan Cenkowski

Ying Chen

Yalçyn Coşkuner

Jacek Dach

Rotimi M. Davies

Bohdan Dobrzański Jr

Ibrahim Doymaz

Ahmed El-Mowafy

Gilad Even-Tzur

Adam Figiel

Jose Teixeira Freire

Roman Galas

Juraj Gašinec

Algirdas Jasinskas

Sławomir Juściński

Shkelqim Karaj

Andrzej Kmieć

Przemysław Kosobucki

Zbigniew Krzysiak

Stanisław Kukla

Roderik C. Lindenbergh

Haitao Liu

Isabel Paula Ramos Marques

Andrzej Młynarczak

Ana M. Pagano

Eimuntas K. Paršeliūnas

Józef Pelc

Cvetanka Popovska

Witold Prószyński

Angelica Marta Ramirez Martinez

Tamas Regert

Ahmet Sivacioğlu

Miroslava Smitková

Jirt Souček

Sesha Srinivasan

Gabriel Strykowski

Aleksandras Stulginskis

Lieonid Szeynicz

Marek Szmytkiewicz

Amin Taheri-Garavand

Dariusz Tomkiewicz

Marek Trojanowicz

Chavdar Vezirov

Vinita Vishwakarma

Sławomir Wierzbicki

Eva Zdravecká

Milan Zmindak

Guide for Autors

Introduction

Technical Sciences is a peer-reviewed research Journal published in English by the Publishing House of the University of Warmia and Mazury in Olsztyn (Poland). Journal is published continually since 1998. Until 2010 Journal was published as a yearbook, in 2011 and 2012 it was published semiyearly. From 2013, the Journal is published quarterly in the spring, summer, fall, and winter.

The Journal covers basic and applied researches in the field of engineering and the physical sciences that represent advances in understanding or modeling of the performance of technical and/or biological systems. The Journal covers most branches of engineering science including biosystems engineering, civil engineering, environmental engineering, food engineering, geodesy and cartography, information technology, mechanical engineering, materials science, production engineering etc.

Papers may report the results of experiments, theoretical analyses, design of machines and mechanization systems, processes or processing methods, new materials, new measurements methods or new ideas in information technology.

The submitted manuscripts should have clear science content in methodology, results and discussion. Appropriate scientific and statistically sound experimental designs must be included in methodology and statistics must be employed in analyzing data to discuss the impact of test variables. Moreover there should be clear evidence provided on how the given results advance the area of engineering science. Mere confirmation of existing published data is not acceptable. Manuscripts should present results of completed works.

There are three types of papers: a) research papers (full length articles); b) short communications; c) review papers.

The Journal is published in the printed and electronic version. The electronic version is published on the Website ahead of printed version of Technical Sciences.

Technical Sciences does not charge submission or page fees.

Types of paper

The following articles are accepted for print:

Reviews

Reviews should present a focused aspect on a topic of current interest in the area of biosystems engineering, civil engineering, environmental engineering, food engineering, geodesy and cartography, information technology, mechanical engineering, materials science, production engineering etc. They should include all major findings and bring together reports from a number of sources. These critical reviews should draw out comparisons and conflicts between work, and provide an overview of the 'state of the art'. They should give objective assessments of the topic by citing relevant published work, and not merely present the opinions of individual authors or summarize only work carried out by the authors or by those with whom the authors agree. Undue speculations should also be avoided. Reviews generally should not exceed 6,000 words.

Research Papers

Research Papers are reports of complete, scientifically sound, original research which contributes new knowledge to its field. Papers should not exceed 5,000 words or about 12 printed pages, including figures and tables.

Short Communications

Short Communications are research papers constituting a concise description of a limited investigation. They should be completely documented, both by reference list, and description of the experimental procedures. Short Communications should not occupy more than 2,000 words, including figures and tables.

Letters to the Editor

Letters to the Editor should concern with issues raised by articles recently published in scientific journals or by recent developments in the engineering area.

Contact details for submission

The paper should be sent to the Editorial Office, as a Microsoft Word file, by e-mail: techsci uwm.edu.pl

Referees

Author/authors should submit, with the manuscript, the names, addresses and e-mail addresses of at least three potential referees. The editor retains the sole right to decide whether or not the suggested reviewers are used.

Submission declaration

After final acceptance of the manuscript, the corresponding author should send to the Editorial Office the author's declaration. Submission of an article implies that the work has not been published previously (except in the form of an abstract or as part of a published lecture or academic thesis or as an electronic preprint), that it is not under consideration for publication elsewhere, that publication is approved by all authors and tacitly or explicitly by the responsible authorities where the work was carried out, and that, if accepted, it will not be published elsewhere in the same form, in English or in any other language.

To prevent cases of ghostwriting and guest authorship, the author/authors of manuscripts is/are obliged to: (i) disclose the input of each author to the text (specifying their affiliations and contributions, i.e. who is the author of the concept, assumptions, methods, protocol, etc. used during the preparation of the text); (ii) disclose information about the funding sources for the article, the contribution of research institutions, associations and other entities.

Language

Authors should prepare the full manuscript i.e. title, abstract and the main text in English (American or British usage is accepted). Polish version of the manuscript is not required.

The file type

Text should be prepared in a word processor and saved in DOC or DOCX file (MS Office).

Article structure

Suggested structure of the manuscript is as follows:
Title
Authors and affiliations
Corresponding author
Abstract
Keywords
Introduction
Material and Methods
Results and Discussion

Conclusions
Acknowledgements (*optional*)
References
Tables
Figures

Subdivision — numbered sections

Text should be organized into clearly defined and numbered sections and subsections (optionally). Sections and subsections should be numbered as 1. 2. 3. then 1.1 1.2 1.3 (then 1.1.1, 1.1.2, ...). The abstract should not be included in numbering section. A brief heading may be given to any subsection. Each heading should appear on its own separate line. A single line should separate paragraphs. Indentation should be used in each paragraph.

Font guidelines are as follows:
– Title: 14 pt. Times New Roman, bold, centered, with caps
– Author names and affiliations:12 pt. Times New Roman, bold, centered, italic, two blank line above
– Abstract: 10 pt. Times New Roman, full justified, one and a half space. Abstract should begin with the word Abstract immediately following the title block with one blank line in between. The word Abstract: 10 pt. Times New Roman, centered, indentation should be used
– Section Headings: Not numbered, 12 pt. Times New Roman, bold, centered; one blank line above
– Section Sub-headings: Numbered, 12 pt. Times New Roman, bold, italic, centered; one blank line above
– Regular text: 12 pt. Times New Roman, one and a half space,full justified, indentation should be used in each paragraph

Title page information

The following information should be placed at the first page:

Title

Concise and informative. Authors should not use abbreviations and formulae where possible.

Authors and affiliations

Author/authors' names should be presented below the title.The authors' affiliation addresses (department or college; university or company; city, state and zip code, country) should be placed below the names. Authors with the same affiliation must be grouped together on the same line with affiliation information following in a single block. Authors should indicate all affiliations with a lower-case superscript letter immediately after the author's name and in front of the appropriate address.

Corresponding author

It should be clearly indicated who will handle correspondence at all stages of refereeing and publication, also post-publication process. The e-mail address should be provided (footer, first page). Contact details must be kept up to date by the corresponding author.

Abstract

The abstract should have up to 100-150 words in length. A concise abstract is required. The abstract should state briefly the aim of the research, the principal results

and major conclusions. An abstract must be able to stand alone. Only abbreviations firmly established in the field may be eligible.Non-standard or uncommon abbreviations should be avoided, but if essential they must be defined at their first mention in the abstract itself.

Keywords

Immediately after the abstract, author/authors should provide a maximum of 6 keywords avoiding general, plural terms and multiple concepts (avoid, for example, 'and', 'of'). Author/authors should be sparing with abbreviations: only abbreviations firmly established in the field may be eligible.

Abbreviations

Author/authors should define abbreviations that are not standard in this field. Abbreviations must be defined at their first mention there. Author/authors should ensure consistency of abbreviations throughout the article.

Units

All units used in the paper should be consistent with the SI system of measurement. If other units are mentioned, author/authors should give their equivalent in SI.

Introduction

Literature sources should be appropriately selected and cited. A literature review should discuss published information in a particular subject area. Introduction should identify, describe and analyze related research that has already been done and summarize the state of art in the topic area. Author/authors should state clearly the objectives of the work and provide an adequate background.

Material and Methods

Author/authors should provide sufficient details to allow the work to be reproduced by other researchers. Methods already published should be indicated by a reference. A theory should extend, not repeat, the background to the article already dealt within the Introduction and lay the foundation for further work. Calculations should represent a practical development from a theoretical basis.

Results and Discussion

Results should be clear and concise. Discussion should explore the significance of the results of the work, not repeat them. A combined Results and Discussion section is often appropriate.

Conclusions

The main conclusions of the study may be presented in a Conclusions section, which may stand alone or form a subsection of a Results and Discussion section.

Acknowledgements

Author/authors should include acknowledgements in a separate section at the end of the manuscript before the references. Author/authors should not include them on the title page, as a footnote to the title or otherwise. Individuals who provided help during the research study should be listed in this section.

Artwork
General points

– Make sure you use uniform lettering and sizing of your original artwork

- Embed the used fonts if the application provides that option
- Aim to use the following fonts in your illustrations: Arial, Courier, Times New Roman, Symbol
- Number equations, tables and figures according to their sequence in the text
- Size the illustrations close to the desired dimensions of the printed version

Formats

If your electronic artwork is created in a Microsoft Office application (Word, PowerPoint, Excel) then please supply 'as is' in the native document format

Regardless of the application used other than Microsoft Office, when your electronic artwork is finalized, please 'Save as' or convert the images to one of the following formats (note the resolution requirements given below):

EPS (or PDF): Vector drawings, embed all used fonts

JPEG: Color or grayscale photographs (halftones), keep to a minimum of 300 dpi

JPEG: Bitmapped (pure black & white pixels) line drawings, keep to a minimum of 1000 dpi or combinations bitmapped line/half-tone (color or grayscale), keep to a minimum of 500 dpi

Please **do not**:
- Supply files that are optimized for screen use (e.g., GIF, BMP, PICT, WPG); these typically have a low number of pixels and limited set of colors
- Supply files that are too low in resolution
- Submit graphics that are disproportionately large for the content

Color artwork

Author/authors should make sure that artwork files are in an acceptable format (JPEG, EPS PDF, or MS Office files) and with the correct resolution. If, together with manuscript, author/authors submit color figures then Technical Sciences will ensure that these figures will appear in color on the Web as well as in the printed version at no additional charge.

Tables, figures, and equations

Tables, figures, and equations/formulae should be identified and numbered consecutively in accordance with their appearance in the text.

Equations/mathematical and physical formulae should be presented in the main text, while tables and figures should be presented at the end of file (after References section). Mathematical and physical formulae should be presented in the MS Word formula editor.

All types of figures can be black/white or color. Author/authors should ensure that each figure is numbered and has a caption. A caption should be placed below the figure. Figure must be able to stand alone (explanation of all symbols and abbreviations used in figure is required). Units must be always included. It is noted that figure and table numbering should be independent.

Tables should be numbered consecutively in accordance with their appearance in the text. Table caption should be placed above the table. Footnotes to tables should be placed below the table body and indicated with superscript lowercase letters. Vertical rules should be avoided. Author/authors should ensure that the data presented in tables do not duplicate results described in figures, diagrams, schemes, etc. Table must be able to stand alone (explanation of all symbols and abbreviations used in table is required). Units must be always included. As above, figure and table numbering should be independent.

References

References: All publications cited in the text should be presented in a list of references following the text of the manuscript. The manuscript should be carefully checked to ensure that the spelling of authors' names and dates of publications are exactly the same in the text as in the reference list. Authors should ensure that each reference cited in the text is also present in the reference list (and vice versa).

Citations may be made directly (or parenthetically). All citations in the text should refer to:

1. Single author

The author's name (without initials, with caps, unless there is ambiguity) and the year of publication should appear in the text

2. Two authors

Both authors' names (without initials, with caps) and the year of publication should appear in the text

3. Three or more authors

First author's name followed by et al. and the year of publication should appear in the text

Groups of references should be listed first alphabetically, then chronologically.

Examples:

"... have been reported recently (ALLAN, 1996a, 1996b, 1999; ALLAN and JONES, 1995). KRAMER et al. (2000) have recently shown..."

The list of references should be arranged alphabetically by authors' names, then further sorted chronologically if necessary. More than once reference from the same author(s) in the same year must be identified by the letters "a", "b", "c" etc., placed after the year of publication.

References should be given in the following form:

KUMBHAR B.K., AGARVAL R.S., DAS K. 1981. *Thermal properties of fresh and frozen fish*. International Journal of Refrigeration, 4(3), 143–146.

MACHADO M.F., OLIVEIRA F.A.R., GEKAS V. 1997. *Modelling water uptake and soluble solids losses by puffed breakfast cereal immersed in water or milk*. In Proceedings of the Seventh International Congress on Engineering and Food, Brighton, UK.

NETER J., KUTNER M.H., NACHTSCHEIM C.J., WASSERMAN W. 1966. *Applied linear statistical models* (4th ed., pp. 1289–1293). Irwin, Chicago.

THOMSON F.M. 1984. *Storage of particulate solids*. In M. E. Fayed, L. Otten (Eds.), Handbook of Powder Science and Technology (pp. 365–463). Van Nostrand Reinhold, New York.

Citation of a reference as 'in press' implies that the item has been accepted for publication.

Note that the full names of Journals should appear in reference list.

Submission checklist

The following list will be useful during the final checking of an article prior to the submission. Before sending the manuscript to the Journal for review, author/authors should ensure that the following items are present:

– Text is prepared with a word processor and saved in DOC or DOCX file (MS Office). One author has been designated as the corresponding author with contact details: e-mail address

– Manuscript has been 'spell-checked' and 'grammar-checked'

– References are in the correct format for this Journal

– All references mentioned in the Reference list are cited in the text, and vice versa

– Author/authors does/do not supply files that are too low in resolution

– Author/authors does/do not submit graphics that are disproportionately large for the content